THE ROLE OF MITOCHONDRIAL PHOSPHOLIPID HYDROPEROXIDE GLUTATHIONE PEROXIDASE IN CANCER THERAPY

by

Hong Wang

An Abstract

Of a thesis submitted in partial fulfillment
of the requirements for the Doctor of
Philosophy degree in Free Radical and Radiation Biology
in the Graduate College of
The University of Iowa

December 2000

Thesis supervisor: Professor Garry R. Buettner

ABSTRACT

Phospholipid hydroperoxide glutathione peroxidase (PhGPx) is a unique selenoenzyme that directly detoxifies lipid hydroperoxides *in situ*. It therefore plays an important role in the protection of cellular membranes. PhGPx is expressed in most mammalian tissues. It is present as a mitochondrial form (L-PhGPx) and a cytosolic form (S-PhGPx). Overexpression of PhGPx has been shown to significantly protect cells from oxidative damage. The hypothesis of this thesis is that mitochondrial PhGPx (L-PhGPx) may play an important role in the resistance of cells to certain oxidative stress-mediated cancer therapies.

A human breast carcinoma MCF-7 cell line was used as a cell model system in this research. It was stably transfected with human L-PhGPx sense cDNA. Four clones (P-1, P-2, P-3, and P-4) with 3- to 7-fold increases in PhGPx activity were selected for study. Overexpression of L-PhGPx did not significantly influence other cellular antioxidants, including superoxide dismutases, cytosolic glutathione peroxidase, catalase, glutathione reductase, and glutathione. However, L-PhGPx did decrease the rate of cell growth. Cell plating efficiency was inversely correlated with effective PhGPx activity, which is defined as the product of cellular PhGPx activity and total glutathione.

The biological functions of L-PhGPx have been investigated in cancer treatment, including photodynamic therapy (PDT) and hyperthermia (HT). Both PDT and HT can induce oxidative stress. Overexpression of L-PhGPx in MCF-7 cells significantly increased the resistance of cells to PDT- and HT-mediated cytotoxicity. The effective PhGPx activity had a remarkable inverse linear correlation ($r = -0.80$) to the rate of

removal of lipid hydroperoxides in living cells, and correlated positively with cell survival after photooxidation ($r = 0.91$). L-PhGPx protected mitochondrial function by preserving the mitochondrial membrane potential.

These data demonstrate that L-PhGPx provides significant protection against lipid peroxidation *via* removal of LOOH and maintaining the mitochondrial membrane potential, suggesting that LOOHs are major mediators in this cell injury process. It also suggests that mitochondria are important targets for PDT and HT. PhGPx activity could contribute to the resistance of tumor cells to the treatments that have oxidative stress as a component in their mechanism of action.

Abstract approved: _____
Thesis supervisor

_____
Title and department

_____
Date

THE ROLE OF MITOCHONDRIAL PHOSPHOLIPID HYDROPEROXIDE GLUTATHIONE PEROXIDASE IN CANCER THERAPY

by

Hong Wang

A thesis submitted in partial fulfillment
of the requirements for the Doctor of
Philosophy degree in Free Radical and Radiation Biology
in the Graduate College of
The University of Iowa

December 2000

Thesis supervisor: Professor Garry R. Buettner

Graduate College
The University of Iowa
Iowa City, Iowa

CERTIFICATE OF APPROVAL

_____

PH.D. THESIS

_____

This is to certify that the Ph.D. thesis of

Hong Wang

has been approved by the Examining Committee for the
thesis requirement for the Doctor of Philosophy degree in
Free Radical and Radiation Biology at the December 2000 graduation.

Thesis committee: _____
Thesis supervisor

_____
Member

_____
Member

_____
Member

_____
Member

To
Yongde and Chris

ACKNOWLEDGEMENTS

I would like to thank my mentor Dr. Garry R. Buettner for his guidance in the 'world of free radicals'. He has provided me with encouragement, independence, and friendship throughout the course of this work.

I would like to thank my committee members Drs. Frederick E. Domann, Kevin C. Kregel, Larry W. Oberley, and Michael E.C. Robbins for their critical evaluation of this work, and more importantly, their time.

I would like to thank Dr. Rugao Liu for providing the human mitochondrial PhGPx sense cDNA.

I would like to thank Dr. Albert W. Girotti for providing the primary PhGPx antibody and the pure PhGPx protein used in these studies.

I would like to thank Messrs. Justin Fishbaugh and Gene Hess for helping in the analyses of flow cytometry.

I would like to thank Drs. Shijun Li, Joseph Nwankwo, Yunxia O'Malley, Steven Y. Qian, Freya Q. Schafer, Douglas R. Spitz, Sujatha Venkataraman, Tao Yan, Hannah J. Zhang, and Weiling Zhao for their critical scientific input and interest in this research project.

I also would like to thank my RRL friends Dr. James W. Osborne, Eric E. Kelley, Sean M. Martin, Brett A. Wagner, Christine Weydert, Lingjie Zhao, and Chunhong Zhu for their help in many ways.

This work was supported by NIH Grants CA-81090 and CA-66081.

TABLE OF CONTENTS

LIST OF TABLES

LIST OF FIGURES

LIST OF SCHEMES

LIST OF ABBREVIATIONS

a^H	hyperfine constant from hydrogen atom
a^N	hyperfine constant from nitrogen atom
ATCC	American Type Culture Collection
ATZ	3-amino-1,2,4-triazole
BGH	bovine growth hormone
BSO	buthionine sulfoximine
CAT	catalase
cDNA	complementary deoxyribonucleic acid
CuZnSOD	copper-zinc superoxide dismutase
DEM	diethylmaleate
DMPO	5,5-dimethyl-pyrroline-1-oxide
dNTP	mixture of dATP. dGTP, dCTP, dTTP
DTNB	5,5'-dithio-*bis*-(2-nitobenzoic acid)
DTT	dithiothreiol
dUTP	deoxyuridine triphosphate
e_{eq}^-	aqueous electron
ECL	enhanced chemiluminescence
EDTA	ethylenediamine tetraacetate
EPR	electron paramagnetic resonance
FBS	fetal bovine serum
G418	Geneticin
G-6-PD	glucose-6-phosphate dehydrogenase
GPx(s)	glutathione peroxidase(s)
GPx1	cytosolic glutathione peroxidase
GPx2	gastrointestinal glutathione peroxidase

GPx3	plasma glutathione peroxidase
GR	glutathione reductase
GSH	glutathione
GST	glutathione S-transferase
GSSG	glutathione disulfide
HT	hyperthermia
$H_2O^{\bullet+}$	ionized water
H_2O_2	hydrogen peroxide
HPD	hematoporphyrin derivative
HPLC	high-performance liquid chromatography
13-HpODE	13-hydroperoxyloctadecadienoic acid
Hsp(s)	heat shock protein(s)
Hsp70c	heat shock protein 70 (constitutive form)
Hsp70I	heat shock protein 70 (inducible form)
$L^{\bullet}$	lipid alkyl radical
LDL	low density lipoprotein
LH	lipid
L-PhGPx	mitochondrial phospholipid hydroperoxide glutathione peroxidase
LOOH(s)	lipid hydroperoxide(s)
$LO^{\bullet}$	lipid alkoxyl radical
$LOO^{\bullet}$	lipid peroxyl radical
MCF-7	human breast carcinoma cells
MEGM	mammary epithelial growth medium
MEM	minimum essential medium
MMLV	moloney-murine leukemia virus
MnSOD	manganese superoxide dismutase
$NADP^+$	oxidized nicotinamide adenine dinucleotide phosphate
NADPH	nicotinamide adenine dinucleotide phosphate

NBT	nitroblue tetrazolium
Neo	vector only control
NFκB	nuclear transcription factor kappa B
$O_2^{\bullet -}$	superoxide
$^1O_2$	singlet oxygen
$^{\bullet}OH$	hydroxyl radical
$^{\bullet}OL$	lipid epoxyallylic radical
$OLOO^{\bullet}$	lipid epoxyperoxyl radical
OLOOH	lipid epoxyperoxyl hydroperoxide
PB	phosphate buffer
PBS	phosphate-buffered saline
PCOOH	phosphatidylcholine hydroperoxide
PCR	polymerase chain reaction
PDT	photodynamic therapy
PE	plating efficiency
PhGPx (GPx4)	phospholipid hydroperoxide glutathione peroxidase
PI	propidium iodide
PLA_2	phospholipase A_2
PPD	4-(methoxy-4-(3-phosphatephenyl) spirol (1,2-dioxentane-3,2'-adamantane)
PUFA	polyunsaturated fatty acid
Rh123	Rhodamine 123
RNasin	RNase inhibitor
ROS	reactive oxygen species
RT	reverse transcriptase
S	ground state of sensitizer
$^1S^*$	singlet excited state of sensitizer
$^3S^*$	triplet excited state of sensitizer

Se	selenium
SDS	sodium dodecyl sulphate
SOD(s)	superoxide dismutase(s)
SSA	sulfosalylic acid
SSC	saline/sodium citrate
SF	surviving fraction
Td	doubling time
TEMED	N,N,N',N'-tetramethyl-ethylenediamine
TNB	5-thio-2-nitrobenzoic acid
3'-UTR	3' untranslated region
2-VP	2-vinylpyridine
Wt	wild type

CHAPTER I
INTRODUCTION

Statement of Problem

Cancer is a leading cause of death in the western world, second only to cardiovascular disease in the United States. Breast cancer has the highest incidence in women, accounting for approximately 30% of all new cancer cases [Phillips DM, 1996; Parker SL, 1997].

Treatment of breast cancer includes surgery, radiation, chemotherapy, and hormonal modification. Breast cancer is often treated by mastectomy alone or with radiation therapy. Chemotherapy is recommended for patients with metastatic spread to regional lymph nodes. Antiestrogen treatment has proven useful in patients with lymph node metastasis. With all these treatments, the 5-year survival is improving [Parker SL, 1997]. However, local regional recurrences of breast cancer are still the cause of severe suffering for patients. It is estimated that 5 – 20% of breast cancer patients have chest wall recurrence [Ottesen G, 1988]. Although rarely the immediate cause of death, chest wall recurrence results in profound physical and psychological morbidity. Therefore, application of a treatment that results in long-term local tumor control would be beneficial to patients.

Photodynamic therapy (PDT) and local hyperthermia treatment (HT) are two options that have recently been studied in clinical trials for treatment of breast cancer local recurrence [Khan SA, 1993; Taber SW, 1998; Robinson DS, 1998; van der Zee J, 1999]. PDT involves administration of a photosensitizer followed by laser light exposure directed at the particular target area. The enhanced retention of the photosensitizer by

tumor tissue provides selective killing of cancer cells while sparing the surrounding normal tissue [Phillips D, 1994]. Therapeutic hyperthermia is an effective cell-killing agent especially to cells in a hypoxic, nutrient-deprived, and low pH environment, conditions that are found specifically in malignant tumors. Both experimental and clinical research have shown that hyperthermia gives valuable additional effects when applied in combination with radiotherapy [Sherar M, 1997; van der Zee J, 1999]. The tumoricidal actions of PDT and HT are believed to result from the generation of reactive oxygen species (ROS) [Jori G, 1980; Wilkinson F, 1981; Lord-Fontaine S, 1999; Freeman ML, 1985; Griffith OW, 1979]. These ROS may disrupt cellular membrane structure, mitochondrial function, and subsequently lead to cell destruction. Nevertheless, resistance to PDT and HT is observed [Adams K, 1999; Marchal C, 1999]. Strategies to improve the therapeutic efficacy of these two procedures are needed.

Objective

The overall objective of this research is to increase the effectiveness of PDT, and HT in breast cancer treatment. The working paradigm of this research is that ROS are important mediators involved in these cancer therapies. The working hypotheses of this research are: 1) PDT and HT induce oxidative stress; 2) the mitochondrial antioxidant enzyme phospholipid hydroperoxide glutathione peroxidase, which detoxifies cellular lipid hydroperoxides (LOOHs), plays an important role in the resistance of cells to these anticancer treatments. These hypotheses were tested by investigating the following specific aims:

1. Develop a tumor cell model that overexpresses mitochondrial PhGPx (L-PhGPx). Determine the expression levels of PhGPx in this cell model system, and investigate the biological and biochemical effects of L-PhGPx on these cells (Chapter II);
2. Determine the effects of L-PhGPx on cellular susceptibility to PDT (Chapter III);

3. Examine the cellular level of LOOHs and the potential free radical reactions induced by PDT; study the effect of L-PhGPx on cellular lipid peroxidation (Chapter III);
4. Study the role of L-PhGPx in HT-induced cellular cytotoxicity (Chapter IV);
5. Determine whether lowering the cellular pool of glutathione (GSH) will affect the enzymatic function of PhGPx (Chapter IV);
6. Study the function of L-PhGPx in providing protection against HT-induced mitochondrial damage (Chapter IV).

Antioxidants are an important cellular defense system against endogenous and exogenous oxidative stresses. A better understanding of the molecular mechanisms of the action of PhGPx and the cytotoxic mechanisms of antitumor treatments will allow us to develop new approaches to enhance tumor tissue killing as well as to protect normal tissue during cancer treatment.

Background

Lipid Peroxidation

Lipid peroxidation is a degenerative process that occurs in cell membranes, lipoproteins, and other lipid-containing cellular structures under conditions of oxidative stress [Girotti AW, 1985; Halliwell B, 1990; Porter NA, 1995]. The unsaturated phospholipids and cholesterol in cell membranes and other organized systems are important targets of oxidant attack. Lipid peroxidation perturbs structure and function of the target system, consequently leading to cell destruction. The oxidation of lipids, particularly phospholipids, in biological tissues has been suggested to be a significant chemical event in a variety of pathological conditions, such as atherosclerosis [Kovacs IB, 1997], ischemia-reperfusion injury [Palace V, 1999], and inflammation [Compton CN, 1997]. Lipid peroxidation also plays an important role in the cytotoxic effects of

reactive oxygen species (ROS)-mediated cancer therapy, including radiotherapy [Weiss JF, 2000; Newton CJ, 1999; Borges HL, 1999; Hanning J, 1999], chemotherapy [Gewirtz DA, 1999], photodynamic therapy (PDT) [Buettner GR, 1993; Kelley EE, 1997] as well as hyperthermia treatment (HT) [Khadir A, 1999; Frank J, 1998].

Lipid hydroperoxides (LOOHs), more long-lived than free radicals, are important intermediates involved in lipid peroxidation [Kappus H, 1985; Girotti AW, 1985]. The formation of LOOHs can result from both free radical species, such as hydroxyl radical ($^{\bullet}$OH), and non-free radical species, *e.g.* singlet oxygen ($^1O_2$) (**Scheme I-1**). The formed LOOHs in the membrane bilayer disturb the structure and the function of membranes [Pradhan D, 1990]; this may lead to cell destruction. LOOHs can also initiate the reaction with lipoprotein forming lipid-hydroperoxide-modified apolipoprotein [Kato Y, 1997], which contributes to the oxidation of low density lipoprotein (LDL). It has also been shown that LOOHs play a role in apoptotic cell death by triggering signal transduction pathways [Suzuki YJ, 1997].

In addition to these direct effects of LOOHs, LOOHs can be degraded *via* reductive reactions (**Scheme I-1**), which either diminish or enhance the cytotoxic potential. These formed LOOHs can be reduced by catalytic metals, such as ferrous iron, and undergo Fenton-type lipid chain reactions *via* initiation, propagation, and termination [Girotti AW, 1985]. Alternatively, LOOHs may be reduced to lipid alcohols by glutathione-dependent peroxidases (**Scheme I-1**), such as cytosolic glutathione peroxidase (GPx1), phospholipid hydroperoxide glutathione peroxidase (PhGPx) [Ursini F, 1982], as well as by nonseleno-dependent glutathione S-transferase (GST) [Flohe L, 1982]. LOOHs can also be detoxified by a newly discovered enzyme, nonselenium-dependent GPx [Fisher AB, 1999].

The balance between these two reductive pathways may play an important role in determining the potential effects of LOOHs on cells, whether the peroxidative injury is enhanced or prevented.

Lipid Hydroperoxide-Mediated Cancer Therapy

In contrast to radical surgery, nonsurgical treatment of cancer provides great advantages to patients as an alternative and promising therapeutic strategy. The most widely used nonsurgical, antineoplastic treatments are radiotherapy, chemotherapy, hyperthermia (HT), and photodynamic therapy (PDT). Oxidative stress is an important mechanism involved in the tumor killing effects of these therapies [Baker A, 1991; Li JJ, 1997; Lord-Fontaines S, 1999].

Ionizing radiation-induced damage can result from direct radiation damage or more importantly, from ROS generated from the ionization of water molecules. Ionized water ($H_2O^{\bullet+}$) and aqueous electrons (e_{aq}^-) are two primary products from the ionization of the water. These two species can subsequently produce superoxide ($O_2^{\bullet-}$) and hydrogen peroxide (H_2O_2). Superoxide can be converted to H_2O_2 by superoxide dismutase (SOD); H_2O_2 can be further reduced to hydroxyl radical ($^{\bullet}OH$) *via* the Fenton reaction. The hydroxyl radical is the most oxidizing species on the pecking order [Buettner GR, 1993], and will react almost immediately with cellular targets where it is formed. A large accumulation of lipid peroxidation products, such as conjugated dienes, ketotrienes and thiobarbituric acid-reactive substances, have been observed after irradiation [Slyshenkov VS, 1999]. Also, lipid peroxidation-mediated permeabilization of cell membranes following ionizing radiation is well documented [Hanning J, 1999].

Lipid peroxidation has also been found as a possible mechanism in the chemotherapeutic antitumor action [Benchekroun MN, 1992; Gewirtz DA, 1999], in

addition to DNA intercalation, free radical formation, DNA binding and alkylation, and DNA cross linking.

Photofrin-based PDT was approved by the U.S. Food and Drug Administration in 1995 as a modality for treating patients with esophageal cancer and lung cancer. PDT selectively destroys tumor tissue *via* two pathways: free radical pathway (type I) and singlet oxygen pathway (type II) [Ochsner M, 1997]. Both of these pathways can lead to lipid peroxidation. Lipid peroxidation has been reported as an early oxidative event involved in PDT cytotoxicity [Buettner GR, 1993; Kelley EE, 1997].

Elevated temperature can increase the generation of ROS *via* metabolic reactions in cells and tissues. The reactivity of these ROS is also increased with temperature [Hall D, 2000]. Therefore, hyperthermia treatment (HT) could result in an imbalance between prooxidants and antioxidants, which could lead to an increase in oxidant-induced damage to cellular proteins, lipids, and nucleic acids.

Success of the above treatments in the clinic has led to further interest in understanding their underlying mechanisms. Oxidative stress is one of the important mechanisms involved in the pathway leading to tumor destruction. The balance between oxidants and antioxidants is an important determinant for potential oxidative damage. Manipulation of the oxidant pressure in cells would be a way to increase tumor tissue cytotoxicity or to provide normal tissue protection.

Cellular Antioxidant System

Eukaryotic cells have developed a network of antioxidants as a defense against potential oxidative damage from the environment [Fridovich I, 1978] (**Scheme I-2**). Mammalian cells can induce the production of antioxidants in response to oxidant stress [Shull S, 1991; Alvares S, 1993; Vile GF, 1993]. The cellular antioxidant system contains small antioxidant molecules as well as antioxidant enzymes. The former

includes exogenous and endogenous antioxidant molecules, such as tocopherol, ascorbate, β-carotene, uric acid, and glutathione (GSH).

The enzymatic defense system involves primary and secondary protection against lipid peroxidation and other oxidative stresses [Fridovich I, 1978]. Primary defenses rely on the direct scavenging and inactivation of the reactive oxygen species (ROS) before lipid peroxidation takes place, while secondary defenses involve excision and repair of the damage. Enzymes involved in primary protection are: *1)* manganese-superoxide dismutase (MnSOD), and copper/zinc superoxide dismutase (CuZnSOD), which convert superoxide ($O_2^{\bullet -}$) to hydrogen peroxide (H_2O_2); *2)* catalase (CAT), which scavenges H_2O_2 at relatively high concentrations; and *3)* cytosolic glutathione peroxidase (GPx1), which scavenges H_2O_2 at relatively low concentrations. Enzymes involved in secondary protection include non-seleno glutathione S-transferase (GST), and seleno-dependent glutathione peroxidases (GPxs), which detoxify fatty acid hydroperoxides, phospholipid hydroperoxides, and cholesterol hydroperoxides. The glutathione peroxidase family is comprised of four members: *1)* cytosolic glutathione peroxidase (GPx1), which is ubiquitously distributed in cytosol [Mills GC, 1957]; *2)* gastrointestinal glutathione peroxidase (GPx2), which is exclusively expressed in the gastrointestinal tract [Chu FF, 1993]; *3)* plasma glutathione peroxidase (GPx3) [Takahashi K, 1987], which is directed to extracellular compartments and expressed in various tissues that are in contact with body fluids; and *4)* phospholipid hydroperoxide glutathione peroxidase (PhGPx or GPx4), which is both a cytosol and membrane-bound protein [Ursini F, 1982]. Among them, PhGPx is a unique enzyme in that it can directly reduce phospholipid- and cholesterol-hydroperoxides present in membranes [Ursini F, 1985; Thomas JP, 1990]. GPx1 can reduce LOOHs only after the peroxidized fatty acids are clipped off by phospholipase A_2 (PLA_2). Moreover, the reduction rate of phospholipid hydroperoxides

through PhGPx is estimated to be about four-orders magnitude higher than that through GPx1 and PLA_2 [Antunes F, 1995].

Phospholipid Hydroperoxide Glutathione Peroxidase

Phospholipid hydroperoxide glutathione peroxidase (PhGPx) was first described in 1982 [Ursini F, 1982] and later verified as a selenoprotein by sequencing [Schuckelt R, 1991]. It is a monomeric enzyme that contains one selenium atom at the active site as selenocysteine. PhGPx can directly reduce phospholipid- and cholesterol-hydroperoxides to corresponding alcohols at the expense of glutathione (GSH) [Ursini F, 1982; Thomas JP, 1990] (**Scheme I-3**). It has been suggested that GPx1 is important in removing cytosolic hydroperoxides, while PhGPx catalyzes the reduction of lipid hydroperoxides (LOOHs) in membranes and lipoproteins [Maiorino M, 1990]. The small size and the hydrophobic surface of PhGPx have been implicated in its ability to react with lipids in membranes. Thus, PhGPx is a crucial enzyme in the protection of cellular membranes against oxidative damage. Overexpression of PhGPx has been demonstrated to protect cells significantly from LOOH-mediated oxidative injury [Imai H, 1996; Yagi K, 1996; Arai M 1999].

The cDNA of PhGPx has been cloned from porcine [Brigelius-Flohe R, 1994], rat [Pushpa-Rekha TR, 1995], and human [Esworthy RS, 1994]. Recently, the gene structure of porcine, rat and human PhGPx has been determined [Kelner MJ, 1998; Knopp EA, 1999]. The human PhGPx gene is located on chromosome 19, spans only 2.8 kilobases and consists of 7 exons [Kelner MJ, 1998]. The sequence of PhGPx is highly conserved across species. The amino acid sequence of rat PhGPx shares 93% and 91% homology with pig and human PhGPx, respectively [Pushpa-Rekha TR, 1995]. The amino acid sequence of rat PhGPx also shares about 40% identity with rat GPx1 [Pushpa-Rekha TR, 1995].

PhGPx is both a cytosolic and membrane-associated enzyme. It is present in cytoplasm and is bound to plasma and nuclear membranes [Roveri A, 1992], as well as in the intermembrane space of mitochondria [Godeas C, 1994]. The sequence analyses of PhGPx cDNA and gene structure provide a structural basis for its subcellular distribution. There are two windows of transcription start sites in the PhGPx gene, which are tissue specific [Pushpa-Rekha TR, 1995]. Multiple transcription start sites generate two populations of PhGPx transcripts. The predominant full-length transcript in testis directs the synthesis of a 197-amino acid protein (L-PhGPx) containing a potential mitochondrial targeting signal, 27-amino acid, at the N-terminus. The 27-amino acid is highly conserved and directs the protein into mitochondria [Pushpa-Rekha TR, 1995]. L-PhGPx is localized in the intermembrane space of the mitochondria [Godeas C, 1994; Arai M, 1996]; higher activity is found in the contact sites of inner- and outer-membranes [Godeas C, 1994]. It has also been found to bind to the chromatin in rat testis nuclei [Godeas C, 1996]. Somatic tissues primarily express shorter transcripts that encode a 170-amino acid protein (S-PhGPx), which represents the cytosolic and membrane-associated form [Pushpa-Rekha TR, 1995].

PhGPx is unique compared to the other seleno-dependent glutathione peroxidases, in that it is not just an enzyme responsible simply for the defense against oxidative stress. By repairing LOOHs in membranes, PhGPx is able to serve as an off-switch for signaling mechanisms of biological events mediated by lipid hydroperoxides (LOOHs) [Ursini F, 1995]. PhGPx may also contribute to redox regulation through the oxidation of its selenium moiety and its reaction with glutathione or susceptible thiols of proteins [Maiorino M, 1998]. It has been found that PhGPx can abrogate interleukin 1-dependent NFκB activation [Brigelius-Flohe R, 1997] and silence lipoxygenases by regulating hydroperoxide concentration [Schnurr K, 1996; Huang HS, 1999]. PhGPx exhibits the

highest activity in testis [Imai H, 1995; Knopp EA, 1999]. This activity is strongly related to spermatid differentiation; its level decreases in well differentiated cells [Godeas C, 1997; Maiorino M, 1998]. Recently, a novel function of PhGPx has been found during sperm maturation [Ursini F, 1999]. PhGPx exists as a soluble peroxidase in spermatids but persists in mature spermatozoa as an enzymatically inactive, oxidatively cross-linked, insoluble protein. The selenol group of PhGPx is oxidized by hydroperoxides, which then reacts with protein thiols as alternate substrates to create protein aggregates that are cross-linked by selenadisulfide or disulfide bonds. These aggregates shield the helix of mitochondrial DNA from oxidative damage. PhGPx serves as a structural protein in the mature spermatozoa.

Cellular Glutathione System

Glutathione, L-γ-glutamyl-cysteinyl glycine tripeptide, is found in most plants, micro-organisms, and all mammalian tissues. It is the dominant nonprotein thiol in mammalian cells at concentrations of 1 – 11 mM [Smith CV, 1996]. In eukaryotic cells, 90% of the glutathione (GSH) is present in the cytosol, 10% in the mitochondria, and a small percentage in the endoplasmic reticulum [Hwang C, 1992; Meredith MJ, 1982; Meister A, 1988]. Total cellular glutathione is referred to as the sum of GSH plus glutathione disulfide (GSSG). Glutathione is essential in maintaining the intracellular redox balance [Meister A, 1988]. It plays a pivotal role in cellular detoxification of harmful oxidative species and various xenobiotics [Meister A, 1983]. GSH also serves as an important substrate in the removal of hydroperoxides by glutathione peroxidases. The intracellular H_2O_2 and LOOHs produced from oxidation are reduced to water and alcohols by GSH in the presence of the selenium-dependent enzymes, GPx1 and PhGPx. As a result, GSH is oxidized to GSSG, which in turn is reduced back to GSH by

glutathione reductase (GR) in the presence of NADPH, forming a redox cycle [Lopez-Barea J, 1990] (**Scheme I-2**).

Maintenance of a homeostatic GSH content is achieved by both *de novo* synthesis and salvage synthesis, and a number of interrelated pathways are involved. Most cell types do not import GSH [Meister A, 1994]. The synthesis of GSH occurs primarily in the cytoplasmic compartment. The rate of synthesis is determined by the availability of cysteine and the activity of the rate-limiting enzyme, γ-glutamylcysteine synthetase (GCS) [Griffith OW, 1999; Lu SC, 1999]. The level of GSH is a major contributing factor to selenium-dependent GSH peroxidase function. Low levels of GSH can limit the capability of GPx1 for removing H_2O_2 [Li S, 2000]. The protective effects of PhGPx are also influenced by the intracellular GSH level. Low levels of GSH inhibit the enzymatic function of PhGPx [Nomura K, 1999; Wang HP, 2000]. GSH has been found to be elevated in a number of tumor cells that are resistant to cancer therapy [Mulcahy RT, 1994]. This resistance might result from the interactions of GSH with therapeutic drugs and with ROS. It could also result from the participation of GSH in the reactions with GSH-dependent peroxidases.

Significance

The main goal of cancer therapy is to destroy tumor tissue and yet not cause damage to normal tissue. Most non-surgical therapeutic strategies are often limited due to the severe side effects on surrounding or even remote normal tissues. Resistance to some radiotherapy, chemotherapies, hyperthermia, and photodynamic therapy is also an important contributing factor that can cause failure of non-surgical therapy [Suzuki Y, 2000; Taber SW, 1998]. Since oxidative stress is a critical mechanism for both PDT and HT, cellular antioxidant levels could play a role on the efficacy of these treatments.

Research on free radicals and antioxidants could therefore provide the possibility to examine oxidant levels and to manipulate antioxidant levels in cells.

This thesis project explores the mechanism of PDT- and HT-induced cytotoxicity. Specifically, this project examines the production of lipid hydroperoxides (LOOHs) and the potential radical reactions from PDT. Mitochondrial function after HT is also examined. More importantly, this work establishes a cell model system (MCF-7 cell) that overexpresses L-PhGPx. MCF-7 cell is a human breast carcinoma cell line widely used as a cell model system in research. Its antioxidant profile is well characterized [Yan T, 1998; Maiorino M, 1991]. Successful transfection of MnSOD has been achieved in this cell line [Zhang J, 1998]. Overexpression of L-PhGPx in this cell line will help us to understand the role of L-PhGPx in response to certain anticancer treatments such as PDT and HT. In this project, the potential role of L-PhGPx in LOOH-mediated oxidative damage has been examined. The impact of cellular GSH on the protective effect of L-PhGPx has also been investigated.

The knowledge gained from this research is of importance in that the efficacy of cancer treatments may be enhanced. It may be possible to better sensitize tumor tissue or protect normal tissue by modulating the intracellular antioxidant levels. The findings from this research also will have wide implications to other disease treatments that have an oxidative component in their action.

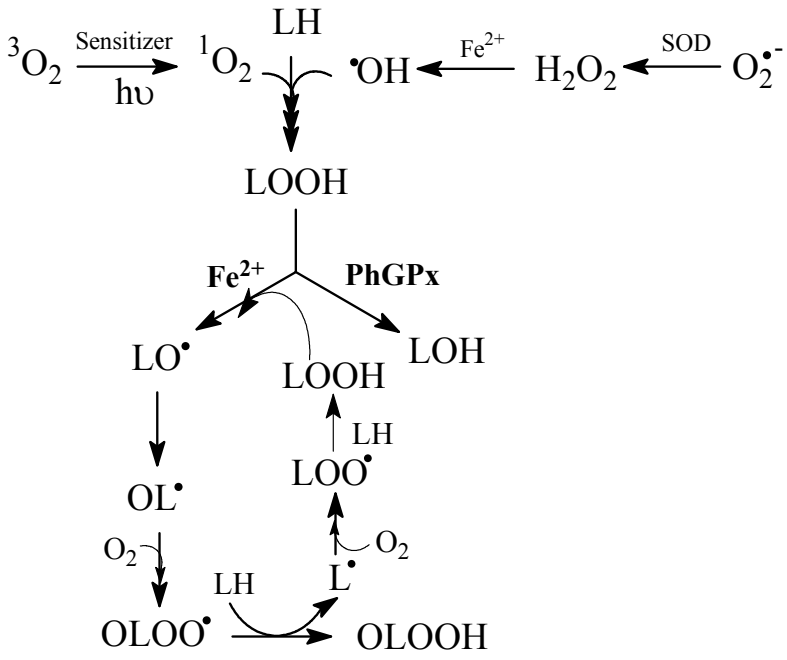

Scheme I-1. The proposed mechanism of lipid peroxidation induced by $^1O_2$ and free radicals.

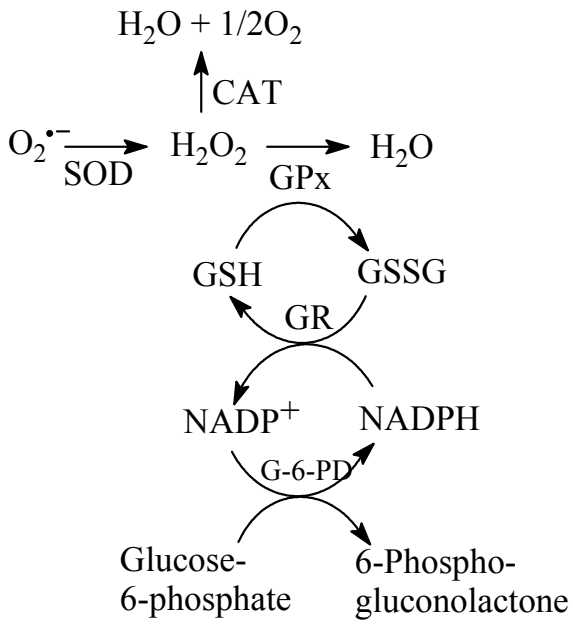

Scheme I-2. The primary intracellular antioxidant enzyme system.

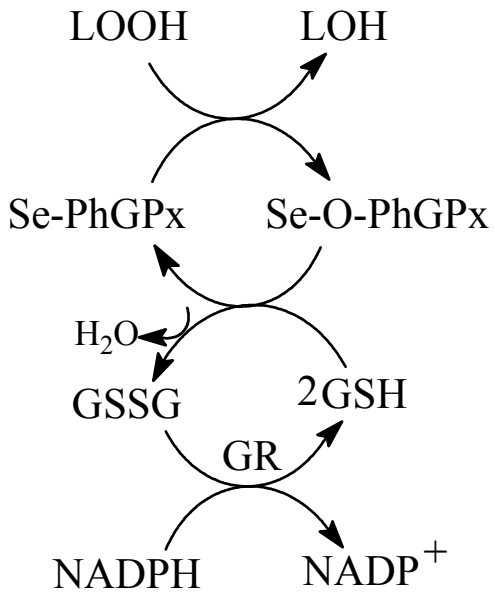

Scheme I-3. The mechanism of PhGPx in detoxifying LOOHs.

CHAPTER II

OVEREXPRESSION OF L-PhGPx IN MCF-7 CELLS

Introduction

The human PhGPx gene is located on the short arm of chromosome 19 [Kelner MJ, 1998]. It is a single copy gene, encoding both cytosolic (S-PhGPx) and mitochondrial (L-PhGPx) forms of the protein. L-PhGPx (~23 kDa) contains 27 amino acids at the N-terminus that serve as a mitochondrial targeting signal. This leader sequence directs the protein to the intermembrane space of the mitochondria, where it is cleaved by a membrane-associated peptidase, yielding a mature protein the same size as cytosolic PhGPx [Pushpa-Rekha TR, 1995]. L-PhGPx is particularly abundant in testis tissue, while S-PhGPx is predominantly present in most somatic tissues. PhGPx is a unique selenoprotein that reduces membrane-bound lipid hydroperoxides (LOOHs) [Ursini F, 1985; Thomas JP, 1990].

PhGPx plays an important role in the regulation of cellular hydroperoxides [Weitzel F, 1993; Schnurr K, 1996; Imai H, 1998]. Lipid hydroperoxides (LOOHs) have, in the past, been considered as toxic compounds. But recent data suggest that they are also signaling molecules. LOOHs have been implicated in a variety of physiological and pathophysiological processes such as aging, cell differentiation, carcinogenesis, inflammation, hypoxia, and atherogenesis [Steinbeck MJ, 1998; Bindoli A, 1988; Shigenaga MK, 1994; Gutteridge JM, 1993]. LOOHs are also involved in NF-κB activation [Kretz-Remy C, 1996; Brigelius-Flohe R, 1997] and play a role in triggering apoptotic cell death [Sandstrom PA, 1994; Nomura K, 1999]. Removal of all LOOHs is

not necessarily advantageous to cells. Rather, the maintenance of a certain peroxide tone, that is the steady-state level of LOOHs, is important for appropriate functioning of cells.

It is of interest to compare the relative abundance of PhGPx and GPx1, because they contribute to the reduction of cellular hydroperoxides. It has been found that the ratio of PhGPx/GPx1 is highest in testis tissue, and very low in other normal tissues, such as liver, kidney, spleen, lung, skeletal muscle, heart, and brain [Imai H, 1995]. However, the ratio of PhGPx/GPx1 is relatively high in tumor tissues derived from liver, kidney, and mammary cells [Imai H, 1995]. This suggests that PhGPx might be related to transformation, immortalization, and growth of cells.

A good cell model system is necessary to better understand the potential biological functions of PhGPx. In this research, a stably transfected cell model with overexpression of L-PhGPx was established. The human mitochondrial PhGPx sense cDNA was stably transfected into MCF-7 cells. MCF-7 cells are a human breast carcinoma cell line widely used in research. The antioxidant profiles are well characterized [Yan T, 1998; Maiorino M, 1991]. Successful transfection of MnSOD has been achieved in this cell line [Zhang J, 1998]. Overexpression of L-PhGPx in MCF-7 cells would provide information on how this enzyme is involved in the cellular response to PDT and HT, which might account for the resistance of MCF-7 cells to cancer therapies. In this part of study, the expression of L-PhGPx was evaluated; its impact on cell growth, cellular antioxidant profiles, and the GSH cycle were examined.

Materials and Methods

Reagents

The primary polyclonal antibody against rat PhGPx was a generous gift from Dr. Albert W. Girotti (Medical College of Wisconsin, Milwaukee, WI). The primary polyclonal

antibodies against MnSOD, CuZnSOD, and GPx1 were developed in Dr. L.W. Oberley's laboratory [Oberley LW, 1989]. The catalase (CAT) primary antibody was obtained from Calbiochem-Novabiochem Corp. (San Diego, CA). Horseradish peroxidase conjugated to goat anti-rabbit IgG, Blocking Reagent®, anti-digoxigenin-AP® and CDPD® were purchased from Boehringer Mannheim (Indianapolis, IN). L-α-phosphatidyl-choline type III/S, lipoxidase type IV, sodium deoxycholate, glutathione (GSH), glutathione reductase (GR), NADPH, Triton X-100 (peroxide-free), sodium azide, sodium selenite, 5-sulfosalylic acid (SSA), 5, 5'-dithio-*bis*-(2-nitrobenzoic acid) (DTNB), dichlorophenol-indophenol, and 3(4,5-dimethythiazolyl-2)-2,5-diphenyl tetrazolium acid were purchased from Sigma (St Louis, MO). LipofectAMINE™, minimum essential medium (MEM), fetal bovine serum (FBS), Geneticin™ (G418), and Tris-HCl were purchased from GIBCO (Grand Island, NY). The pcDNA3.1(-) plasmid was obtained from Invitrogen (Carlsbad, CA). Methanol (HPLC grade), chloroform (HPLC grade), acetic acid, crystal violet, acetic acid, and disodium ethylenediamine tetraacetate (EDTA) were purchased from Fisher Scientific Co. (Pittsburgh PA). 2-Vinylpyridine (2-VP) was obtained from Aldrich (Milwaukee, WI). Sep-Pak Plus C_{18} cartridge (Part No. WAT 020515) was from Waters Co. (Milford, MA).

Cell Culture

MCF-7 cells, from American Type Culture Collection (ATCC), were cultured routinely in MEM containing 10% FBS, 1% non-essential amino acids, and 30 nM sodium selenite. After stable transfection, the selected clones were grown in the above medium with selection antibiotic G418 (350 μg/mL). The antibiotic was removed one cell passage before an experiment. Cells were incubated at 37°C in a humidified atmosphere with 5% CO_2. Cell medium was changed every 3 – 4 days. Cells were changed to fresh medium 24 h before harvesting for the experiments.

Construction of L-PhGPx Expression Vector

The pBluescript plasmid containing the human mitochondrial form of PhGPx (L-PhGPx) cDNA was kindly provided by Dr. Rugao Liu (Howard Hughes Institute, Roseville, MN). The cDNA, an 800-base pair fragment, was prepared by RT-PCR and inserted between EcoRI and HindIII restriction enzymes. It was then ligated into the pcDNA3.1(-) mammalian expression vector between the EcoRI and HindIII with a 5′ to 3′ orientation. The cDNA insert was sequenced bidirectionally from the T7 priming site and the BGH (bovine growth hormone) reverse priming site, using the Sanger-based dideoxy sequencing strategy. The sequence was compared to the PhGPx cDNA from the gene bank (GenBank/EMBL accession No. X71973).

Transfection of L-PhGPx into MCF-7 Cells

Cells (1×10^5) were seeded into 6-well plates 24 h before transfection. The expression vector pcDNA3.1(-) only and the plasmid containing human PhGPx cDNA were transfected into MCF-7 cells using LipofectAMINE reagent according to the instructions provided by the manufacturer (LifeTech Inc., NY). The PhGPx-containing plasmid (5 μg) and LipofectAmine reagent (10 μL) were mixed and incubated at room temperature for 45 min to allow the formation of DNA-lipid complexes. The same preparation was used for the vector-only control solution. Cells were incubated with these complexes in serum free medium for 5 h at 37°C and 5% CO_2. Following this incubation, 1 mL of growth medium containing twice the normal concentration of serum was added to the cells without removing the transfection mixture. Cells were provided with fresh, complete growth medium 24 h after transfection. At 72 h after transfection, cells were subcultured into G418 (1 mg/mL) selective medium with 1:10, 1:100, 1:1000 dilutions, and incubated for 15 days. Resistant colonies were selected and grown in MEM

containing 10% FBS, 1% non-essential amino acids, 30 nM sodium selenite, and G418 (350 μg/mL).

Northern Blot for PhGPx

Total cellular RNA was isolated from transfected and nontransfected cells using Qiagen RNeasy Kit [QIAGEN Inc., Valencia, CA] and quantified by UV spectrophotometer at 260 nm. Ten μg of total cellular RNA were denatured in a formaldehyde (4%)-formamide (40%) solution at 65°C for 5 min and immediately cooled on ice for 5 min. The RNA was size-fractionated on a 1.5% denaturing formaldehyde agarose gel and transferred to a nylon membrane [Boehringer Mannheim, Indianapolis, IN]. The membrane was prehybridized in the standard hybridization buffer (5x saline/sodium citrate (SSC), 0.1% N-lauroylsarcosine, 0.2% SDS, 1% blocking reagent) for 4 h and then hybridized in the same buffer with digoxigenin-11-dUTP labeled L-PhGPx cDNA probe. The probe was prepared by the random primed method based on the standard protocol provided by the manufacturer [Boehringer Mannheim, Indianapolis, IN], at 68°C. After hybridization, the membrane was washed twice with washing buffer (0.3% Tween 20, 0.1 M maleic acid, 0.15 M NaCl, pH 7.5) at room temperature and then washed twice at 68°C. The hybridized bands were detected by incubation of the membrane with anti-digoxigenin-alkaline phosphatase (1:10,000) for 30 min at room temperature. The subsequent dephosphorylation of the chemiluminescent substrate lumigen PPD [4-(methoxy-4-(3-phosphatephenyl) spirol (1,2-dioxentane-3,2'-adamantane)] resulted in light emission. The membrane was then exposed to X-ray film (Kodak) at room temperature.

Cell Homogenization

The cell homogenization process was performed on ice to prevent denaturation of the antioxidant enzymes. Eighty percent confluent cells on a 100-mm culture dish were washed twice with phosphate-buffered saline (PBS, pH 7.8). Cells were harvested using a scraper. Cells were then centrifuged at 1000 g for 5 min at 4°C, and the supernatant was removed. The cell pellet was resuspended in 0.05 M phosphate buffer (PB, pH 7.8) and sonicated, four bursts of 30 s, using a Vibra Cell Sonicator (Sonics & Materials, Danbury, CN) with a cup horn at full power. The concentration of total cellular proteins was determined with the Bio-Rad Protein assay kit (Bio-Rad Laboratories, Hercules, CA)] using IgG as standard. The homogenate was used for western analyses and activity assays.

Western Blot for PhGPx

Cells were grown to 80% confluency in 100-mm dishes, washed twice with phosphate-buffered saline (PBS, pH 7.8), and harvested by scraping. The cell pellet was sonicated and protein concentration was determined. Total denatured protein (200 μg) was separated on a 12.5% SDS-PAGE and electrotransferred onto a nitrocellulose membrane (Schleicher and Schuell, Keene, NH). The membrane was blocked in 10% non-fat milk for 1 h at room temperature, followed by incubation with rabbit anti-rat PhGPx polyclonal antibody (1:100) overnight at 4°C. After washing three times with TTBS (0.02 M Tris-HCl buffer pH 7.5, 0.137 M NaCl, and 0.1% Tween 20), the membrane was incubated with horseradish peroxidase conjugated to goat anti-rabbit IgG (1:5000). Detection by the chemiluminescence reaction was carried out using the enhanced chemiluminescence (ECL) kit (Amersham Pharmacia Biotech, Piscataway, NJ), followed by exposure to Kodak X-ray film.

Densitometry Measurement

The bands from western blotting were quantified with densitometry analysis using a computerized digital imaging system, AlphaImager™ 2000 software (Alpha Innotech, San Leandro, CA). The intensity of each band was obtained by integrating the pixel values after subtracting the background.

Phosphatidylcholine Hydroperoxide Preparation

The assay for the activity of PhGPx is similar to that of GPx1 except that the PhGPx assay uses a substrate specific for PhGPx, *e.g.* phosphatidylcholine hydroperoxide (PCOOH). The preparation of PCOOH is critical for the activity assay. The substrate was prepared by enzymatic hydroperoxidation of phosphatidylcholine using soybean lipoxidase type IV [Roveri A, 1994]. A mixture of 22 mL of 0.2 M Tris-HCl pH 8.8, containing 3 mM sodium deoxycholate and 0.3 mM phosphatidylcholine was incubated at room temperature under continuous stirring. The reaction was started by adding 0.7 mg of soybean lipoxidase type IV to the mixture with stirring for 30 min. The mixture was then loaded on a Sep-Pak Plus C_{18} cartridge that was equilibrated with 4 mL methanol followed by 40 mL of water. The mixture was applied to the cartridge and washed with 220 mL water. PCOOH was then eluted with 2 mL methanol. After dilution in methanol (100 times) the substrate was quantitated spectrophotometrically at 234 nm using an extinction coefficient of 25,000 $M^{-1}cm^{-1}$ [Chan H W-S, 1984]. The final concentration of PCOOH in methanol was about 2 mM. The methanolic solution of PCOOH is stable for months at –20°C. Because this assay is not specific for PCOOH, as other oxidized lipid products can result in conjugated diene formation, we used one batch for all experiments insuring that the concentration of PCOOH was always the same.

PhGPx Activity Assay

Because measurement of PhGPx activity is an essential step in this work, I established the PhGPx activity assay in our laboratory [Wang HP, 2000]. The activity was measured by coupled enzymatic assay with some modification [Roveri A, 1994], using GSH, GR, PCOOH, and NADPH. The spectrophotometric test mixture contained, in 1 mL, the following: 0.1 M Tris-HCl (pH 8.0), 2 mM EDTA, 1.5 mM NaN_3, 0.1% Triton X-100 (peroxide free), 3 mM GSH, and 1.5 U/mL GR. Sample (1 mg) was added to the test mixture, and incubated at 37°C for 8 min. Then 0.2 mM NADPH was added and incubated for 8 min to allow PhGPx and GSH to be converted to reduced forms. The nonspecific NADPH oxidation rate was recorded for 4 min at 340 nm, and then the enzyme reaction was started with the addition of PCOOH (10-30 mM). The rate of NADPH oxidation was recorded every 20 s for 4 min at 340 nm using a Beckman DU-70 spectrophotometer. The activity was calculated by subtracting the nonspecific NADPH oxidation rate from the observed NADPH oxidation rate after substrate addition. The specific activity of PhGPx is expressed as units per milligram protein (U / mg protein), 1 unit being the amount of enzyme catalyzing the oxidation of 1 μM of NADPH per minute.

RT-PCR for PhGPx

Total cellular RNA was isolated from transfected and nontransfected cells using Qiagen RNeasy Kit [QIAGEN Inc., Valencia, CA] and quantified by UV spectrophotometer at 260 nm. Five μg of total RNA were converted into cDNA by priming in a reaction solution containing 2 μL oligo (dT) primer (20 μM), 2 μL of dNTP mixture (10 mM each of dATP, dGTP, dCTP, dTTP), 2 μL of dithiothreiol (DTT) (100 mM), 1 μL of RNase inhibitor (RNasin) (40 units/μL), 2 μL of Moloney-Murine Leukemia Virus (MMLV) reverse transcriptase (200 units/μL), 8 μL of 5× first strand

buffer (50 mM Tris-HCl, pH 8.3, 3 mM $MgCl_2$, 75 mM KCl). The mixture was incubated to synthesize cDNA for 1 h at 42°C, and then to inactivate the enzyme at 70°C for 15 min. The synthesized cDNA was diluted to 100 μL with PCR water and stored at –20°C.

PCR primers were designed based on the human PhGPx cDNA sequence [Esworthy RS, 1994]. The sequences of oligonucleotide primers were as follows: L-PhGPx sense, 5'-CTTTGCCGCCTACTGAAG-3'; S-PhGPx sense, 5'-TCCATGCACGAGTTTCC-3'; antisense, 5'-GATCCGCAAACCACACTC-3'. The PCR products of L-PhGPx and S-PhGPx were 275 bp long and 174 bp long, respectively. PCR was carried out in a 50 μL mixture containing 5 μL 10× PCR buffer, 1 μL 10 mM dNTP, 1 μL Tag DNA polymerase (5 units/μL), 5 μL of cDNA, 1 μL of sense and antisense primer mixture (20 μM each), 1 μL of antisense primer, and 37 μL PCR water. PCR was conducted in a thermal cycler (Perkin Elmer GeneAmp PCR System 2400). After 3 min denaturation at 94°C, the amplification was carried out with 30 cycles. The thermal cycling profile consists of denaturation at 94°C for 1 min, annealing at 55°C for 1 min, and extension at 72°C for 1:30 min, followed by a final extension at 72°C for 7 min. The PCR products (30 μL) were resolved in a 1.5% agarose gel with ethidium bromide staining. Positive controls: pure L-PhGPx cDNA was amplified in PCR mixture; negative controls: the PCR mixture was amplified without template cDNA.

Glutathione Measurement

The GSH/GSSG assay was adapted from Anderson [Anderson ME, 1985] with minor modification. The total intracellular GSH was determined by the colorimetric reaction of DTNB (5,5'-dithio-*bis*(2-nitrobenzoic acid)) with GSH to form TNB (5-thio-2-nitrobenzoic acid). The rate of TNB formation, which is proportional to the total GSH concentration, was measured spectrophotometrically at 412 nm. Cellular GSSG is

reduced to GSH by GR, using NADPH as co-factor. The assay started with lysing the cell pellet in 5% SSA. The total GSH was measured by mixing 50 μL sample with 100 μL water, 700 μL working buffer [2 mM NADPH in stock solution (0.143 M sodium phosphate, 6.3 mM EDTA)], and 100 μL DTNB (6 mM DTNB stock solution). The assay was initiated by addition of 50 μL GR solution (266 U/mL). The rate of TNB formation was followed at 412 nm, every 20 seconds for 3 min using a Beckman DU-70 spectrophotometer. Total GSH of a sample was calculated from a standard curve of GSH concentration as a function of the rate (change in absorbance/time). The cellular GSSG level was determined by the same DTNB assay after the reduced GSH was masked by 2-VP. 2-VP (3 μL) was added to 100 μL of sample prepared as above for total GSH measurement. After 2 h incubation at 4°C, GSSG was measured as described in the DTNB assay. The reduced GSH was determined by subtracting the GSSG content from the total GSH content. The GSSG levels in the cell line we studied were below the detection limit of this assay.

Cell Growth Curve

The growth rates of various clones were determined by counting the number of cells as a function of time. Cells were seeded in 24-well plates at 2×10^4 cells per well containing 1 mL medium. Three parallel wells for each clone were plated for each time point. Cells were counted 24 h after seeding and then counted every 48 h for 13 days using a hemocytometer. Doubling time (Td) was calculated from the logarithmic phase on the growth curve using the following formula:

$$Td = 0.693t/\ln(N_t/N_0)$$

where t is the time in days, N_t is the cell number at time t, N_0 is the cell number at initial time.

Plating Efficiency

A single cell suspension was plated in 60-mm dishes. The cell number plated was calculated to yield about 100 colonies per dish. The cells were kept in culture medium and incubated at 37°C for 14 days to allow colony formation. Cells were fixed with methanol:acetic acid (3:1, *v/v*) and stained with 0.1% crystal violet. Colonies containing 50 cells or more were counted. The plating efficiency (PE) was calculated as:

$$PE = (\text{Colonies formed} / \text{Cells seeded}) \times 100\%$$

Lipid Hydroperoxide Assay

The steady-state level of cellular LOOHs was determined using the Lipid Hydroperoxide Kit. Briefly, cells were seeded into 100-mm dishes until 80% confluence. Cells were washed with metal-free PBS (pH 7.8), and sonicated in metal-free phosphate buffer (pH 7.8). The lipids were then extracted with 1.5 mL deoxygenated chloroform:methanol (2:1, *v/v*) mixture. Ferrous iron was added to the chloroform layer and the formation of ferric thiocyanate was measured at 500 nm on a Beckman DU-70 spectrophotometer. 13-Hydroperoxyloctadecadienoic acid (13-HpODE) was used as the standard. The amount of LOOHs was normalized by total cellular protein.

Western Analysis for MnSOD, CuZnSOD, CAT

The western analysis described above for PhGPx was used for the examination of the protein levels of MnSOD, CuZnSOD, and CAT in the cells after PhGPx transfection. Briefly, cell homogenate (30 μg) was electrophoresed in a 12.5% SDS-polyacrylamide running gel with a 5% stacking gel. After that, the proteins were transferred to nitrocellulose membranes (Schleicher & Schell, Keene, NH), and the membranes were blocked in 10% non-fat milk with TTBS (0.02 M Tris buffer pH 7.5, 0.137 M NaCl, and 0.1% Tween 20) for 1 h at room temperature. The membranes were probed with specific

antibodies, MnSOD (1:1,000 dilution), CuZnSOD (1:250 dilution), and CAT (1:1,000 dilution) overnight at 4°C. After that membranes were incubated with horseradish peroxidase conjugated with goat-anti-rabbit IgG (1:10,000) for 1 h at room temperature. The membranes were exposed to X-ray film using an enhanced chemiluminescence (ECL) kit (Amersham Pharmacia Biotech, Piscataway, NJ).

In Gel Activity Assay for MnSOD and CuZnSOD

Native activity gel assay [Beauchamp C, 1971] was used as an alternative to examine the activity of SOD enzymes in the cells with PhGPx transfection. Cells were harvested by scraping from 60-mm dishes. The cell pellet was homogenized and the protein was quantified. Total cellular protein of 200 μg was separated in a 12% native polyacrylamide gel with 5% stacking gel that had been run in pre-electrophoresis buffer (Tris 22.76 g/L, disodium EDTA 0.38 g/L, pH 8.8). The protein was electrophoresed in pre-electrophoresis buffer for 3 h at 4°C, followed by 4 h in electrophoresis buffer (Tris 6.06 g/L, glycine 22.5 g/L, disodium EDTA 0.68 g/L, pH 8.3) at 4°C. The gel was stained with 2.34 mM NBT, 28 μM riboflavin, and 28 mM TEMED for 20 min in the dark. After that, the gel was washed in ddH_2O and then exposed to a bright fluorescent light. The achromatic bands indicated the presence of the corresponding SOD activities.

In Gel Activity Assay for Catalase

A native activity gel assay was used to measure the activity of CAT in these cells. The cell pellet was homogenized and the protein was quantified. Total cellular protein (30 μg) was separated in a 12% native polyacrylamide gel with a 5% stacking gel which had been run in pre-electrophoresis buffer (Tris 22.76 g/L, disodium EDTA 0.38 g/L, pH 8.8). The protein was electrophoresed in pre-electrophoresis buffer for 3 h at 4°C, followed by 4 h in electrophoresis buffer (Tris 6.06 g/L, glycine 22.5 g/L, disodium

EDTA 0.68 g/L, pH 8.3) at 4°C. After incubation with 0.003% H_2O_2 for 10 min, the gel was stained with 2% ferric chloride and 2% potassium ferricyanide. The achromatic bands that appeared on the gel represented the presence of CAT activity.

Native Immunoblotting Analysis for GPx1

The protein level of GPx1 was examined using a native immunoblotting method [Li S, 2000]. The 12% native polyacrylamide gel with a 5% stacking gel was electrophoresed in pre-electrophoresis buffer (Tris 22.76 g/L, disodium EDTA 0.38 g/L, pH 8.8) at 4°C for 1 h. Total cellular protein (700 μg) was then loaded onto the gel and run in the pre-electrophoresis buffer for 3 h at 4°C, followed by 4 h in electrophoresis buffer (Tris 6.06 g/L, glycine 22.5 g/L, disodium EDTA 0.68 g/L, pH 8.3) at 4°C. The native protein was transferred to a nitrocellulose membrane, and probed with GPx1 primary antibody to human GPx1 (1:300 dilution) overnight at 4°C. After that the membrane was incubated with horseradish peroxidase conjugated with goat-anti-rabbit IgG (1:10,000) for 1 h at room temperature. The membranes were exposed to X-ray film using an enhanced chemiluminescence (ECL) kit (Amersham).

In Gel Activity Assay for Glutathione Reductase

A native activity gel assay was used to measure the activity of GR in the cells with PhGPx transfection. Cells were homogenized and the protein concentration was determined. Total cellular protein (500 μg) was separated on a 12% native polyacrylamide gel with a 5% stacking gel that had been run in pre-electrophoresis buffer (Tris 22.76 g/L, disodium EDTA 0.38 g/L, pH 8.8). The protein was electrophoresed in pre-electrophoresis buffer for 3 h at 4°C, followed by 4 h in electrophoresis buffer (Tris 6.06 g/L, glycine 22.5 g/L, disodium EDTA 0.68 g/L, pH 8.3) at 4°C. The gel was placed in a freshly made dye solution (3.4 mM GSSG, 0.36 mM NADPH, 0.052 mM

dichlorophenol-indophenol, 1.1 mM 3(4,5-dimethythiazolyl-2)-2,5-diphenyl tetrazolium acid prepared in 250 mM Tris, pH 8.0). The GR activity was indicated by the presence of a purple precipitate in the gel.

Statistics

Mean values, standard errors, and the linear regression were determined using Microsoft Excel program (Excel 97 SR-1). ANOVA-Tukey test was used to compare the differences between two groups. In all cases, the statistical significance of differences between the two variants was determined at the level of $p < 0.05$. All the data presented were from the average of at least three independent experiments. In the cases of western, northern analyses and RT-PCR, representative results that were repeated at least three times are shown.

Results

Mapping of Human L-PhGPx cDNA Sequence

The human L-PhGPx sense cDNA was prepared and inserted into pBluescript vector using RT-PCR by Dr. Rugao Liu (Howard Hugh Institute). After construction into pcDNA3.1(-) mammalian expression vector, the insert cDNA sequence of L-PhGPx was verified bidirectionally using the Sanger-based dideoxy sequencing strategy. The sequence was compared to the PhGPx cDNA from the gene bank (GenBank/EMBL accession No. X71973). A point mutation was found around 200 bp downstream of the selenocysteine active site, which causes a transition of adenine (A) to guanine (G). This point mutation results in an amino acid change of isoleucine to valine (**Figure II-1**).

Overexpression of L-PhGPx in MCF-7 Cells

To better characterize the role of PhGPx in cancer therapy, we chose MCF-7 cells as a model cell line and stably transfected these cells with L-PhGPx sense cDNA. MCF-7 cells have been widely used in our research laboratories and their antioxidant profile has been well characterized [Yan T, 1998]. The presence of L-PhGPx after transfection was assessed using western and northern blotting analysis. The potential activity of PhGPx was quantified. After screening 20 different clones, the parent cells (Wt), the vector control cells (Neo) and the four clones (P-1, P-2, P-3, P-4) with PhGPx transfection were selected for study. **Figure II-2** shows the immunoreactive protein (panel A), and the steady-state level of mRNA (panel B) in the cells used in this study. Both the Wt and the Neo had detectable levels of PhGPx protein, but mRNA levels were below the limit of detection. It has been reported that PhGPx mRNA remains stable even in the condition of selenium deficiency [Flohe L, 1997]. Thus, the nondetectable level of PhGPx mRNA should not be due to mRNA instability but rather the limited loading amount. P-1 and P-2 cells had low and medium expression of PhGPx, while P-3 and P-4 cells strongly expressed PhGPx at both protein and mRNA levels. Total PhGPx activity increased 3- to 4-fold in P-1 and P-2 cells, and increased 7- to 8-fold in P-3 and P-4 cells, compared to the Wt and Neo controls, **Figure II-3A**. There was a direct linear correlation between PhGPx protein and its activity ($r = 0.99$), **Figure II-3B**. Thus, a cell model system with different levels of PhGPx was established.

L-PhGPx and S-PhGPx

PhGPx is present in two forms: mitochondrial form (L-PhGPx) and nonmitochondrial form (S-PhGPx). The L-PhGPx expresses dominantly in testis tissues, and the S-PhGPx is primarily in somatic tissues. The difference in subcellular distribution results from the unique gene structure of PhGPx. Multiple transcription start

sites generate two populations of PhGPx mRNAs that have different translation start sites [Pushpa-Rekha TR, 1995]. It has been found that there are two translation start sites, AUG^{61} and AUG^{141}, in testis tissues [Pushpa-Rekha TR, 1995]. However, the transcripts in somatic tissues lack the first AUG codon [Pushpa-Rekha TR, 1995]. It should be noted that AUG^{61} is predominantly used as the translation initiation codon in the full-length transcript [Pushpa-Rekha TR, 1995]. To confirm the form of PhGPx transfected into the cells used in this study, we examined the L- and S-forms of PhGPx in MCF-7 cells using RT-PCR (**Figure II-4**). The S-PhGPx was found in all the cells. The L-PhGPx was found only in the PhGPx transfected cells.

This implies that the increased mRNA and protein levels of PhGPx in the transfected cells result primarily from the L-form. Although the transfection of L-PhGPx could result in the increase of S-PhGPx, the effect should be minor. The RT-PCR data provide only qualitative but not quantitative information due to the lack of an internal standard.

Effective PhGPx Activity

The enzymatic activity of the GPx family is dependent on the presence of glutathione (GSH). In fact, the observed K_m for GPx is a function of the concentration of GSH [Flohe L, 1971]; at normal physiological concentrations of GSH, the activity of GPx cannot be saturated [Kosower NS, 1978]. The typical kinetic assays used to determine the activity of the GPx family of enzymes contain high levels of GSH in the incubation. These assays therefore, measure the potential maximum enzyme activity. However, in cells and tissues GSH levels vary. Thus, a more appropriate representation of enzyme activity would be the product of maximum enzyme activity and cellular GSH level. The "effective" GPx1 activity has been shown to correlate with biological variables [Li S, 2000]. In this research study, the effective activity of PhGPx (**Table II-1**) was used as an

independent variable to examine the correlation with various measures of biochemical and biological responses. Better correlation resulted when effective PhGPx activity was used rather than the measured PhGPx activity. Even though L-PhGPx is located in mitochondrial, effective PhGPx activity should be appropriate because PhGPx is located in the intermembrane space and GSH in this subcellular site is freely diffusible through the outer-membrane of mitochondria.

Overexpression of L-PhGPx Inhibited MCF-7 Cell Growth

Excessive generation of ROS can cause cell death, while moderate ROS production may stimulate signal transduction and gene activation [Dypbukt JM, 1994]. Hydroperoxides have been reported to play a role in cell proliferation and differentiation [Steinbeck MJ, 1998; Kuhn H, 1990]. The stage-specific expression pattern of PhGPx in spermatogenesis suggests that LOOHs are involved in the maturation of sperm [Maiorino M, 1998]. We hypothesized that PhGPx may modulate cell growth by regulating cellular hydroperoxide tone. Cell proliferation was examined with growth curves and cell doubling time. The ability of cells to undergo attachment and division was measured with plating efficiency.

Growth curves are a measure of the balance between cell proliferation and cell death. Cells transfected with different levels of L-PhGPx (P-1, P-2, P-3, P-4) exhibited different growth rates compared to controls (Wt and Neo) (**Figure II-5A**). The cell doubling time varied from 49.7 h to 74.5 h in the transfected cells, while Wt and Neo had 43.5 h and 50.5 h (**Figure II-5B**). However, the statistic analysis showed that only the cells with the highest PhGPx activity (P-4 cells) had significantly greater doubling time compared to the Wt control. Interestingly, PhGPx significantly influenced the plating efficiency. Control cell lines (Wt, Neo) had higher plating efficiency, 20.5% and 15.3%,

compared to transfected cells, 4.6% to 9.7% (**Figure II-6A**). The plating efficiency inversely correlated with the effective PhGPx activity (r = -0.86) (**Figure II-6B**).

These results suggest that overexpression of L-PhGPx influences cell growth. It increases cell doubling time, and significantly decreases the plating efficiency.

Overexpression of L-PhGPx Did Not Change the Steady-State Levels of LOOHs in MCF-7 Cells

The oxidized phospholipids produced by spontaneous or pathologic oxidation may affect membrane structure and cell function. The glutathione peroxidases (GPxs) and the non-selenium glutathione S-transferases (GSTs) [Leyland-Jones BR, 1991; Hurst R, 1998] play an important role in reducing hydroperoxides. Detoxification of phospholipid hydroperoxides can be accomplished through the coupled reactions of phospholipase A_2 (PLA_2) and GPx1, or through GST. However, the kinetic rate constants for both PLA_2 [Antunes F, 1995] and GST [Hurst R, 1998] are much lower than that of PhGPx. Recently a new non-selenium GPx has been found, which can reduce phospholipid hydroperoxides at the same rate as PhGPx [Fisher AB, 1999]. The non-selenium GPx has the same order of magnitude of rate constant as PhGPx in reducing phospholipid hydroperoxides. To examine whether transfection of PhGPx changes the steady-state level of LOOHs, we analyzed Neo and P-4 cell lines for lipid hydroperoxides. Cellular LOOH levels were measured without any oxidative stress. A slight decrease in LOOH steady-state level was found in P-4 cells compared to Neo (**Figure II-7**). It appears that PhGPx does not significantly lower the steady-state level of LOOHs; a certain peroxide tone is maintained allowing normal cellular functions.

Overexpression of L-PhGPx Appeared Not to Influence the Antioxidant Enzyme Profiles in MCF-7 Cells

The antioxidant system is important for cells in the defense against endogenous and exogenous oxidative stress. The antioxidant enzymes work coordinately to achieve an equilibrium between prooxidant and antioxidant systems. Tumor cells appear to have an unbalanced antioxidant system. MnSOD and GPx1 in general are lower in tumor cells compared to their normal counterparts [Yan T, 1998]. PhGPx is found at higher levels in tumor cell lines than in the normal tissues [Maiorino M, 1991; Huang HS, 1999]. To test if overexpression of PhGPx influences other antioxidant enzymes, the expression levels of MnSOD, CuZnSOD, CAT, and GPx1 were examined in the PhGPx transfectants.

The protein levels and activities of both MnSOD and CuZnSOD did not change significantly after PhGPx transfection (**Figure II-8**). Stable transfection of L-PhGPx also did not cause alteration of CAT at both the protein and activity levels (**Figure II-9**). The protein level of GPx1 in MCF-7 cells was below the detection limit before and after the transfection (**Figure II-10**).

These observations indicate that overexpression of L-PhGPx does not significantly change the other cellular antioxidant enzyme levels.

Overexpression of L-PhGPx Had a Minor Effect on Cellular GSH Pool

PhGPx is a seleno-dependent glutathione peroxidase. The selenium is incorporated as selenocysteine into the active site of the enzyme by the 3' untranslated region (3'-UTR) [Brigelius-Flohe R, 1994]. The selenocysteine is oxidized by hydroperoxides. The oxidized form of the enzyme can be reduced by reacting with free GSH and possibly with protein thiol groups. Thus, PhGPx might be involved in cellular redox regulation by oxidizing GSH to GSSG.

Transfection of L-PhGPx resulted in a minor change of GSH in MCF-7 cells (**Table II-1**). Total GSH levels in cells with PhGPx transfection were slightly decreased compared to Wt and Neo controls, ranging from 5 to 9 μmol GSH per mg protein. The Neo cells had the highest level of GSH (10 μmol / mg protein) compared to Wt and other transfected cells. However, there were no statistical differences in these variations. The GSSG levels in all the cells examined were below the detection limit. The level of GR after L-PhGPx transfection was also studied and no change in its activity was observed (**Figure II-11**).

In contrast to GPx1 transfection [Li S, 2000], overexpression of L-PhGPx appears not to dramatically influence the cellular GSH system. This difference might be explained by the different location of GPx1 and L-PhGPx inside cells. GPx1 is primarily present in the cytosol, with some detectable in the mitochondria [Esworthy RS, 1997]. L-PhGPx is located in the intermembrane space of the mitochondria [Godeas C, 1994]. The main source of GSH for GPx1 and L-PhGPx differs. GPx1 utilizes dominantly the cytosolic GSH, whereas L-PhGPx uses mitochondrial GSH. Typically, only 10% of all the cellular GSH is found in the mitochondria [Meredith MJ, 1982]. Changes in mitochondrial GSH might not be displayed in terms of total cellular GSH.

Discussion

PhGPx has received extensive interest recently because of its major function in the defense against lipid hydroperoxide-mediated oxidative damage. Oxidative stress is one of the major mechanisms involved in nonsurgical cancer treatments. Lipid hydroperoxides (LOOHs) are an important mediator in oxidative stress. LOOHs have been implicated in many cancer therapies, such as photodynamic therapy. Our research hypothesis was that PhGPx might be the important enzyme involved in cell resistance to cancer therapy. To test this hypothesis, MCF-7 cells were used as a model cell line and

stably transfected with PhGPx (L-PhGPx sense cDNA). The expression of PhGPx in transfected cells and nontransfected control cells was examined. The forms of PhGPx transfected into cells were verified using RT-PCR (**Figure II-4**). Four clones (P-1, P-2, P-3, and P-4) overexpressing L-PhGPx were selected (**Figure II-2**). The enzymatic activity directly correlated with the amount of protein (**Figure II-3**). The antioxidant enzyme profile of MCF-7 cells has been well characterized [Zhang J, 1998; Yan T, 1998]; they have very low levels of MnSOD, and GPx1. We confirmed that MCF-7 cells have PhGPx [Maiorino M, 1991]. Transfection of MnSOD and GPx1 into MCF-7 cells has been successfully carried out previously, and the changes in tumor growth and tumor phenotypic were documented [Zhang J, 1998; Li S, 2000]. Overexpression of MnSOD can significantly inhibit cell growth while double transfection of MnSOD and GPx1 reverses this inhibition of cell growth, suggesting that hydroperoxide levels are critical in governing cell differentiation and proliferation. Overexpression of L-PhGPx has an impact on tumor cell proliferation (**Figures II-5 & II-6**), with a minor change in cell doubling time and significant decrease in plating efficiency. These changes may come from the enzymatic reduction of intracellular LOOHs. Hydroperoxides were found to either stimulate cell proliferation or inhibit cell growth, depending on their concentration [Li S, 2000]. Enzymes that control peroxide tone are therefore critical for cell growth. Although our results found that the average steady-state level of LOOH in a cell ensemble did not change (**Figure II-7**), this should not be interpreted as contradictory. The cells we analyzed were not a synchronized population; different proliferation levels are present in that whole population. PhGPx is a unique enzyme that directly regulates intracellular LOOHs. To reduce LOOHs, PhGPx requires GSH and NADPH, the two major sources of reducing equivalents in cells. During the reduction reaction, GSH and NADPH are oxidized to GSSG and $NADP^+$. PhGPx could therefore cause a change in the redox state

of cells. The oxidation of NADPH, a major product of the pentose pathway, may affect cell glycolysis. All these changes may possibly feedback to affect cell proliferation. Maintenance of a certain hydroperoxide tone could be an important role for PhGPx.

Modulation of PhGPx can be achieved by selenium manipulation [Lin F, 1992]. However, alteration of selenium can also influence the other selenium-dependent enzymes, such as GPx1. Stable transfection of PhGPx does not significantly alter the major cellular antioxidants, including MnSOD, CuZnSOD, CAT, GPx1, GR, and GSH (**Figures II-8 – II-11**). Therefore, this cell model is a good system for study of the specific roles of PhGPx in cells.

Figure II-1. cDNA sequence of L-PhGPx.

The human L-PhGPx cDNA was constructed into pcDNA3.1(-) expression vector. The inserted cDNA sequence of PhGPx was verified bidirectionally from the T7 priming site and the BGH reverse priming site.

* indicates the point mutation, which is a transition from adenine (A) to guanine (G). This point mutation results in an amino acid change of Isoleucine to Valine. Two potential start codons are underlined. The stop codon is italicized. The overlined sequences of the L-form primer, S-form primer, and antisense primer were used in PCR experiments.

CTCGAGCGGCCGCCACTGTGCTGGATATCTGCAGAATTCGATGCCGCGATGA
_____*L-form primer*_____
GCCTCGGCCCGCCTTTGCCGCCTACTGAAGCCGGCGCTGCTCTGTGGGGCTCT
GGCCGCGCCTGGCCTGGCCGGGACCATGTGCGCGTCCCGGGACGAATGGCGC
_____*S-form primer*_____
TGTGCGCGCTCCATGCACGAGTTTTCCGCCAAGGACATCGACGGGCACATGG
TTAACCTGGACAAGGACCGGGGCTTCGTGTGCATCGTCACCAACGTGGCCTC
CCAGTGAGGCAAGACCGAAGTAAACTACACTCAGCTCGTCGACCTGCACGCC
_____*antisense primer*_____
CGATACGCTGAGTGTGGTTTGCGGATCCTGGCCTTCCCGTGTAACCAGTTCGG
GAAGCAGGAGCCAGGGAGTAACGAAGAGATCAAAGAGTTCGCCGCGGGCTA
CAACGTCAAATTCGATATGTTCAGCAAGATCTGCGTGAACGGGGACGACGCC
CACCCGCTGTGGAAGTGGATGAAGG*TCCAACCCAAGGGCAAGGGCATCCTG
GGAAATGCCATCAAGTGGAACTTCACCAAGTTCCTCATCGACAAGAACGGCT
GCGTGGTGAAGCGCTACGGACCCATGGAGGAGCCCCTGGTGATAGAGAAGG
ACCTGCCCCACTATTTC*TAG*CTCCACAAGTGTGTGGCCCCGCCCGAGCCCCTG
CCCACGCCCTTGGAGCCTTCCACCGGCACTCATGACGGCCTGCCTGCAAACC
CTGCTGGTGGGGCAGACCCGAAAATCCAGCGTGCACCCCGCCGGAGGAAGG

Figure II-2. Stable transfection of human L-PhGPx sense cDNA increased both mRNA and protein levels of PhGPx in MCF-7 cells.

A. Western blot for PhGPx. Protein (200 μg) from each cell line was separated on a 12.5% SDS polyacrylamide gel. An increased expression of PhGPx is observed in the ~20 kDa band in the four transfected cell lines (P-1, P-2, P-3, and P-4). The Neo cells (vector only) had a similar expression level as the Wt (wild type).

B. Northern blot for PhGPx. Total RNA (10 μg) was separated on a 1.5% RNA agarose gel. A band corresponding to PhGPx mRNA was found in the transfected cells. No bands were detectable in Wt and Neo cells.

C. Loading control. The 28S rRNA was used as the loading control for northern blotting analysis.

Data are representative of three independent experiments.

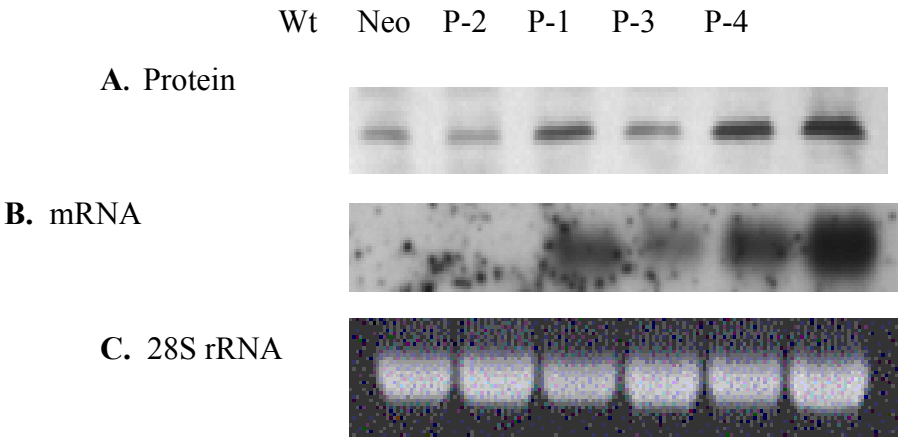
Wt
Neo
P-2
P-1
P-3
P-4
A. Protein
B. mRNA
C. 28S rRNA

Figure II-3. Stable transfection of human L-PhGPx sense cDNA increased PhGPx activity in MCF-7 cells.

A. Cellular PhGPx activity was measured by a coupled enzymatic assay at 340 nm. The phosphatidylcholine hydroperoxide (20 μM) was used as the substrate. One unit of PhGPx activity is defined as the amount of protein required to oxidize 1 μM of NADPH per minute. Results were mean ± SE, n = 3, * $p < 0.05$, ** $p < 0.001$ compared to Wt.

B. Correlation of PhGPx activity and protein. Data are derived from Figures II-2A and 1A (The protein level was quantified using densitometry based on the intensities of the western blots, triplicate data were obtained).

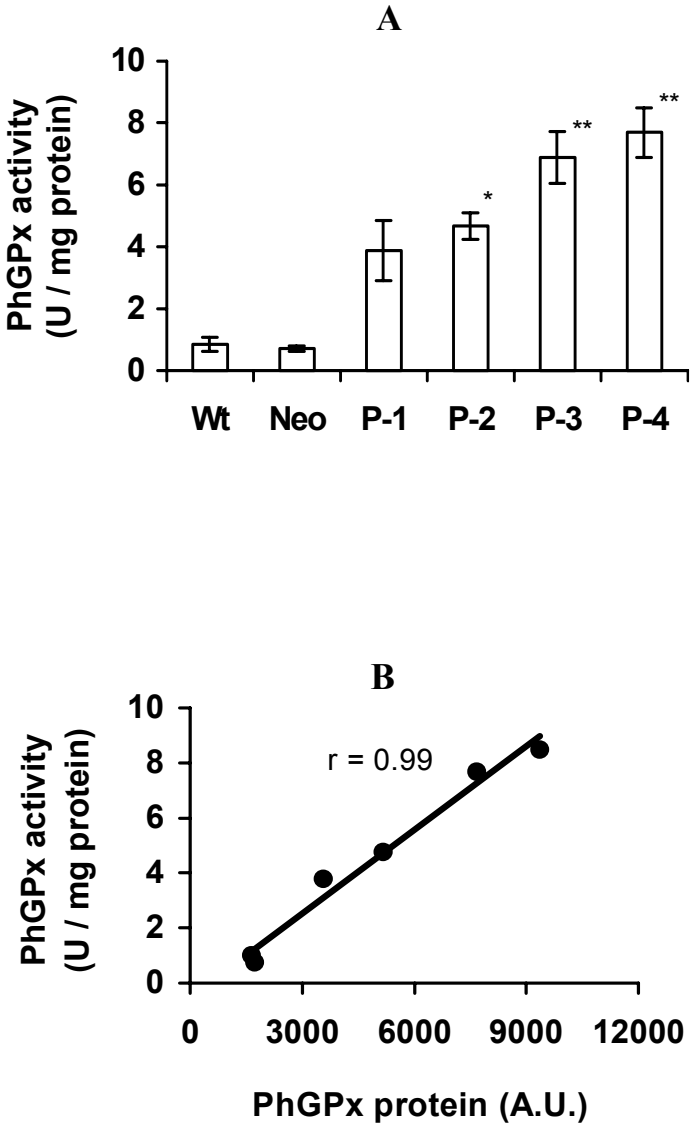
A
PhGPx activity
(U / mg protein)
10
8
6
4
2
0
*
**
**
Wt
Neo
P-1
P-2
P-3
P-4
B
PhGPx activity
(U / mg protein)
r = 0.99
0
3000
6000
9000
12000
PhGPx protein (A.U.)

Figure II-4. Examination of L-PhGPx and S-PhGPx in MCF-7 cells using RT-PCR. PhGPx cDNA was prepared by the reaction of total cellular RNA (5 μg) with oligo (dT) using MMLV-RT. The resulting cDNA was amplified in a 50 μL PCR mixture for 30 thermal cycles. The PCR products (30 μL) were separated in a 1.5% agarose gel staining with ethidium bromide.

Positive control: pure L-PhGPx cDNA was amplified in the PCR mixture; negative control: the PCR mixture was amplified without template cDNA; Lanes 1: with the L-form primer; Lanes 2: with the S-form primer. Figure shown is representative of three independent experiments.

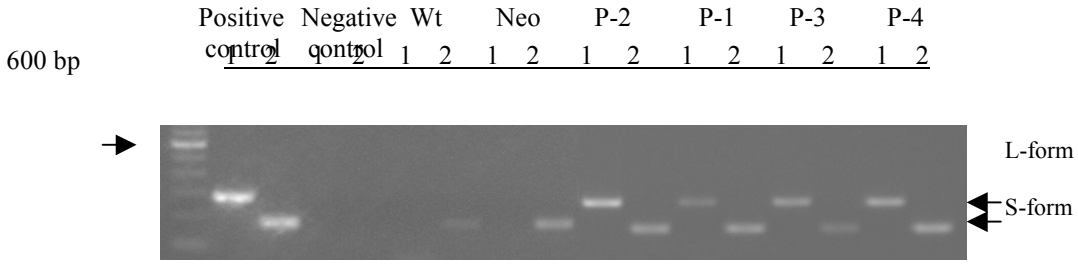
Positive control
Negative control
Wt
Neo
P-2
P-1
P-3
P-4
1 2 1 2 1 2 1 2 1 2 1 2 1 2 1 2
600 bp
L-form
S-form

Table II-1: Effective PhGPx Activity

Cell Lines	GSH (μmol/mg protein)	Maximum PhGPx Activity (U/mg protein)	Effective PhGPx Activity [a,b]
Wt	8.2 ± 2.3	0.84 ± 0.22	6.9 ± 2.8
Neo	10.1 ± 3.2	0.71 ± 0.09	7.2 ± 2.6
P-1	5.4 ± 1.5	3.87 ± 0.43	21 ± 6
P-2	8.8 ± 3.6	4.67 ± 0.97[c]	41 ± 18[c]
P-3	6.9 ± 1.5	6.89 ± 0.84[d]	48 ± 12[c]
P-4	7.8 ± 2.3	7.70 ± 0.80[d]	60 ± 20[c]

The effective PhGPx activity is defined as the product of total cellular GSH and the maximum PhGPx activity. [a] Units are: (μmol GSH • Units PhGPx) / $(\text{mg protein})^2$; [b] Because effective PhGPx is a derived quantity (GSH • Max PhGPx activity), the errors quoted were determined by the propagation of errors method; [c] $P < 0.05$ compared to Wt; [d] $P < 0.001$ compared to Wt.

Figure II-5. **Overexpression of L-PhGPx inhibited cell growth.**

A. Growth curves. 2×10^4 cells were seeded into 24-well plates, and counted every 48 h. The mean cell numbers are shown. ♦ represents Wt; □ Neo; ▲ P-1; Δ P-2; ○ P-3; ● P-4.

B. Cell doubling time. The doubling time was calculated from the growth curves during logarithmic growth phase. Data are mean ± SE, n = 3, *$p < 0.05$ compared to Wt.

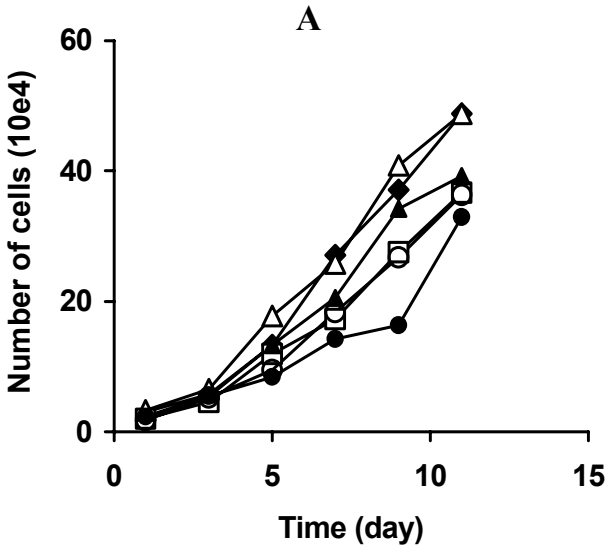
A
60
40
20
0
Number of cells (10e4)
0
5
10
15
Time (day)

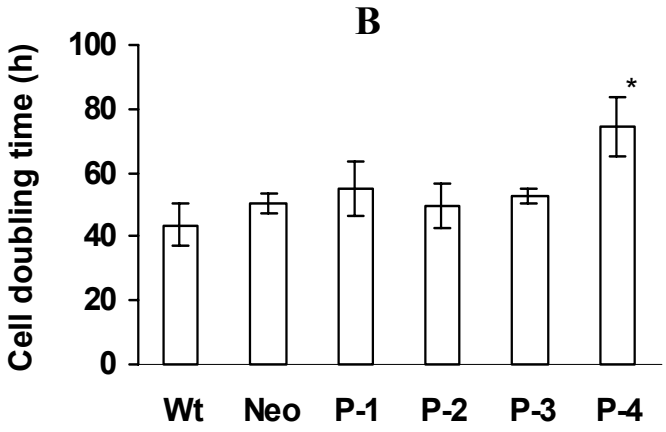
B
100
80
60
40
20
0
Cell doubling time (h)
*
Wt
Neo
P-1
P-2
P-3
P-4

Figure II-6. Overexpression of L-PhGPx decreased plating efficiency.

A. Plating efficiency. Cells were seeded into 60-mm dishes at a certain cell number. After 2 weeks incubation at 37°C, cells were fixed and stained. Colonies containing more than 50 cells were counted. The plating efficiency (PE) was calculated as:

PE = (Colonies formed / number of cells seeded) × 100%

Data are mean ± SE, n = 3; * $p < 0.05$ compared to Wt.

B. Correlation of plating efficiency and effective PhGPx activity. Data are derived from Figure II-5A and Table II-1. The unit for effective PhGPx activity is: (μmol GSH • Units PhGPx) / $(\text{mg protein})^2$.

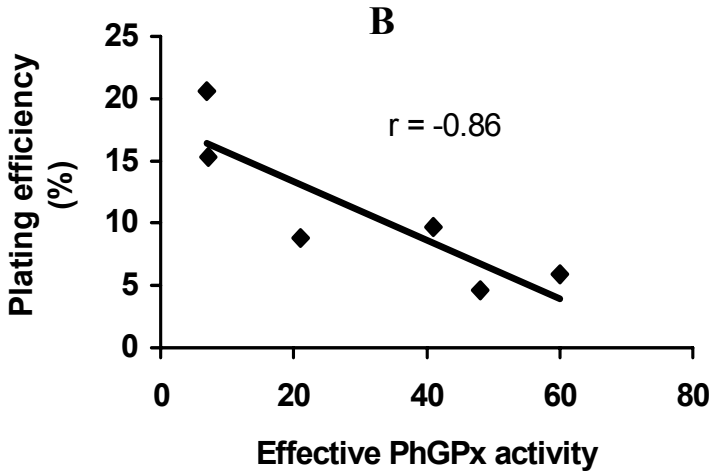
B
Plating efficiency (%)
25
20
15
10
5
0
r = -0.86
0
20
40
60
80
Effective PhGPx activity

Figure II-7. Overexpression of L-PhGPx did not influence the steady-state level of cellular LOOHs.

Neo and P-4 Cells were grown on 100-mm dishes to 80% confluency. Cellular lipids were extracted with chloroform:methanol (2:1, *v/v*). The chloroform layer was used for LOOH determination using the Cayman Lipid Hydroperoxide Assay Kit. Total LOOHs were normalized to total cellular protein. Data are mean ± SE, n = 3.

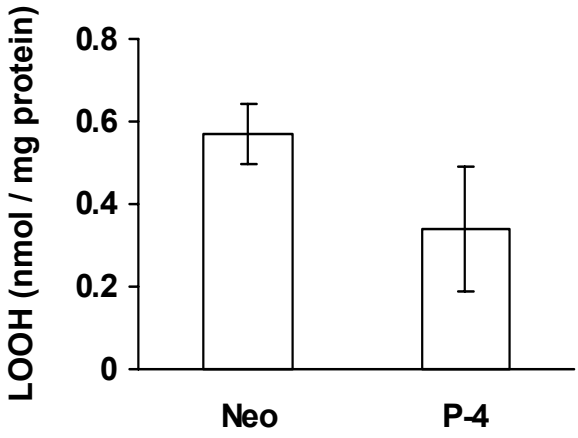
LOOH (nmol / mg protein)
0.8
0.6
0.4
0.2
0
Neo
P-4

Figure II-8. Overexpression of L-PhGPx did not influence the levels of MnSOD and CuZnSOD in MCF-7 cells.

A. Western blot for MnSOD. Total cellular protein (30 μg) was electrophoresed on a 12.5% SDS-polyacylamide gel and detected using anti-human MnSOD polyclonal antibody.

B. Western blot for CuZnSOD. Total cellular proteins (30 μg) were electrophoresed on a 12.5% SDS-polyacylamide gel and detected using anti-human CuZnSOD polyclonal antibody.

C & D. In gel activity assay for MnSOD and CuZnSOD. Total cellular proteins (200 μg) were electrophoresed on a 12% native gel, followed by incubation in nitroblue tertrazolium (NBT) and riboflavin-TEMED solution. The gel was washed with water and illuminated under a bright fluorescent light. Achromatic bands indicate the presence of SOD.

Data are representative of three independent experiments.

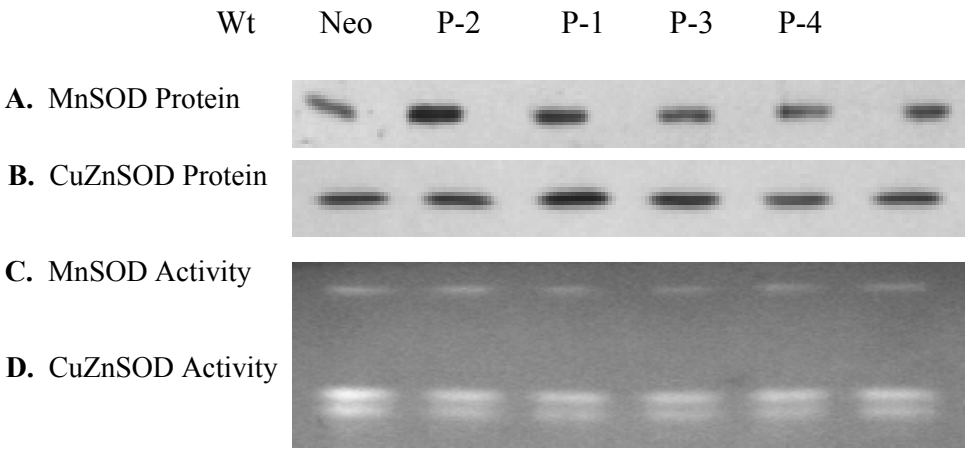
Wt
Neo
P-2
P-1
P-3
P-4
A. MnSOD Protein
B. CuZnSOD Protein
C. MnSOD Activity
D. CuZnSOD Activity

Figure II-9. Overexpression of L-PhGPx did not affect catalase level in MCF-7 cells.

A. Western blot for catalase. Total cellular proteins (30 μg) were electrophoresed on a 12.5% SDS-polyacylamide gel, and detected by the anti-human catalase polyclonal antibody.

B. In gel activity assay for catalase. Total cellular proteins (30 μg) were electrophoresed on a 12% native gel, followed by incubation with 0.003% H_2O_2. The activity of catalase was determined by staining the gel with ferric chloride and potassium ferricyanide.

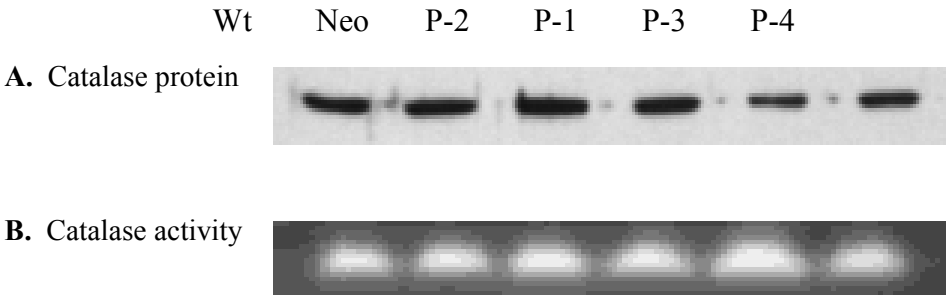
Wt
Neo
P-2
P-1
P-3
P-4
A. Catalase protein
B. Catalase activity

Figure II-10. Overexpression of L-PhGPx did not change GPx1 protein level in MCF-7 cells.

The native immunoblotting assay for GPx1. Total cellular protein (700 μg) was separated on a 12% native gel. After transferring onto a nitrocellulose membrane, GPx1 was detected by a polyclonal antibody against human GPx1.

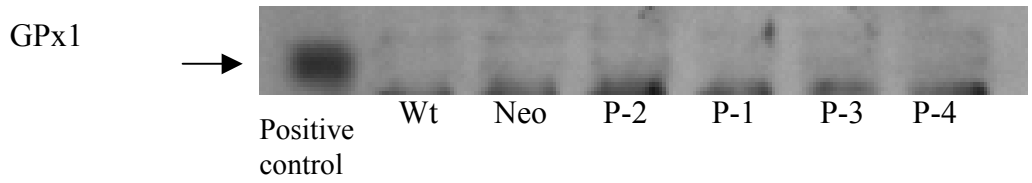
GPx1
Positive control
Wt
Neo
P-2
P-1
P-3
P-4

Figure II-11. Overexpression of L-PhGPx did not change glutathione reductase activity in MCF-7 cells.

In gel activity assay for GR. Cellular protein (500 μg) was separated onto a 12% native gel. GR activity was detected by staining the gel with 3.4 mM GSSG, 0.36 mM NADPH, 0.052 mM dichlorophenol-indophenol, and 1.1 mM 3(4,5-dimethythiazolyl-2)-2,5-diphenyl tetrazolium.

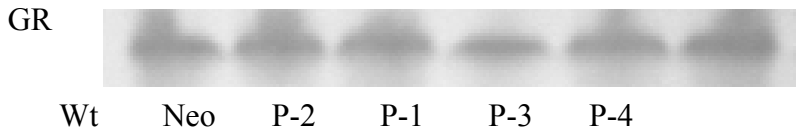
GR
Wt
Neo
P-2
P-1
P-3
P-4

CHAPTER III
THE ROLE OF L-PhGPx IN PDT-MEDIATED OXIDATIVE STRESS

Introduction

Photodynamic therapy (PDT) is a promising modality for the treatment of various solid tumors [Pass HI, 1992; Evensen JF, 1995]. The therapy relies on the preferential accumulation of a photosensitizer in tumor tissue followed by irradiation of the tumor with visible light [Phillips D, 1994]. Photofrin (sodium porfimer), a purified hematoporphyrin derivative (HPD), is the only photosensitizer approved by the U.S. Food and Drug Administration in 1995 for use in clinical therapy. It has been found that PDT with Photofrin is effective against solid tumors in humans [Pass HI, 1992; Dougherty TJ, 1986]. Evidence from *in vitro* studies has demonstrated that PDT can rapidly induce oxidative stress that results in many events, including activation of phospholipase and release of the lipid second messengers [Agarwal ML, 1993], induction of $p21^{WAF1/CIP1}$ [Ahmad N, 1998], activation of nitric oxide synthase and release of nitric oxide [Gupta S, 1998], activation of stress kinases and increase of early response genes [Tao JS, 1996].

Photofrin is a hydrophobic compound that accumulates in cellular membranes, including mitochondrial membranes. Upon photoactivation, it generates singlet oxygen ($^1O_2$). The generation of $^1O_2$ has been suggested as a primary mechanism involved in PDT-mediated photooxidation [Jori G, 1980; Wilkinson F, 1981]. The phosphorescence of $^1O_2$ has been directly observed at 1270 nm after Photofrin was exposed to light [Baker A, 1991]. Due to the short lifetime and limited diffusion range of $^1O_2$ [Ochsner M, 1997], the site of production determines the site and type of damage. Singlet oxygen reacts with

polyunsaturated fatty acid (PUFA) in membranes forming LOOHs [Weishaupt K, 1976; Gomer CJ, 1989; Henderson BW, 1992; Buettner GR, 1993; Kriska T, 1996]. The LOOHs formed within the bilayer of membranes alter the membrane structure [Pradhan D, 1990] and may disrupt membrane function, subsequently leading to cell destruction.

Lipid peroxidation has been shown to be an early oxidative event during photooxidation with Photofrin [Buettner GR, 1993; Kelley EE, 1997]. Upon photo-activation, the sensitizer is elevated from its ground state (S) to a singlet excited state ($^1S^*$); this singlet state relaxes to a longer-lived energetic triplet state ($^3S^*$) (reaction 1).

$$S \xrightarrow{h\nu} {}^1S^* \rightarrow {}^3S^* \qquad (1)$$

The triplet state of the sensitizer physically transfers its energy to ground state oxygen ($^3O_2$), yielding $^1O_2$ (reaction 2). Singlet oxygen covalently adds to carbon-carbon double bonds forming LOOH (reaction 3).

$$^3S^* + {}^3O_2 \rightarrow {}^1O_2 + S \qquad (2)$$

$$^1O_2 + LH \rightarrow LOOH \qquad (3)$$

The formed LOOHs can undergo reductive degradation. LOOHs can initiate lipid radical chain reactions in the presence of iron, which can enhance the cytotoxicity. Alternatively, LOOHs can be repaired by cellular antioxidant enzymes. The seleno-dependent and nonseleno-dependent enzymes are implicated in LOOH detoxification: GPx1, PhGPx, and GST, as well as a newly discovered nonselenium-dependent GPx [Fisher AB, 1999]. The selenium-dependent peroxidases have been studied extensively and are considered to be more important in overall LOOH repair. It has been found that selenium-deficient cells accumulate LOOHs more rapidly under oxidative challenge than their normal counterparts and die faster [Geiger PG, 1993; Lin F, 1992]. PhGPx can directly act on phospholipid hydroperoxides in membranes, whereas GPx1 is nonreactive unless the fatty acyl bonds are cleaved to liberate fatty acid hydroperoxides [Grossman A,

1983; van Kuijk FJGM, 1987]. It has been estimated from a kinetic model that the reduction rate of LOOHs through PhGPx is at least 10^4-fold greater than that through GPx1 and PLA_2 [Antunes F, 1995]. It has been shown that cells transfected with PhGPx sense cDNA are better equipped to detoxify LOOHs and survive peroxidative stress than the nontransfected counterparts [Yagi K, 1996; Imai H, 1996]. Therefore, we hypothesized that increased PhGPx could play a critical role in the resistance of tumor cells to PDT-induced cytotoxicity.

Materials and Methods

Reagents

Lipid hydroperoxide assay kit and reagents were purchased from Cayman Chemical Co. (Ann Abor, MI). Chloroform (HPLC grade), methanol (HPLC grade), crystal violet, acetic acid, and trypan blue were obtained from Fisher Scientific Co. (Pittsburgh, PA). Sodium selenite, and 5,5-dimethyl-pyrroline-1-oxide (DMPO) were obtained from Sigma (St. Louis, MO). DMPO was purified with activated charcoal/benzene, and then prepared as a 1.0 M aqueous stock solution [Buettner GR, 1978; Kotake Y, 1994]. MEM, fetal bovine serum (FBS), non-essential amino acids, Geneticin™ (G418) were bought from GIBCO (Grand Island, NY). Photofrin® (porfimer sodium) was a gift from QLT Phototherapeutics, Inc. (Vancouver, British Columbia, Canada). A stock solution was made in 5% dextrose (pH 7.4), filtered and stored at –20°C. Annexin V apoptosis assay kit and reagents were purchased from Biovision (Palo Alto, CA).

Cell Culture

Cells were routinely grown in T-25 cell culture flasks at 37°C with 5% CO_2. The Wt cells were grown in MEM supplemented with 10% FBS, 1% non-essential amino

acids, and 30 nM sodium selenite. The Neo and P-1, P-2, P-3, P-4 cells were grown in the above medium with G418 (350 μg/mL). G418 was removed from the medium one cell passage number before an experiment. Cells were subcultured into 100-mm dishes for LOOH assay and EPR measurement, and 6-well plates for viability assays.

Photosensitization with Photofrin

Cells were incubated with Photofrin (6 μg/mL) in serum-containing medium for 24 h. After being washed with medium three times, cells were illuminated with visible light (5 J/m^2s) on a light box for different time point [Schafer FQ, 2000]. Cells were then incubated for 6 h at 37°C in the dark. After this incubation, cells were subjected to assays. Cells treated with Photofrin but without light exposure were used as controls.

Activity Assay for PhGPx

The measurement of PhGPx activity is an essential step in this work. PhGPx activity assay is a newly established method in our lab [Wang HP, 2000]. The activity was measured by coupled enzymatic assay with some modification, using GSH, GR, PCOOH, and NADPH [Roveri A, 1994]. The spectrophotometric test mixture contained, in 1 mL, the following: 0.1 M Tris-HCl (pH 8.0), 2 mM EDTA, 1.5 mM NaN_3, 0.1% Triton X-100 (peroxide free), 3 mM GSH, and 1.5 U/mL GR. Sample (1 mg) was added to the test mixture and incubated at 37°C for 8 min. Then 0.2 mM NADPH was added and incubated for 8 min to allow PhGPx and GSH to be converted to the reduced forms. The nonspecific NADPH oxidation rate was recorded for 4 min at 340 nm and the enzyme reaction started with the addition of PCOOH (10-30 mM). The rate of specific NADPH oxidation was recorded every 20 s for 4 min at 340 nm using a Beckman DU-70 spectrophotometer. The activity was calculated by subtracting the nonspecific NADPH oxidation rate from the observed NADPH oxidation rate after substrate addition. The

specific activity of PhGPx is expressed as units per milligram protein, 1 unit being the amount of enzyme catalyzing oxidation of 1 μM of NADPH per min.

Lipid Hydroperoxide Assay

The level of cellular LOOHs was determined using the Lipid Hydroperoxide Assay Kit as described in Chapter II. Briefly, cells were seeded into 100-mm dishes until 80% confluence. After photosensitization with Photofrin, cell membranes were extracted with 1.5 mL deoxygenated chloroform:methanol (2:1, *v/v*) mixture. Ferrous iron was added to the chloroform layer and the formation of ferric thiocyanate was measured at 500 nm on a Beckman DU-70 spectrophotometer. 13-Hydroperoxyloctadecadienoic acid (13-HpODE) was used as the standard. The amount of LOOHs was normalized to total cellular protein.

EPR Spin Trapping Measurement for Lipid Radical Chain Reactions

The potential lipid chain reactions were determined using a newly developed EPR spin trapping method from our lab [Qian SY, 2000]. Cells (3×10^6) were seeded into 100-mm dishes 24 h before the experiment. After photosensitization treatment, cells were washed twice with metal-free PBS (pH 7.4) and then incubated with 150 mM DMPO and 100 μM $Fe(NH_4)_2(SO_4)_2 \bullet 6H_2O$ in metal-free PBS buffer for 5 min at room temperature. Cells were then scraped off and extracted using 20 mL chloroform:methanol (2:1, *v/v*) mixture. After phase separation overnight, the lower layer of chloroform was collected and dried completely under argon. The residue was resuspended in 500 μL deoxygenated ethyl acetate and immediately transferred into an EPR flat cell for EPR measurement. EPR spectra were recorded on a Bruker ESP-300 spectrometer (Billerica, MA) equipped with a TM_{110} cavity operating at 9.76 GHz with

modulation frequency 100 kHz, modulation amplitude 1.0 G, and microwave power 40 mW. All experiments were performed at room temperature.

Trypan Blue Dye Exclusion Assay

Cells (1×10^5) were seeded into 6-well plates 24 h before Photofrin photosensitization. After photooxidation, cells were incubated 6 h to allow the enzymatic repair and then washed and trypsinized. Cells were stained with 0.2% trypan blue for 2 min at room temperature. The cells excluding or stained with the dye were counted using a hemocytometer. Membrane integrity was expressed as the percentage of cells that excluded the dye.

Clonogenic Survival Assay

A clonogenic survival assay was used to measure the cytotoxicity from PDT photooxidation. Cells (3×10^5) were seeded in 60-mm dishes 24 h before the experiment. After photosensitization, cells were trypsinized. The resulting single-cell suspension was counted and diluted. A certain cell number of cells, which yielded 50 – 100 surviving colonies per well, were seeded into 6-well plates for colony survival analysis. After a two-week incubation at 37°C, cells were fixed with methanol:acetic acid (3:2, *v/v*) mixture and stained with crystal violet. A colony containing more than 50 cells was considered as a survivor and counted. The cell survival fraction (SF) was calculated as following:

$$SF = \text{Colonies formed} / (\text{Number of cells seeded} \times \text{Plating efficiency})$$

Survival data following treatment were normalized to appropriate control plating efficiencies.

Flow Cytometry Analysis

Cells (2×10^5) were seeded into 6-well plate 24 h before the experiment. After Photofrin treatment and 10 min light exposure, cells were incubated in the dark for 6 h. Cells were then washed, trypsinized, and resuspended in the Annexin V binding buffer with Annexin V (2 μg/mL) and PI (5 μg/mL). After incubation with Annexin V and PI for 5 min at room temperature, cell death was examined *via* flow cytometry (FACScan, Becton Dickinson).

Statistics

Mean values, standard errors, and the linear regression parameters were determined using Microsoft Excel program (Excel 97 SR-1). ANOVA-Tukey test was used to compare the differences between two groups. In all cases, the statistical significance of differences between the two variants were determined at a level of $p < 0.05$. All the data presented are from the average of at least three independent experiments.

Results

Photosensitization Minimally Induced PhGPx Activity

It has been reported that mammalian cells can overproduce antioxidant enzymes such as GPx1, CAT, and SODs in response to sublethal or lethal oxidant pressure [Shull S, 1991; Alvarez S, 1993; Lemaitre D, 1997]. Overexpression of these proteins is believed to be a defensive strategy against oxidative stress. PDT induces oxidative stress to cells. Our hypothesis was that Photofrin photosensitization might modulate PhGPx activity. Neo and P-4 cells were exposed to Photofrin and 5-min visible light, and then allowed to recover for 6 h in the dark. After photosensitization, there was only a minimal (not statistically different) increase in PhGPx activity in both Neo and P-4 cells (**Figure**

III-1), suggesting that $^1O_2$ might be involved in the up-regulation of PhGPx expression. It has been reported that $^1O_2$ can induce the activation of the transcription factor AP-2 [Grether-Beck S, 1996]. The AP-2 binding site is found in the PhGPx promoter region [Huang HS, 1999]. Thus, PDT may have an effect in inducing PhGPx expression *via* the generation of $^1O_2$. The minor induction effect found in this study might be due to the low doses of Photofrin and irradiation.

L-PhGPx Decreased PDT-Induced Lipid Hydroperoxide Levels in MCF-7 Cells

Lipid peroxidation is involved in PDT [Kelley EE, 1997]. We hypothesized that cells with higher PhGPx levels would more rapidly remove these LOOHs. To test this hypothesis, cells were incubated with Photofrin and then illuminated to produce LOOHs in cell membranes. Immediately after light exposure all six cell lines had a significant increase in LOOHs compared to their non-irradiated controls. LOOHs were increased from a background level of approximately 1 nmol/mg protein to 5 nmol/mg protein in each cell line. These results suggest that an increase in PhGPx, at the level we were able to obtain, does not influence the formation of LOOHs from singlet oxygen. However, when the cells were incubated in the dark after light exposure to allow for repair, significant differences in LOOH levels were observed (**Figure III-2A**). After 6 h post-PDT, Wt and Neo cells still had 4- to 5-fold more LOOHs compared to their non-illuminated controls. The two clones with low to medium PhGPx levels (P-1, P-2) had 2- to 3-fold more LOOHs compared to their controls. However, the two clones having the highest PhGPx activity (P-3, P-4) fully repaired the $^1O_2$-induced LOOHs as only background levels of LOOHs were observed in these cells.

Thus, L-PhGPx did not appear to influence the formation of LOOHs but rather their removal. In fact, the removal of LOOHs by the various cell lines correlated directly with their effective PhGPx activity (r = 0.8) (**Figure III-2B**).

These results demonstrate that LOOHs are a critical and early mediator of photooxidation with Photofrin. L-PhGPx is an effective repair enzyme in removing LOOHs. The rate of removal by this protein is dose dependent.

L-PhGPx Removed Component Needed for Free Radical Chain Reactions

In the presence of trace amounts of ferrous iron, LOOHs can be decomposed to enter the free radical chain reactions, which lead to cell death [Porter NA, 1995]. To test our hypothesis that PhGPx could decrease lipid radical chain reactions, we examined lipid-derived radical formation using EPR spin trapping. LOOHs were seeded into cells by exposure to Photofrin and light. After a 6-h recovery period in the dark, the spin trap DMPO was added followed by ferrous iron to initiate radical-mediated lipid peroxidation. Lipid-derived radical adducts of DMPO (a^N = 15.2 G, a^H = 10.2 G) were observed by EPR (**Figure III-3A**). Each spectrum represents the signal-averaged result of 45 scans. The height of the low-field line of the DMPO/lipid-derived radical adduct was used as a measure of radical yield. Cells treated with Photofrin but no light exposure were considered as controls, and their radical yield was below the detection limit (data not shown). Quantification of the spin adducts after $^1O_2$-induced lipid peroxidation showed that cells with the lowest PhGPx activity produced the most spin adducts, while those with higher levels of PhGPx produced less spin adducts. A strong inverse correlation (r = -0.96) was found between the amount of DMPO spin adduct formed and the effective PhGPx activity (**Figure III-3B**). This result demonstrates that PhGPx is effective in preventing potential lipid radical reactions.

L-PhGPx Protected against $^1O_2$-Induced Membrane Permeability

LOOH formed in the bilayer can cause the disruption of cell membranes. Because PhGPx removes LOOHs formed in cells, we hypothesized that cells with higher PhGPx activity would be better able to maintain membrane integrity upon exposure to $^1O_2$. To test this hypothesis we examined trypan blue dye exclusion from cells after photosensitization and 6 h recovery. Membrane integrity was preserved in cells that expressed higher levels of PhGPx; P-3 and P-4 cells were up to 4-times more resistant than Wt and Neo (**Figure III-4A**). Membrane integrity, expressed as percentage of dye exclusion at 10 min light exposure, correlated directly with the effective PhGPx activity ($r = 0.96$) (**Figure III-4B**). PhGPx is capable of protecting cell membranes from PDT-mediated oxidation.

L-PhGPx Decreased $^1O_2$-Induced Cytotoxicity

The formation of LOOHs within the bilayer of membranes alters the membrane structure [Pradhan D, 1990] and thus, may disrupt membrane function consequently leading to cell destruction. To examine whether removal of LOOHs modulates $^1O_2$-induced cytotoxicity, cell survival was determined by clonogenic assay. As seen in **Figure III-5A**, L-PhGPx greatly enhanced clonogenic survival. At 10 min of light exposure, P-4 cells exhibited a 10-fold higher survival than Wt and Neo cells. Cell survival at 10 min light exposure had a strong direct correlation with effective PhGPx activity ($r = 0.91$) (**Figure 5B**). The cytoprotective effect of L-PhGPx was also observed from the flow cytometry analysis. Cells were double stained with Annexin V and PI for measurement of apoptosis and necrosis, respectively. The changes observed in PI staining patterns clearly demonstrated that $^1O_2$ induced necrotic cell death (**Figure III-6**). For Neo cells, the percentage of cells that gated PI-positive increased from 21% before $^1O_2$

exposure to 94% after exposure (**Figures III-6A to III-6B**). However, this same treatment of P-3 cells resulted in a change in the PI positive cells from 22% to 65% (**Figures III-6C to III-6D**). There was no Annexin V positive cells found after Photofrin photosensitization (data not shown). DNA agarose gel results also showed that there was no apoptotic DNA fragmentation in all six cells (Wt, Neo, P-1, P-2, P-3, P-4) after Photofrin photosensitization (data not shown). This observation is consistent with previous finding that MCF-7 cells exhibit minimal apoptotic response to PDT [Fisher AMR, 1999].

These data suggest that overexpression of L-PhGPx can protect cells from $^1O_2$-induced necrosis, and that PhGPx is an important enzyme responsible for cellular resistance to PDT.

Discussion

Lipids are one of the major targets for oxidative damage in cells. Lipid hydroperoxides (LOOHs) are key intermediates in the lipid peroxidation process, acting as initiator for free radical chain reactions. It has become clear that lipid peroxidation is involved in a variety of different types of cell injury [Yoshikawa T, 1987] and that use of this mechanism of cell injury can be applied to advantage in the therapy of cancer. The enzymatic repair of these LOOHs is critical for cells to avoid potential lethal damage. There are three important enzyme systems (GPx1, GST, and PhGPx) that can detoxify LOOHs and thereby reduce or prevent hydroperoxide-mediated cell damage. Of these three enzymes, PhGPx is unique in that it directly reduces phospholipid hydroperoxides, *i.e.* it detoxifies LOOHs inside the cell membrane. Thus, PhGPx could play an important role in protecting cells from the effects of lipid peroxidation [Thomas JP, 1990; Arai M, 1999].

Singlet oxygen is an ideal tool to introduce LOOHs into cell membranes. PhGPx was not able to block the formation of LOOHs, but rather removed them. The rate of removal of LOOHs correlated directly with effective PhGPx activity (**Figure III-2)**. Removal of LOOHs by PhGPx prevented potential free radical formation as observed by EPR spin trapping, (**Figure III-3)**.

Because lipid peroxidation can be detrimental to cells, we hypothesized that increasing PhGPx activity would increase the resistance of cells to oxidative stress. Formation of LOOHs and the subsequent lipid peroxidation reactions can interrupt the integrity of cell membranes. Indeed, L-PhGPx was able to maintain membrane integrity upon exposure to singlet oxygen (**Figure III-4)**. Cell survival, as assessed by clonogenic assay and flow cytometer with PI, was also significantly increased in cells with high levels of PhGPx activity (**Figures III-5 and III-6)**.

As shown in Chapter II, transfection of L-PhGPx did not change the intracellular antioxidant profile (GPx1, CAT, MnSOD, CuZnSOD, GR, and total cellular GSH levels). Thus, the removal of LOOHs and the increase in cell survival in response to $^1O_2$ are probably due to the overexpression of L-PhGPx.

Effective PhGPx activity correlates inversely with intracellular levels of lipid hydroperoxides and potential radical formation upon exposure to singlet oxygen. The importance of the removal of lipid hydroperoxides is supported by the strong direct correlation seen between effective PhGPx activity and cell survival after an oxidative stress. Taken together, these data support LOOHs as being major mediators in cell injury. PhGPx is a key enzyme in protecting cells from the damaging effects of lipid peroxidation resulting from oxidative stress.

Many xenobiotics, be they drugs for treatment of disease or pollutants from environmental exposure, result in the production of reactive oxygen species. Resistance

to such an oxidative stress will depend on the antioxidant capacity of the cells and tissues. It has been estimated that, under physiological conditions, the rate of removal of LOOHs through PhGPx is about four-orders of magnitude greater than through the GPx1 and PLA_2 system [Antunes F, 1995]. In addition, a dietary study of selenium deficiency in mice found that PhGPx activity was more slowly depleted by Se deficiency than GPx1 [Weitzel F, 1990]. Our findings that effective PhGPx activity strongly correlated with various biological endpoints support the importance of PhGPx as an antioxidant enzyme. The ability of PhGPx to remove LOOHs *in situ* could confer resistance of cells and tissues to an oxidative stress that results in the formation of LOOHs. This could be an advantage or disadvantage, depending on the situation. It would be a disadvantage if PhGPx affords cells and tissues (e.g. tumor) to be resistant to the oxidative stress induced by treatments such as PDT. On the other hand, PhGPx could aid in the resistance of cells to oxidative stress due to xenobiotic exposure; this property could protect normal tissue during certain disease treatments.

Figure III-1. Photooxidation had minor effects on the induction of PhGPx activity. Neo and P-4 cells were exposed to PDT. The total cellular protein was assayed for PhGPx activity. The activity is expressed as U / mg total cellular protein, one unit of enzyme activity catalyzes the oxidation of 1 μM NADPH per min.

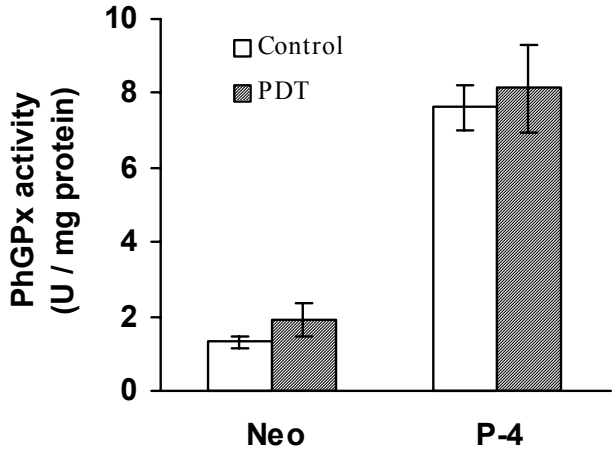
10
8
6
4
2
0
PhGPx activity
(U / mg protein)
Control
PDT
Neo
P-4

Figure III-2. L-PhGPx removed PDT-induced LOOHs in MCF-7 cells.

A. Cells were pretreated with Photofrin (6 μg/mL) for 24 h in full media. After a 5-min light exposure, cells were incubated for 6 h in the dark. The level of LOOH was assessed using the Cayman Lipid Hydroperoxide Kit. (Mean ± SE, n = 3, * $p < 0.05$ compared to the corresponding no-light exposed control)

Solid bars: control, cells exposed to Photofrin, but no light.

Open bars: cells treated with Photofrin and light;

B. Removal of LOOHs correlates with effective PhGPx activity; data are derived from Table II-1 and Figure III-2A (in 2A, data were normalized to controls). The units for effective PhGPx activity are: (μmol GSH • Units PhGPx) / $(\text{mg protein})^2$.

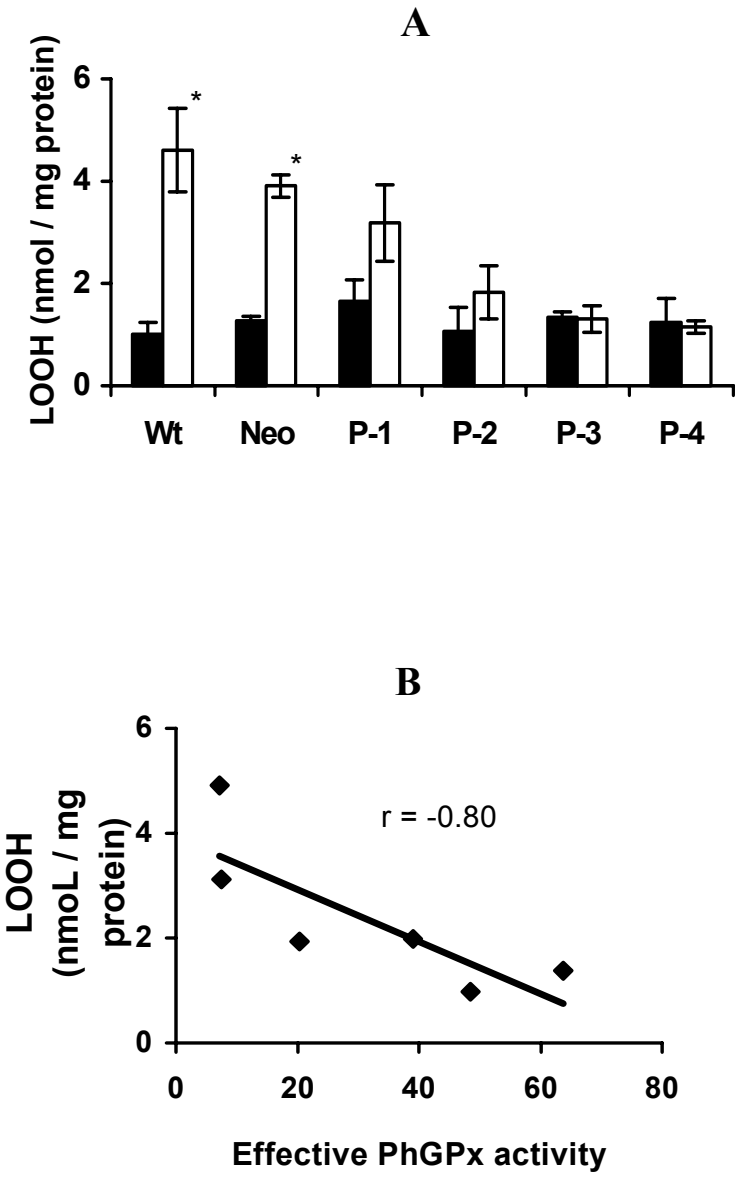
A
LOOH (nmol / mg protein)
6
4
2
0
*
*
Wt
Neo
P-1
P-2
P-3
P-4
B
LOOH (nmoL / mg protein)
r = -0.80
6
4
2
0
0
20
40
60
80
Effective PhGPx activity

Figure III-3. L-PhGPx inhibited PDT-induced lipid-derived radical generation.

A. Cells (3×10^6) were pretreated with Photofrin (6 μg/mL) for 24 h in full media. After 5-min light exposure, cells were incubated for 6 h in the dark. Radical formation was then assessed using EPR spin trapping. Each spectrum represents the signal-averaged result of 45 scans. The height of the low-field line of the DMPO/lipid-derived radical adduct was used as a measure of radical yield. **Inset:** An example X-band EPR spectrum of the DMPO adduct (a^N = 15.2 G, a^H = 10.2 G in ethyl acetate) formed from MCF-7 cells. Control cells were incubated with Photofrin but not exposed to light. The yield of DMPO adduct in the control samples was below the limit of detection (data not shown).

(Mean ± SE, n = 3, * $p < 0.05$, ** $p < 0.005$ compared to Wt.)

B. Lipid radical formation correlates inversely with effective PhGPx activity. Data are derived from Table II-1 and Figure III-3A. The units for effective PhGPx activity are: (μmol GSH • Units PhGPx) / $(\text{mg protein})^2$.

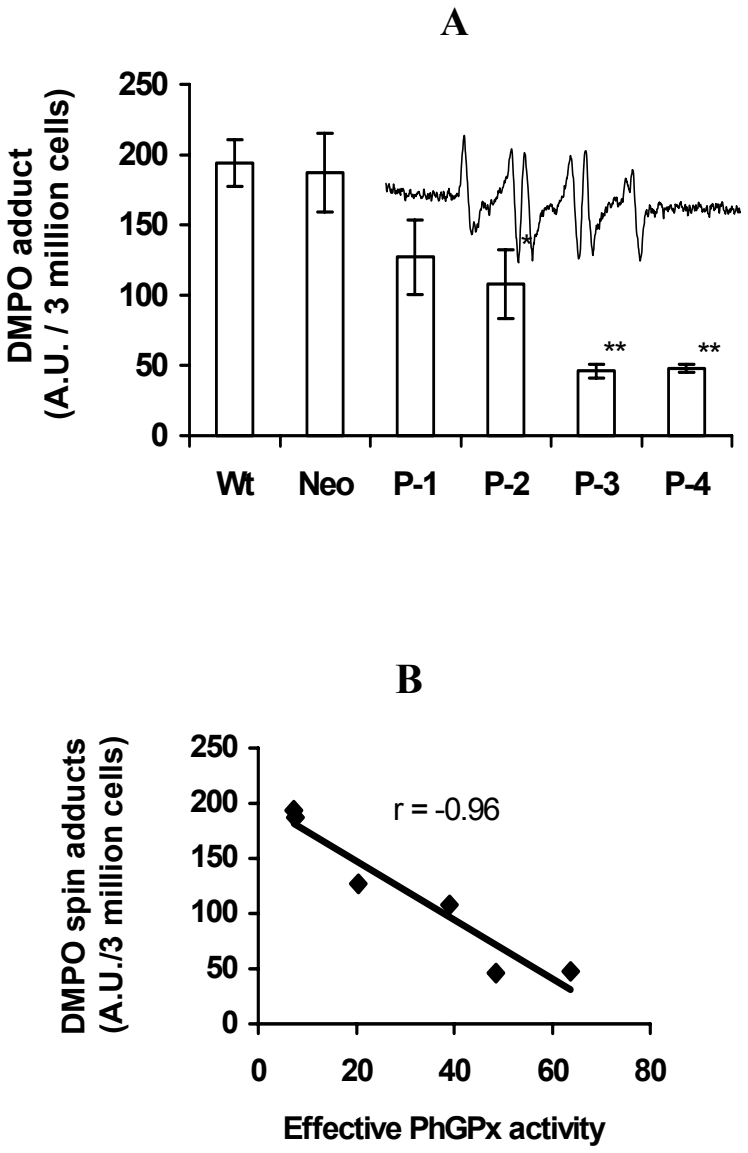
A
DMPO adduct
(A.U. / 3 million cells)
250
200
150
100
50
0
**
**
Wt
Neo
P-1
P-2
P-3
P-4
B
DMPO spin adducts
(A.U./3 million cells)
250
200
150
100
50
0
r = -0.96
0
20
40
60
80
Effective PhGPx activity

Figure III-4. L-PhGPx blunted PDT-induced membrane permeability changes in MCF-7 cells.

A. Membrane permeability was assayed by trypan blue dye exclusion. Cells were incubated with Photofrin (6 μg/mL) for 24 h, and then irradiated with visible light (0 to 15 min). After light exposure, cells were incubated 6 h in the dark at 37°C. Cells were then trypsinized and assayed for viability. Symbols: ▲ represents Wt; Δ Neo; ● P-1; o P-2; ■ P-3; □ P-4. (Mean ± SE, n = 3, * $p < 0.05$ compared to Wt).

B. Cell viability at 10 min correlates directly with effective PhGPx activity. Data are derived from Table II-1 and Figure III-4A. The units for effective PhGPx activity are: (μmol GSH • Units PhGPx) / $(\text{mg protein})^2$.

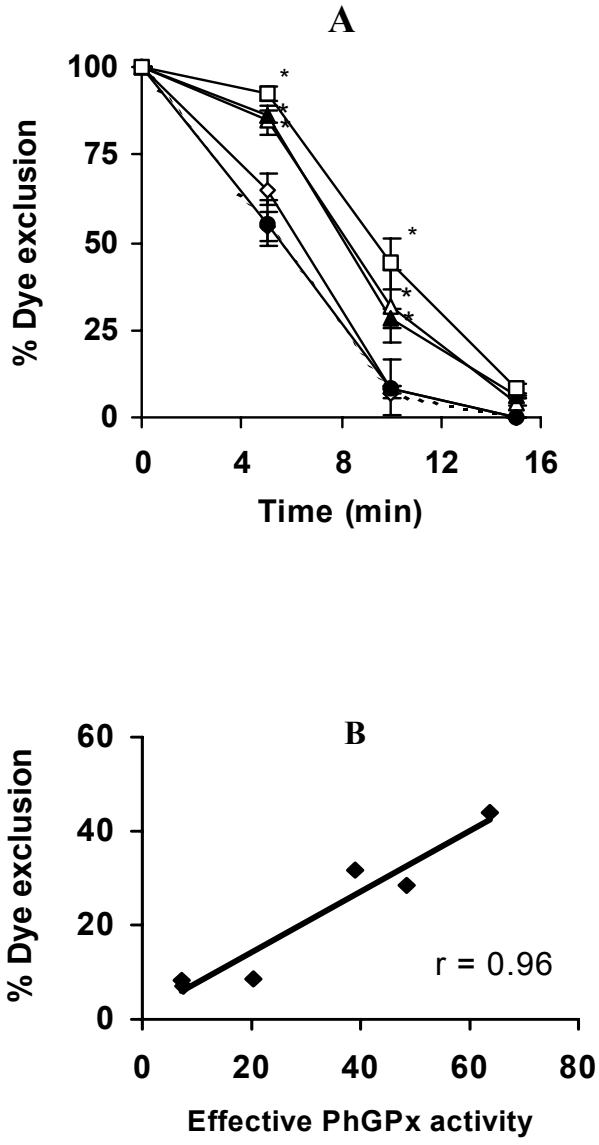
A
100
75
50
25
0
% Dye exclusion
0
4
8
12
16
Time (min)
*
B
60
40
20
0
% Dye exclusion
r = 0.96
0
20
40
60
80
Effective PhGPx activity

Figure III-5. L-PhGPx protected against PDT-induced cytotoxicity in MCF-7 cells.

A. Cell cytotoxicity was measured by clonogenic assay. Cells were incubated with Photofrin (6 μg/mL) for 24 h, and then irradiated with visible light (0 to 10 min). After light exposure, cells were incubated 6 h in the dark at 37°C and then seeded into 6-well plates and incubated for 2 weeks to allow colony formation. Surviving fraction (SF) is expressed as:

(colonies formed / number of cells seeded × plate efficiency) × 100%.

Symbols: ▲ represents Wt; Δ Neo; ● P-1; ○ P-2; ■ P-3; □ P-4.

(Mean ± SE, n = 3; * $p < 0.05$, the error bars are smaller than the symbols).

B. Cell viability at 10 min correlates directly with effective PhGPx activity. Data are derived from Table II-1 and Figure III-5A. The units for effective PhGPx activity are: (μmol GSH • Units PhGPx) / $(\text{mg protein})^2$.

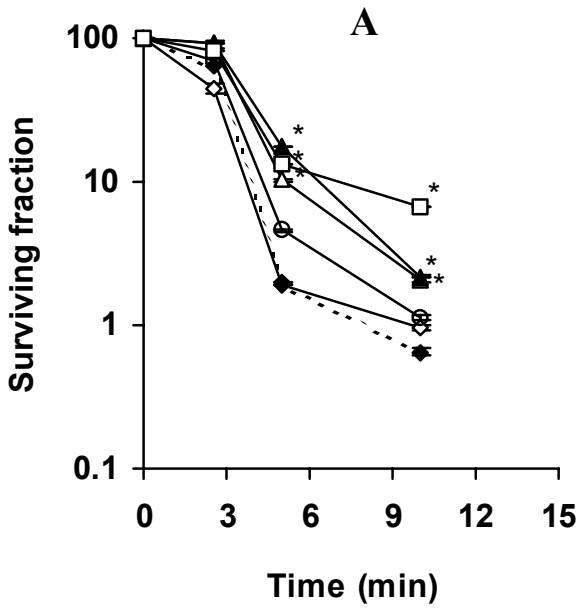
A
100
10
1
0.1
Surviving fraction
0
3
6
9
12
15
Time (min)

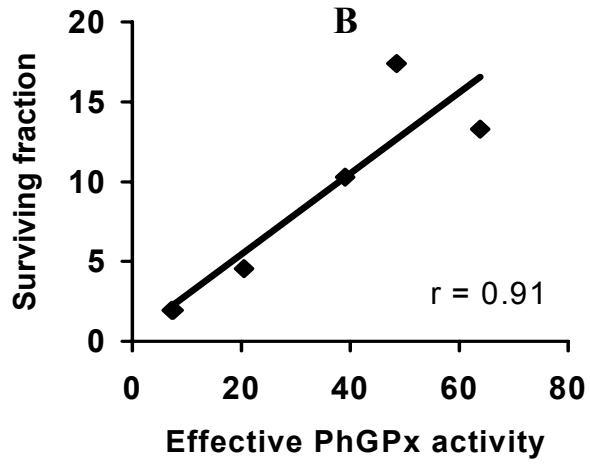
B
20
15
10
5
0
Surviving fraction
r = 0.91
0
20
40
60
80
Effective PhGPx activity

Figure III- 6. **L-PhGPx protected against PDT-induced necrosis in MCF-7 cells.**

Flow cytometric analysis of Neo and P-3 cells exposed to $^1O_2$. Cells were incubated with Photofrin (6 μg/mL) for 24 h, followed by irradiation with visible light (10 min). Cells were then incubated 6 h in the dark at 37°C. Cells were washed and trypsinized, stained with PI (5 μg/μL) in MEM. Cells were analyzed by flow cytometry. The percentage in the figure represents the percent of cells that were PI positive.

A. MCF-7 Neo without light; **B.** MCF-7 Neo with light;

C. P-3 cells without light; **D.** P-3 cells with light.

Data are representative of three independent experiments.

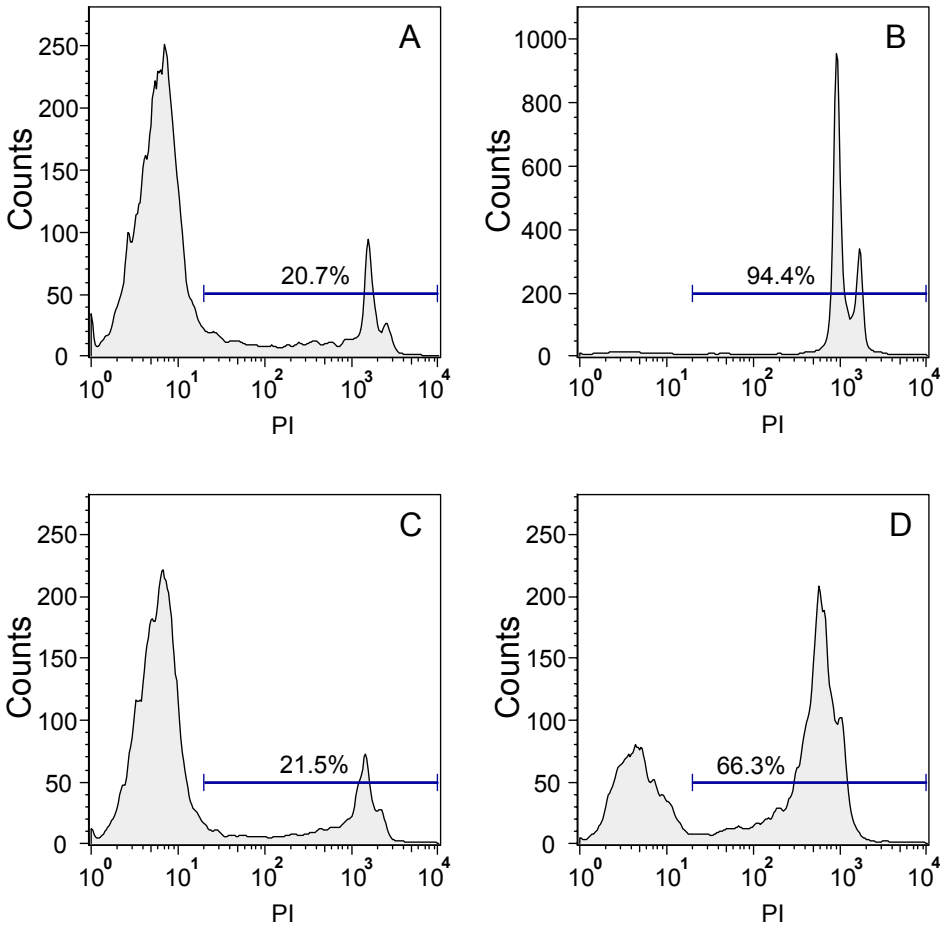
A
Counts
PI
20.7%
B
94.4%
C
21.5%
D
66.3%

CHAPTER IV

THE ROLE OF L-PhGPx IN HYPERTHERMIA-MEDIATED OXIDATIVE STRESS

Introduction

Therapeutic hyperthermia utilizes super-physiological temperatures for treatment of disease. Regional hyperthermia combined with radiotherapy or chemotherapy is a promising treatment for breast cancer [Sherar M, 1997;van der Zee J, 1999]. The mechanism responsible for the antitumor effect of elevated temperatures has been under investigation both at the tumor and cellular levels. At the level of tumor, the microvasculature may play an important role in the heat-induced cytotoxicity [Eddy HA, 1980]. At the cellular level, elevated temperatures cause irreversible damage to many cellular structures, including plasma membrane, cytoskeletal elements, and chromosome [Roti Roti JL, 1988]. Denaturation of a large number of cellular proteins [Lepock JR, 1992], decreases in ATP levels and alteration in Ca^{2+} homeostasis are found in heat-induced stress [Welch WJ, 1992]. Oxidative stress has been suggested as a potential mechanism involved in heat-induced cell killing [Lord-Fontaine S, 1999; Freeman ML, 1985; Griffith OW, 1979]. Heat can increase the rates of many chemical and biochemical reactions. Therefore, heat could increase the generation of ROS *via* metabolic reactions in cells and tissues. The reactivity of ROS with cellular components would also increase with temperature. The production of superoxide and other oxygen-centered radicals has been shown to increase during heat stress [Issels RD, 1986; Flanagan SW, 1998]. Superoxide produced from heat stress can be dismutated to H_2O_2. The latter can generate

hydroxyl radicals ($^{\bullet}OH$) *via* the Fenton reaction. Hydroxyl radical is an extremely potent oxidant [Buettner GR, 1993]. It is able to cause degradation of most biological macromolecules: peroxidation of lipids, oxidation of sugars, oxidation of protein thiols, DNA base damage, and strand breaks to nucleic acids [Skibba JL, 1986; Skibba JL, 1989; Khadir A, 1999]. On the other hand, heat can induce intracellular antioxidants. Glutathione levels, superoxide dismutase (SOD) activity, glutathione peroxidase (GPx) activity, and glutathione S-transferase (GST) activity have been reported to increase after heat stress [Spitz DR, 1990]. Increases in these antioxidants indicate the involvement of oxidative stress. It has been shown that overexpression of MnSOD by stable transfection confers cell resistance to hyperthermia treatment at 43°C and 45°C [Li JJ, 1997]. Depletion of GSH by L-buthionine sulfoximine (BSO) or inhibition of catalase by 3-amino-1,2,4-triazole (ATZ) can increase cell susceptibility to killing [Lord-Fontaine S, 1999]. Cells resistant to H_2O_2 are resistant to hyperthermia treatment [Spitz DR, 1990]. These findings suggest that superoxide radicals and their reaction products are critical mediators involved in hyperthermia-mediated cytotoxicity.

There is growing evidence that mitochondria are highly susceptible to oxidative stress [Arai M, 1999; Sharkey SM, 1993] because of adjacency to the site of phosphorylation [Shigenaga MK, 1994]. Mitochondria have been considered as a major source for ROS generation *via* the respiratory chain [Guarnieri C, 1992]. The levels of ROS in mitochondria are regulated by mitochondrial enzymes, such as MnSOD, GPx1, and the mitochondrial form PhGPx (L-PhGPx). PhGPx is the enzyme that directly reduces phospholipid- and cholesterol- hydroperoxides present in membranes [Ursini F, 1985; Thomas JP, 1990]. Two forms of PhGPx are expressed in tissues, L-PhGPx and S-PhGPx. L-PhGPx, containing a mitochondrial target sequence, is located in the intermembrane space of mitochondria. S-PhGPx, without the leader sequence, is present

in the cytosol. Overexpression of PhGPx *in vitro* has been shown to significantly suppress cell death mediated by LOOHs [Imai H, 1996; Yagi K 1996]. L-PhGPx is able to block the loss of mitochondrial membrane potential, being more efficient than S-PhGPx in preventing ROS-induced cell death [Arai M, 1999; Nomura K 1999].

The generation of ROS during heat may also play a role in the induction of heat shock proteins (Hsps) [Gorman AM, 1999]. The Hsps are stress proteins that are evolutionary conserved. Among them, the Hsp70 family has been investigated for its role in thermotolerance. The expression of Hsp70 is related to the development of heat resistance. It appears that tolerance to higher temperature is directly correlated to elevated levels of Hsp70 [Su CY, 1998; Anderson RL, 1988]. Prevention of Hsp70 induction results in heat sensitization [Gorman AM, 1999].

The objective of this part of the study was to explore the mechanism of heat-induced cytotoxicity. We hypothesized that L-PhGPx could contribute to protection against heat-induced damage by reducing intracellular hydroperoxides generated as a result of oxidative stress in mitochondria.

Materials and Methods

Reagents

L-Buthionine sulfoximine (BSO), glutathione reductase (GR), glutathione (GSH), and sodium selenite were obtained from Sigma (St. Louise, MO). Lipid Hydroperoxide Assay kit and reagents were purchased from Cayman (Ann Abor, MI). Chloroform (HPLC grade), methanol (HPLC grade), crystal violet, and acetic acid were obtained from Fisher Scientific Co. (Pittsburgh, PA). Minimum essential medium (MEM), fetal bovine serum (FBS), MEM non-essential amino acids, and Geneticin™ (G418) were bought from GIBCO (Grand Island, NY). NADPH, 5-sulfosalylic acid (SSA), 5, 5'-dithio-*bis*-

(2-nitrobenzoic acid) (DTNB). 2-vinylpyridine (2-VP) was obtained from Aldrich (Milwaukee, WI). The mouse monoclonal antibody to Hsp70 inducible form (Hsp70i) and the rat monoclonal antibody to Hsp70 constitutive form (Hsp70c) were bought from StressGen Co. (Victoria BC, Canada). The secondary antibodies of horseradish peroxidase conjugated IgG anti-mouse and anti-rat were obtained from Sigma (St. Louis, MO). Rhodamine 123 (Rh123) was bought from Molecular Probes Inc. (Eugene, OR), a stock solution (32 mM) was made in 100% ethanol and stored at −20°C.

Cell Culture

Neo and P-4 cell lines were selected for the hyperthermia studies. Cells were routinely cultured in T-25 cell culture flasks at 37°C, 5% CO_2. Cells were grown in MEM supplemented with 10% FBS, 1% non-essential amino acid, 30 nM sodium selenite and G418 (350 μg/mL). G418 was removed from the medium one cell passage number before an experiment.

Hyperthermia Treatment

Neo and P-4 cells (1×10^6) were seeded into 100-mm dishes, or ($1 - 2 \times 10^5$) into 6-well plates 24 h before heating. Medium was replaced with fresh complete medium immediately before heating. Cells were heated in a water bath at 43°C for 1 and 3 h. After heating, cells were incubated at 37°C for different post incubation time, and then assayed.

GSH Measurement

Total intracellular glutathione, defined as GSH plus two glutathione disulfide (GSSG), was determined by colorimetric reaction of DTNB (5,5'-dithio-*bis*(2-nitrobenzoic acid)) with GSH to form TNB (5-thio-2-nitrobenzoic acid). The rate of TNB formation, which is proportional to total GSH concentration, was measured

spectrophotometrically at 412 nm. Cellular GSSG is reduced to GSH by GR, using NADPH as co-factor. The assay started with lysis of the cell pellet in 5% 5-sulfosalicylic acid (SSA). Total GSH was measured by mixing 50 μL sample with 100 μL water, 700 μL working buffer [2 mM NADPH in stock solution (0.143 M sodium phosphate, 6.3 mM EDTA)], and 100 μL DTNB (6 mM DTNB in stock solution). The assay was initiated by addition of 50 μL GR (266 U/mL). The rate of TNB formation was followed at 412 nm, every 20 s for 3 min using a Beckman DU-70 spectrophotometer. Total glutathione of a sample was calculated from a standard curve of GSH concentration as a function of the rate (change in absorbance/time). Cellular GSSG was determined by the same DTNB assay after GSH was masked by 2-vinylpyridine (2-VP). 2-VP (3 μL) was added to 100 μL of sample prepared as above for total GSH measurement. After 2 h incubation at 4°C, GSSG was measured as described in the DTNB assay. The level of GSSG in the cells we studied was below the detection limit.

PhGPx Activity Assay

The activity was measured by coupled enzymatic assay as described in Chapter II. Briefly, the spectrophotometric test mixture contained in 1 mL, the following: 0.1 M Tris-HCl (pH 8.0), 2 mM disodium ethylenediamine tetraacetate (EDTA), 1.5 mM NaN_3, 0.1% Triton X-100 (peroxide free) (Sigma, St. Louis, MO), 3 mM GSH, and 1.5 U/mL GR. Sample (1 mg) was added to the test mixture and incubated at 37°C for 8 min. Then 0.2 mM NADPH was added and the mixture was incubated for another 8 min to allow the enzyme and GSH to be converted to the reduced forms. The nonspecific NADPH oxidation rate was recorded for 4 min at 340 nm, and then the enzyme reaction started by the addition of PCOOH (10-30 mM). The rate of specific NADPH oxidation was recorded every 20 s for 4 min at 340 nm using a Beckman DU-70 spectrophotometer. The activity was calculated by subtracting the nonspecific NADPH oxidation rate from

the observed NADPH oxidation rate after substrate addition. The specific activity is expressed as units per milligram protein, 1 unit being the amount of enzyme catalyzing oxidation of 1 μM of NADPH per minute.

Clonogenic Survival Assay

The Neo and P-4 cells ($1 - 2 \times 10^5$) were seeded into 6-well plates 24 h before heating. After 1 h and 3 h heat, cells were trypsinized. The resulting single-cell suspension was counted and diluted. A certain cell number of cells, which yielded 50 – 100 surviving colonies, were seeded into 6-well plates for colony survival. After two-week incubation at 37°C, cells were fixed with methanol:acetic acid (3:2, *v/v*) mixture and stained with 0.1% crystal violet. A colony containing more than 50 cells was considered as a survivor and counted. The cell survival fraction (SF) was calculated as following:

$$SF = \text{Colonies formed} / (\text{Cell seeded} \times \text{Plating efficiency})$$

Survival data following treatment were normalized to appropriate control plating efficiencies.

Flow Cytometric Analysis of Rh123

Changes in the mitochondrial membrane potential were examined by monitoring staining with Rh123. Rh123 is a cell-permeable, cationic, green-fluorescence dye that is readily sequestered by active mitochondria without inducing cytotoxic effects [Johnson LV, 1980]. It is widely used to study mitochondrial transmembrane potential [Aria M, 1999; Scaduto RC, 1999]. In this study, 1×10^5 cells were seeded in 6-well plates 24 h before heating. After 1 and 3 h heat at 43°C, cells were immediately stained with 25 μM Rh123 in MEM for 30 min. Cells were then washed three times with medium and

trypsinized. The intensity fluorescence from Rh123 in cells was analyzed with a flow cytometer (FACScan, Becton Dickinson).

Western Analysis for Hsp70

The western analysis described in Chapter II was used for the examination of the heat shock protein levels. Both the inducible form of Hsp70 (Hsp70i) and the constitutive form (Hsp70c) were analyzed after hyperthermia treatment. Briefly, total cellular protein (30 μg) was electrophoresed in a 12.5% SDS-polyacrylamide running gel with 5% stacking gel. After that the protein was transferred to a nitrocellulose membrane (Schleicher & Schell, Keene, NH), and the membrane was blocked in 10% non-fat milk with TBST (0.02 M Tris buffer pH 7.5, 0.137 M NaCl, and 0.1% Tween 20) for 1 h at room temperature. The membranes were then probed with primary antibodies specific to Hsp70i and Hsp70c (1:1,000 dilution) overnight at 4°C. After that, the membrane was incubated with secondary antibody of horseradish peroxidase conjugated IgG (1:10,000). Membranes were exposed to X-ray films using enhanced chemiluminescence (ECL) kit (Amersham Pharmacia Biotech Inc., Piscataway, NJ).

Statistics

Microsoft Excel program (Excel 97 SR-1) was used in calculating mean values and standard errors. ANOVA-Tukey test was used to compare the differences between two groups. In all cases, the statistical significance of differences was determined at a level of $p < 0.05$.

All the data presented are from an average of at least three independent experiments. In the cases of western and flow cytometric analyses, representative figures of at least two independent experiments are given.

Results

Heat Did Not Change the Activity of PhGPx

Hyperthermia treatment has been found to induce the synthesis of cellular antioxidants such as glutathione, superoxide dismutase, and glutathione peroxidase [Mitchell JB, 1983; Loven DP, 1985; Privalle, CT, 1987; Kapoor M, 1987]. The increased syntheses of these antioxidants indicate a cellular response to the oxidative challenge produced by hyperthermia treatment (HT). We examined whether HT at 43°C might induce the activity of cellular PhGPx. Both Neo and P-4 cells were heated in a water bath for 3 h at 43°C, followed by post-incubation at 37°C overnight. Cells were harvested and PhGPx activity was assayed. Heat did not cause statistical changes of PhGPx activty in either cell line (**Figure IV-1**).

The Effect of L-PhGPx on Heat-Induced Cytotoxicity

Oxidative stress has been suggested as a possible mechanism in heat-induced cell killing. This concept is strengthened by the finding that overexpression of MnSOD confers cell resistance to heat in human T-cells [Wong GH, 1991] and breast cancer cells (MCF-7) [Li JJ, 1997], and by the fact that H_2O_2-resistant cells with elevated catalase activity increase resistance to hyperthermic toxicity [Spitz DR, 1990]. Also, decreases in cellular antioxidant levels using SOD and catalase inhibitors increase heat sensitivity in Chinese hamster ovary cells [Khadir A, 1999; Lord-Fontaine S, 1999]. L-PhGPx, as a unique repair enzyme, may be able to protect cells from heat by reduction of hydroperoxide levels as a result of heat cytotoxicity. We investigated whether the cytotoxicity of HT can be inhibited when MCF-7 cells overexpress L-PhGPx. Clonogenic survival was determined after Neo and P-4 cells were exposed to heat for 1 and 3 h (43°C) (**Figure IV-2**). The findings here demonstrate that overexpression of L-

PhGPx decreases the sensitivity of MCF-7 cells to hyperthermia. P-4 cells were more resistant to hyperthermia than Neo cells.

It can be concluded that L-PhGPx plays an important role in the tolerance of MCF-7 cells to the cytotoxic effect of hyperthermia at 43°C.

Inhibition of GSH Lowered the Protective Effect of L-PhGPx

Glutathione (γ-glutamylcysteinyl glycine) is a ubiquitous tripeptide. It is the dominant nonprotein thiol in mammalian cells with multiple functions ranging from antioxidant defense to modulation of cell proliferation. Total cellular glutathione includes glutathione (GSH) and glutathione disulfide (GSSG). The ratio of GSH to GSSG in eukaryotic cells ranges from 10:1 to 100:1 [Hwang C, 1992; Meredith MJ, 1982; Meister A, 1988]. GSH has been shown to be an important modifier of hyperthermia-induced cytotoxicity [Freeman ML, 1985; Lord-Fontaine S, 1999]. GSH depletion by buthionine sulfoximine (BSO) or diethylmaleate (DEM) was found to significantly increase thermal toxicity of cells heated at both 42.5°C and 43°C [Mitchell JB, 1983]. GSH depletion can prevent the syntheses of heat shock proteins (Hsps) [Mitchell JB, 1983]. Furthermore, inhibition of GSH can decrease the enzymatic activities of GPx [Flohe L, 1982; Lord-Fontaine S, 1999] as well as PhGPx [Nomura K, 1999].

GSH is compartmentalized inside cells. GSH is synthesized primarily in the cytoplasmic compartment and utilized in the nucleus, mitochondrial matrix, endoplasmic reticulum, and extracellular spaces [Meister A, 1991]. The availability of GSH in these compartments is determined by the complex interactions of utilization, transport, synthesis, and reduction of GSSG. It has been reported that the nuclear GSH pool is distinct from other subcellular pools in that it resists depletion after exposure of cells to

BSO [Edgren MR, 1987]. The mitochondrial pool of GSH relies more on the transport of cytosolic GSH into the matrix [Griffith OW, 1985; Smith CV, 1996]. Depletion of cytosolic GSH results in the decrease of the GSH pool in the mitochondria [Masini A, 1994; Kurokawa T, 1996]. However, mitochondrial GSH decreases much more slowly than that of cytoplasm [Romero FJ, 1984; Griffith OW, 1985; Freeman ML, 1988]. The half life of GSH in mitochondria is about 30 h, however, the turnover time in cytoplasm is 1 - 2 h [Meredith MJ, 1982]. GSH plays a crucial role in protecting mitochondria against oxidative injury [Masini A, 1994; Kurokawa T, 1996].

As an important cofactor for PhGPx, the level of GSH could affect the enzymatic activity of PhGPx. We hypothesized that GSH depletion could decrease PhGPx enzymatic activity and therefore sensitize cells to heat-induced cytotoxicity. Cells were preincubated with BSO (5 mM, 10 mM) for 24 h. Cells were then heated at 43°C for 3 h in the presence of BSO. The inhibition by 5 mM or 10 mM BSO caused 42 or 60% decrease in total intracellular GSH levels in Neo cells and 55% or 67% in P-4 cells (**Figure IV-3**). The decrease in GSH did not significantly influence the activity of PhGPx in either cell; however, it lowered the effective PhGPx activity (**Table IV-1**). The effective PhGPx activity is defined as the product of total cellular GSH and the maximum PhGPx activity. PhGPx requires GSH as a cofactor to function. The enzyme kinetics of PhGPx is first order in GSH. The product of PhGPx activity and GSH level better represents the activity of PhGPx in the cell. The effective PhGPx activity was reduced significantly by BSO in P-4 cells but not in Neo cells (**Table IV-1**). Inhibition of GSH sensitized P-4 cells to 43°C heat (**Figure IV-4**). In contrast, the Neo cells were slightly resistant to heat following GSH depletion (**Figure IV-4**).

Overexpression of L-PhGPx Did Not Influence Hsp70

Heat shock proteins (Hsps) are the products of heat responsive genes. They are evolutionarily conserved and contribute to the acquired thermotolerance. Among them, the Hsp70 family has been well investigated for its role in induced thermoprotection. The inducible form of Hsp70 (Hsp70i) is synthesized after heat treatment. However, in humans Hsp70i is not only elevated in response to stress, but is also present at basal levels in unstressed cells [Williams RS, 1993; Karlseder J, 1996]. The constitutive form, Hsp70c, is highly homologous to Hsp70i. Overexpression of Hsp70c confers upon cells a marked resistance to thermal killing [Chong KY, 1998], suggesting that Hsp70c actively participates in heat-induced oxidative protection. Heat can cause both Hsp70i and Hsp70c enhancement [Su CY, 1998]. However, the mechanism of Hsp70 induction by heat remains unclear. ROS may contribute to the induction of heat shock proteins during stress response. We hypothesized that LOOHs may play a role in the induction of Hsp70, and the LOOH removal enzyme, L-PhGPx, may be involved in the regulation of Hsp induction. To test this hypothesis, we stressed Neo and P-4 cells with heat (43°C, 3h). After 0 to 18 h of post-incubation, the protein expression of both inducible and constitutive forms of Hsp70 was analyzed by western blotting (**Figure IV-5**). The expression of Hsp70i was increased immediately after heat, reached a maximum after 6 h, and was maintained for 18 h. However, there was no difference in the increase in Hsp70i between Neo and P-4 cells, suggesting that LOOHs appear not to be involved in the induction of Hsp70i. Hsp70c did not change significantly before or after heating in both Neo and P-4 cells (**Figure IV-5**). Although the expression levels of Hsp70i and Hsp70c were not different between Neo and P-4 cells, these two cells exhibited different sensitivity to heat. These findings suggest that the thermoprotection of L-PhGPx is probably not mediated by Hsp70 induction.

L-PhGPx Protected Mitochondrial Function from Heat

Mitochondrial membrane potential was assessed by flow cytometric analysis with Rh123 staining. Rh123, a lipophilic cation, is selectively sequestered by active mitochondria. The uptake of Rh123 is directly proportional to mitochondrial membrane potential [Aria M, 1999; Scaduto RC, 1999]. Neo and P-4 cells were heated for 1 and 3 h at 43°C. After heat, cells were immediately stained with Rh123 for 30 min and assayed *via* flow cytometer. The fluorescence intensity of Rh123 in Neo and P-4 cells without heat was 174 and 116 arbitrary units, respectively (**Figures IV-6A, & IV-6B**). After 1 and 3 h heating, the intensity from Neo cells was decreased to 105 and 97 (**Figures IV-6C, & IV-6E**). However, P-4 cells retained at intensities of 179 and 150 units (**Figures IV-6D, & IV-6F**).

These observations indicate that L-PhGPx protects cells from hyperthermia-mediated damage by preventing loss of the mitochondrial membrane potential.

Discussion

Multiple antitumor treatments have been developed such as surgery, chemotherapy, radiotherapy, PDT, and hyperthermia. Hyperthermia has the potential for human cancer treatment, particularly in combination with radiotherapy or chemotherapy. Advances have been made in these areas, but resistance to treatment remains common.

Elevated temperature is likely to increase the generation of oxidants in cells and to increase their reactivity with cellular components. Thus, thermal stress is likely to cause an imbalance between prooxidants and antioxidants. The sensitivity of cells to heat can be modulated by changing intracellular antioxidant levels. Overexpression of MnSOD results in cytoprotection against heat [Li JJ, 1997], while inhibition of catalase by ATZ leads to a reduction in resistance to heat [Lord-Fontaine S, 1999]. Modulation of intracellular L-PhGPx levels also changes the susceptibility of cells to heat. This is

clearly illustrated in cell survival. P-4 cells with a 7-fold increase in PhGPx activity are more resistant to heat (43°C) than Neo cells (**Figure IV-2**).

PhGPx, as a glutathione dependent enzyme, relies on cellular GSH to achieve its effective function. MCF-7 cells have relatively high levels of GSH but nondetectable GSSG levels. They are resistant to the depletion by BSO. BSO treatment (10 mM) only results in about 60% inhibition of total GSH (**Figure IV-3**). This inhibition of GSH blunts the protection of L-PhGPx against heat cytotoxicity (**Figure IV-4**). However, the reasons underlying this observation are not yet apparent. Mitochondrial GSH decreases more slowly than the cytoplasmic GSH after BSO depletion [Romero FJ, 1984; Freeman ML, 1988]. Therefore, the inhibition of mitochondrial GSH by 10 mM BSO would be less than 60% in MCF-7 cells. These cells, however, contain very few mitochondria (unpublished data from Dr. T.D. Oberley, University of Wisconsin-Madison). We were not successful in isolating the mitochondria from MCF-7 cells. It remains unknown how inhibition by BSO would influence the levels of mitochondrial GSH as well as the mitochondrial PhGPx. The effective activity (**Table IV-1**) may only represent the PhGPx activity in terms of the total cellular compartment rather than the situation in the mitochondria.

Generation of $O_2^{\bullet -}$ has been hypothesized as a critical mechanism in heat-induced cytotoxicity [Privalle CT, 1987]. Superoxide can be dismutated to H_2O_2. In a biological system, H_2O_2 is a weak oxidant. In the presence of iron, H_2O_2 can generate hydroxyl radical ($^{\bullet}OH$) by scission of the peroxide bond through the Fenton reaction. The hydroxyl radical is able to cause the oxidation of lipids, sugars, protein thiols, and DNA [Halliwell B, 1999]. L- PhGPx can reduce free radical-induced lipid peroxidation in mitochondria [Arai M, 1999], thereby protecting the mitochondrial function. L-PhGPx could also play an important role in reducing H_2O_2 to compensate for the lack of GPx1 in mitochondria

[Esworthy RS, 1997] of MCF-7 cells (Chapter II). Although PhGPx reduces H_2O_2 less effectively than GPx1 [Maiorino M, 1990], L-PhGPx might limit the local increases in H_2O_2 concentration. Removal of H_2O_2 in mitochondria by L-PhGPx could prevent mitochondrial injury as a result of the generation hydroxyl radical. Overexpression of L-PhGPx protected against the loss of the mitochondrial membrane potential in MCF-7 cells as examined with Rh123 staining (**Figure IV-6**). The uptake of Rh123 is directly proportional to the membrane potential [Scaduto RC, 1999]. The reason that P-4 cells have lower basal levels of membrane potential than Neo is not clear. However, the fluorescence intensity of Rh123 remains higher in P-4 cells even after 3 h heating; cells without transfection (Neo) lose the Rh123 fluorescence intensity. Thus, L-PhGPx appears to preserve the functions of mitochondria by reducing intracellular hydroperoxides generated as a result of damage to the mitochondrial respiratory machinery.

Interestingly, there was no difference in the expression of the Hsp 70 family between Neo and P-4 cells (**Figure IV-5**). The inducible form of Hsp70 was induced immediately after heat, and reached to maximum 6 h after heat in both cells. The constitutive form did not change before or after heat. These findings suggest that the protective effect of L-PhGPx is not through the induction of heat shock proteins. It also suggests that the induction of Hsp70 may not be mediated by LOOHs.

The different responses to heat between L-PhGPx transfected cells and nontransfected cells indicate that mitochondria appear to be a primary target for hyperthermia-mediated cytotoxicity.

Figure IV-1. Heat stress did not influence PhGPx activity.

Neo and P-4 cells were heated for 3 h in a water bath at 43°C followed by incubation at 37°C overnight. The activity of PhGPx was then assayed. One unit of enzyme activity is defined as the amount of enzyme catalyzing oxidation of 1 μM NADPH per min.

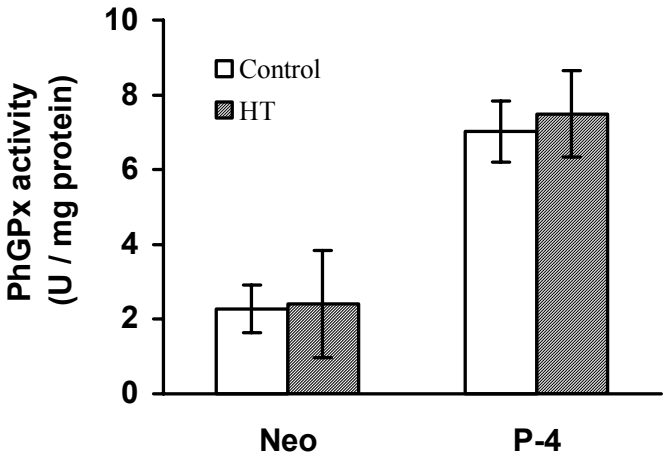
PhGPx activity
(U / mg protein)
10
8
6
4
2
0
Control
HT
Neo
P-4

Figure IV-2. L-PhGPx protected cells from hyperthermia-induced cytotoxicity. Neo and P-4 cells were exposed to 43°C for 1 and 3 h. Cell survival was examined by clonogenic survival assay. Data are mean ± SE, n = 3, *$p < 0.05$ when compared to the corresponding non-transfected cells.

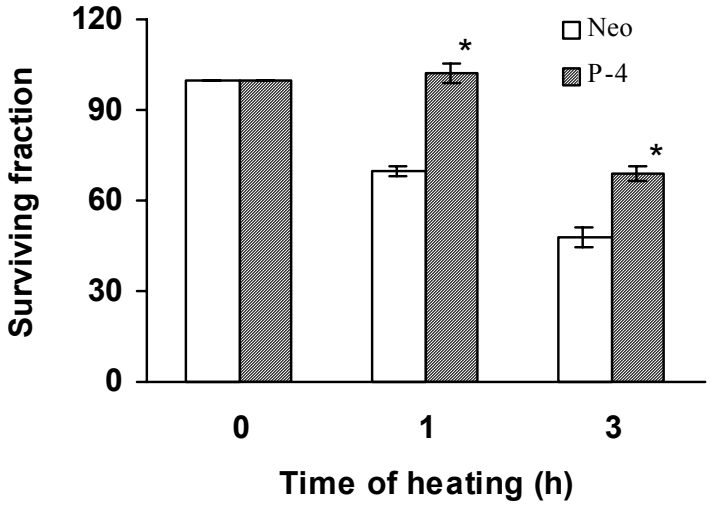
120
90
60
30
0
Surviving fraction
Neo
P-4
*
*
0
1
3
Time of heating (h)

Figure IV-3. BSO decreased total GSH levels in MCF-7 cells.

Neo and P-4 cells were treated with BSO (5 mM or 10 mM) for 27 h in full media. The level of total GSH was determined by GSH assay. The GSSG level in the cells were below the detection limit. Data are mean ± SE, n = 3, *$p < 0.05$ compared to the corresponding non-BSO treated controls.

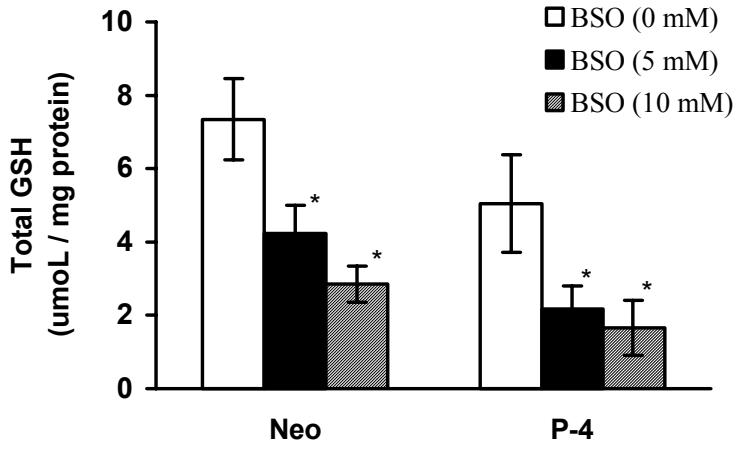
BSO (0 mM)
BSO (5 mM)
BSO (10 mM)
Total GSH
(umoL / mg protein)
10
8
6
4
2
0
*
*
*
*
Neo
P-4

Figure IV-4. BSO attenuated the protective effect of L-PhGPx against hyperthermia.

Neo and P-4 cells were treated with 0, 5, or 10 mM BSO for 24 h in full media. Cells were then heated for 3 h at 43°C in the presence of BSO. Cell survival was determined by clonogenic assay. Data are mean ± SE, n = 3, *$p < 0.05$ compared to corresponding non-transfected controls.

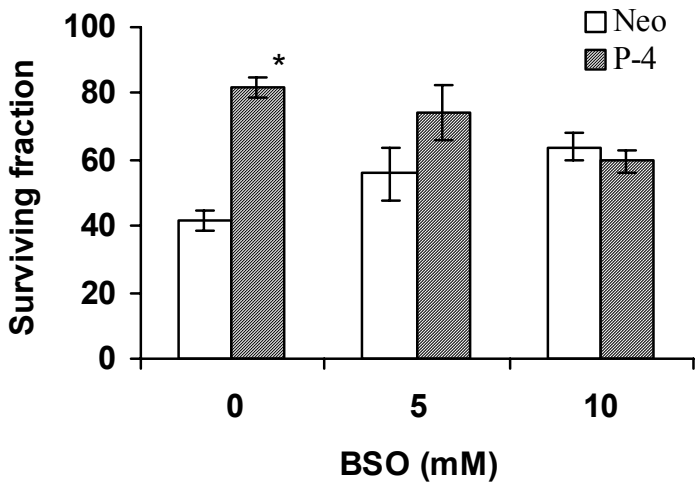
Neo
P-4
100
80
60
40
20
0
Surviving fraction
*
0
5
10
BSO (mM)

Figure IV-5. L-PhGPx did not affect the expression of Hsp70 in MCF-7 cells before or after heat stress.

Neo and P-4 cells were heated for 3 h. The protein levels of Hsp70i and Hsp70c were examined using western blot. Total cellular protein homology (30 μg) was separated on 12.5% SDS PAGE. Hsp70i and Hsp70c were detected by anti-mouse Hsp70i and anti-rat Hsp70c antibodies, respectively. Control represents cells without heat; HT/0, HT/2, HT/6, and HT/18: cells assayed immediately, 2, 6, and 18 h after heat. Data are representative of two independent experiments.

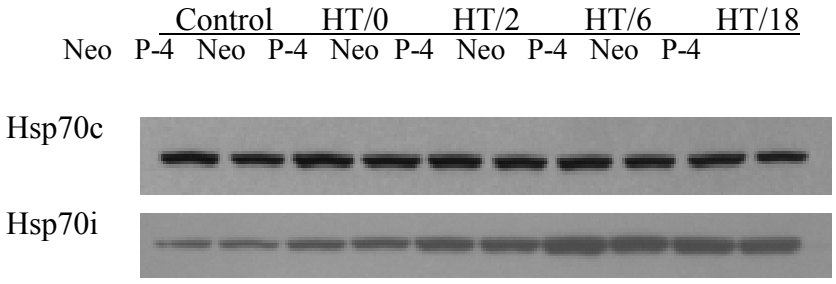
Control HT/0 HT/2 HT/6 HT/18
Neo P-4 Neo P-4 Neo P-4 Neo P-4 Neo P-4
Hsp70c
Hsp70i

Figure IV-6. L-PhGPx protected the mitochondrial membrane potential from heat. Neo and P-4 cells were heated for 1 or 3 h at 43°C. After heating, cells were stained with 25 μM Rh123 for 30 min and assayed *via* the flow cytometer. The events of cell counted were plotted against the arbitrary fluorescence intensity of Rh123. Neo cells (A, C, E), P-4 cells (B, D, F); Cells without heating (A, B); 1 h heating (C, D); 3 h heating (E, F). Data are representative of three independent experiments.

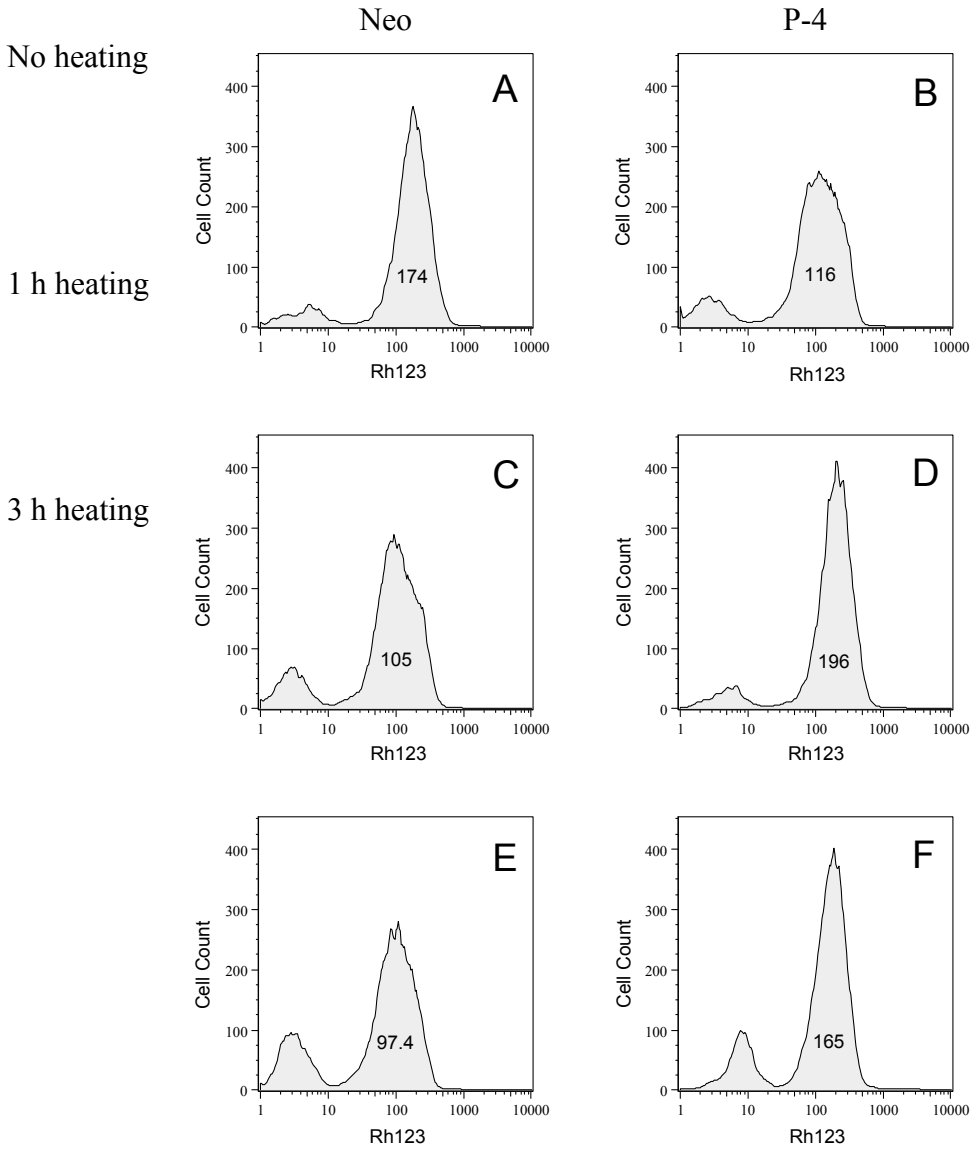
Neo
P-4
No heating
1 h heating
3 h heating
A
B
C
D
E
F
Cell Count
Rh123
174
116
105
196
97.4
165
0
100
200
300
400
1
10
100
1000
10000

Table IV-1. Depletion of GSH by BSO Lowered the Effective PhGPx Activity in L-PhGPx Overexpressing Cells.

Cells	BSO (mM)	GSH (μmol/mg protein)	PhGPx activity (U/mg protein)	Effective PhGPx activity[a, b]
Neo	0	7.3 ± 1.1	1.5 ± 0.4	11 ± 3.4
	5	4.2 ± 0.8[c]	2.3 ± 0.3	9.7 ± 2.2
	10	2.9 ± 0.5[c]	2.7 ± 0.2	7.8 ± 1.5
P-4	0	5.1 ± 1.3	6.3 ± 0.3	32.1 ± 8.3
	5	2.2 ± 0.6[c]	6.6 ± 1.4	14.4 ± 5.0[c]
	10	1.7 ± 0.8[c]	8.2 ± 0.5	13.9 ± 3.1[c]

The effective PhGPx activity is defined as the product of total cellular GSH and maximum PhGPx activity. Data are mean ± SE, n = 3. [a] Units are: (μmol GSH • Units PhGPx) / , $(\text{mg protein})^2$; [b] the errors quoted were determined by the propagation of errors method; [c] $p < 0.05$ compared to their corresponding controls.

CHAPTER V

CONCLUSIONS AND FUTURE DIRECTIONS

Conclusions

The main goal of cancer treatment is to destroy tumor tissue. However, it is important that the treatment has only minor side effects on the surrounding normal tissues. Most current cancer therapies are often limited in their effectiveness because of their cytotoxicity to normal tissues. However, the mechanisms that induce cytotoxicity in cancerous cells *versus* normal cells can be different because their replication, metabolism, antioxidant levels, and redox state differ. We may be able to achieve greater success in cancer treatment by utilizing these differences between normal and tumor tissues.

PhGPx is a seleno-dependent peroxidase. It specifically reduces lipid hydroperoxides (LOOHs), particularly, phospholipid- and cholesterol-hydroperoxides. PhGPx requires several secondary enzymes (GR, G-6-PD), and cofactors (GSH, NADPH) to function with high efficiency. The enzymatic function of PhGPx is shown in **Scheme I-3**. There are two forms of PhGPx found in mammals: a mitochondrial form (L-PhGPx), and a nonmitochondrial form (S-PhGPx). L-PhGPx is located in the intermembrane space of the mitochondria, S-PhGPx is in the cytosol. L-PhGPx is dominantly expressed in testis tissue, while S-PhGPx is present in most somatic tissues.

In this project, a cell model system that stably overexpresses sense L-PhGPx was established and characterized (Chapter II). Stable transfection of L-PhGPx results in the expression of L-PhGPx in MCF-7 cells, while the nontransfected controls only have S-PhGPx. Our newly developed activity assay allows the successful assessment of PhGPx.

Overexpression of the L-PhGPx results in up to 7-fold increase in PhGPx activity. This increase in PhGPx activity directly correlates to mRNA and protein levels. A new concept introduced in this thesis is "effective PhGPx activity", which is defined as the product of PhGPx activity and total cellular GSH. Because GSH is the main substrate for PhGPx, the combination of PhGPx activity and GSH levels provides a better evaluation of the function of PhGPx in cells.

Transfection of L-PhGPx does not cause significant changes in other cellular antioxidant enzymes or the GSH pool in MCF-7 cells. Overexpression of L-PhGPx, however, can inhibit cell growth. The plating efficiency decreases with elevated effective PhGPx activity.

We exposed the L-PhGPx overexpression cell model system to the anti-cancer treatments of photodynamic therapy (PDT) and hyperthermia (HT). Both PDT and HT have been demonstrated to induce oxidative stress. Thus, increases in cellular antioxidant enzymes could protect cells from PDT- and HT-mediated oxidative damage. PhGPx is a critical enzyme in detoxifying intracellular peroxidized lipids. It is an important antioxidant defense enzyme in biomembranes. L-PhGPx is located in the mitochondria. Mitochondria are a major target for oxidative stress. We hypothesized that L-PhGPx could play a role in the cell resistance to PDT and HT by reducing the level of LOOHs, thereby protecting mitochondrial function. This hypothesis was tested in Chapter III and Chapter IV. Cells with higher activity level of PhGPx were found to survive better after both PDT and HT treatments. A direct correlation was found between cell survival and effective PhGPx activity. Overexpression of L-PhGPx prevents cell death from PDT by repairing LOOHs generated by $^1O_2$. Measurement of LOOHs with a lipid hydroperoxide assay and EPR spin trapping confirm that LOOHs are an important mediator in PDT-induced cytotoxicity.

Overexpression of L-PhGPx protects cells from heat. Cell survival is decreased when the effective activity of PhGPx in cells is lowered by depletion of GSH with BSO. Evidence from hyperthermia experiments shows that L-PhGPx protects cells from heat-induced damage by preventing the loss of mitochondrial membrane potential. Mitochondrial enzymes are critical for protecting against $O_2^{\bullet-}$- and H_2O_2 -mediated cytotoxicity. PhGPx repairs not only lipid hydroperoxides, but can also remove H_2O_2. Although the rate constant is lower for removing H_2O_2 compared to GPx1 [Maiorino M, 1990], PhGPx in mitochondria could play an important role in H_2O_2 removal and may compensate for the lack of GPx1 in MCF-7 cells (Chapter II).

An interesting finding in this thesis work is that tumor cells contain higher levels of PhGPx activity than their normal counterparts (**Figure V-1**). The activity of PhGPx in MCF-7 cells is found 10-fold greater than that in MCF-10A cells, an adhering human breast epithelial cell line derived from fibrocystic tissues and immortalized by long-term passage in calcium-deficient medium [Soule H, 1990].

In summary, increased level of L-PhGPx contributes to the resistance of cells to PDT and HT. L-PhGPx appears to maintain the functions of mitochondria by removal of intracellular hydroperoxides generated as a result of oxidative stress in mitochondria. Cells transfected with L-PhGPx are more resistant to PDT and HT than the non-transfected cells, suggesting that mitochondria are a primary target for PDT and HT. Thus, inhibition of PhGPx levels in tumor cells might increase the efficacy of PDT and HT.

Figure V-1. Comparison of PhGPx activity in MCF-7 and MCF-10A cells.
The maximum potential PhGPx activity was determined in both MCF-7 and MCF-10A cells. MCF-10A (kindly provided by Dr. Frederick Domann) is an immortalized epithelial cell line derived from human breast fibrocystic tissue. Cells were cultured in MEGM (Mammary Epithelial Growth Medium) supplemented with 100 ng/mL cholera toxin and 30 nM sodium selenite. MCF-7 cells were grown in MEM with 10% FBS, 1% non-essential amino acids, and 30 nM sodium selenite. Cells were grown in 100-mm dishes and fed with fresh medium 24 h before harvesting. Data are mean ± SE, n = 3, *$p < 0.01$ compared to MCF-10A.

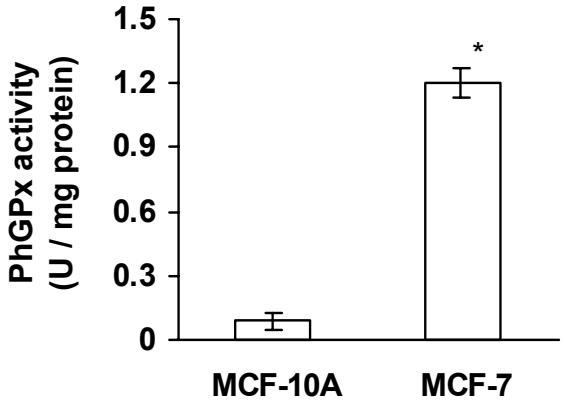
PhGPx activity
(U / mg protein)
1.5
1.2
0.9
0.6
0.3
0
*
MCF-10A
MCF-7

Future Directions

This work has addressed the role of mitochondrial PhGPx (L-PhGPx) in PDT- and HT-mediated cytotoxicity. It has demonstrated that increasing the level of L-PhGPx in cells leads to their resistance to these hydroperoxide-mediated cancer therapies. These findings could have wide implications, as there are other cancer treatments that have an oxidative component in their action. Modulation of PhGPx (L- and/or S-forms) in normal and tumor tissues would be a feasible way to increase the efficacy of anticancer therapies such as PDT and HT. From our data and others [Huang HS, 1999], it is found that tumor cells contain higher PhGPx levels than their normal counterparts. It can be expected that inhibition of PhGPx in tumor tissue will sensitize the tumor to treatment, while increase in normal tissues will protect surrounding healthy cells. There are no known specific chemical inhibitors of PhGPx that could be used to blunt the activity of this enzyme in tumor tissue. Antisense oligonucleotides would be a possible approach to inhibit this protein. Antisense oligonucleotides are short sequences of DNA designed to inhibit the production of a protein of interest. Antisense inhibition has been applied in clinical trials for acute myelogenous leukemia, human immunodeficiency virus, and human papilloma virus infection [Phillips MI, 1997]. We will use molecular strategies to develop antisense oligonucleotides for mitochondrial or nonmitochondrial PhGPx to decrease the enzyme levels in tumors. Therefore, we will be able to sensitize the tumor cells to LOOH-mediated cancer treatment.

Although this work provides a better understanding of the mechanisms of PhGPx in causing cell resistance to PDT and HT, there are still unresolved questions. For instance, the exact subcellular distribution of L-PhGPx in the transfected MCF-7 cells is not known. In a compartmentalized cell, location is important in terms of antioxidants and prooxidants. For example, MnSOD rather than CuZnSOD is responsible for

dismutation of $O_2^{\bullet -}$ generated in mitochondria. PhGPx can be present in mitochondria or in cytosol, as L-PhGPx and S-PhGPx, respectively. PhGPx in mitochondria (L-PhGPx) lowers the level of hydroperoxides, protects against the loss of plasma membrane integrity, and the loss of mitochondrial membrane potential (Chapters III, & IV). L-PhGPx plays a major role in the protection against mitochondria-mediated apoptosis [Nomura K, 1999]. The cDNA of PhGPx used in our study is that of L-PhGPx as examined by DNA sequencing. However, we were not able to directly visualize the localization of PhGPx due to the lack of specific antibody to PhGPx. Development of a monoclonal or polyclonal antibody to PhGPx will be necessary for future studies of this enzyme. Alternatively, measurement of PhGPx activity in the different subcellular compartments could be an approach. For example, comparison of PhGPx activity between the mitochondria and the rest of the cell could provide the information of the location of L-PhGPx.

In this work, we limited our studies to the function of L-PhGPx in anticancer therapies. The role of S-PhGPx is still not clear. It should be noted that most somatic tissues contain S-PhGPx. It will be of importance to establish a cell model with overexpression of S-PhGPx. Since both L- and S-PhGPx have the same enzymatic function, except that they are located in different subcellular compartments. Comparison of the effects of L-PhGPx and S-PhGPx would allow for determination of the targets of oxidative stress. We would then be able to better understand the mechanisms involved in oxidation.

An interesting finding in this thesis work is that overexpression of L-PhGPx significantly inhibits cell growth. Decrease in cell plating efficiency is directly correlated with the effective PhGPx activity, suggesting that PhGPx might play a role in cell proliferation. However, due to the limitation of *in vitro* study, it is still not clear how

PhGPx could influence the differentiation and invasiveness of tumor cells. Further studies on the effects of PhGPx on tumor growth such as soft agar and *in vivo* nude mice experiments need to be done. It is also important to investigate the expression level of PhGPx in human tumor cells. Using the available PhGPx activity assay, RT-PCR, we will be able to screen the levels and the forms of PhGPx in tumor cells. Correlation of PhGPx levels with cell growth and tumor invasiveness will provide important information on the role of PhGPx in cell proliferation, differentiation, and tumor malignancy.

This work has demonstrated the protective effects of L-PhGPx against hydroperoxide-mediated cancer therapy. However, the pathways from LOOH to cell death remain unknown. ROS are known to play an important role as mediators in cellular signaling pathways, such as the activation of nuclear factor κB (NFκB) [Piette J, 1997], and the Ras signaling pathway [Lander HM, 1995]. The activation of NFκB can be inhibited by overexpression of PhGPx in a human umbilical endothelial cell line [Brigelius-Flohe R, 1997], suggesting a possible regulatory role of LOOH in the activation of NFκB. Mitochondria appear to be susceptible to various oxidative injuries. It has been found that the inner membranes of mitochondria contain significant amounts of highly unsaturated fatty acids [Yamaoka S, 1990]. Oxidation of mitochondrial membrane lipids might trigger the opening of mitochondrial permeability transition pores, which could result in cytochrome *c* release. Cytochrome *c* release from mitochondria is considered as a crucial step in the activation of apoptosis [Reed JC, 1997]. L-PhGPx might exert a protective function in the mitochondrial-mediated apoptotic cell death by preserving mitochondrial permeability. Thus, L-PhGPx could play a role in the signal transduction pathways *via* regulation of cellular peroxide tone. Clearly, further study of PhGPx in signaling pathways should be pursued.

REFERENCES

Adams, K.; Rainbow, A.J.; Wilson, B.C.; and Singh, G. In vivo resistance to photofrin-mediated photodynamic therapy in radiation-induced fibrosarcoma cells resistant to in vitro photofrin-mediated photodynamic therapy. *J. Photochem. Photobiol. B-Biol*. 49: 136-141, 1999.

Agarwal, M.L.; Larkin, H.E.; Zaidi, S.I.A.; Mukhtar, H.; and Oleinick, N.L. Phospholipase activation triggers apoptosis in photosensitized mouse lymphoma cells. *Cancer Res*. 53: 5897-5902, 1993.

Ahmad, N.; Feyes, D.; Agarwal, R.; and Mukhtar, H. Photodynamic therapy results in induction of WAF1/CIP1/P21 leading to cell cycle arrest and apoptosis. *Proc. Natl. Acad. Sci*. 95: 6977-6982, 1998.

Alvarea, S.; and Boveris, A. Induction of antioxidant enzymes and DT-diaphorase in human blood mononuclear cells. *Arch. Biochem. Biophys*. 305: 247-251, 1993.

Anderson, M.E. Tissue glutathione. In: *Handbook of Methods for Oxygen Radical Research.* (Greenwald, R.A. ed.), Boca Raton CRC Press, 1985.

Anderson, R.L.; Herman, T.S.; van Kersen, I.; and Hahn, G.M. Thermotolerance and heat shock protein induction by slow rates of heating. *Int. J. Rad. Onco. Biol. Phys.* 15: 717-725, 1988.

Antunes, F.; Salvador, A.; and Pinto, R.E. PhGPx and phospholipase A_2/GPx: comparative importance on the reduction hydroperoxides in rat liver mitochondria. *Free Radic. Biol. Med.* 19: 669-677, 1995.

Arai, M.; Imai, H.; Koumura, T.; Yoshida, M.; Emoto, K.; Umeda, M.; Chiba, M.; and Nakagawa, Y. Mitochondrial phospholipid hydroperoxide glutathione peroxidase plays an important role in preventing oxidative injury to cells. *J. Biol. Chem.* 274: 4924-4933, 1999.

Arai, M.; Imai, H.; Sumi, D.; Imanaka, T.; Takano, T.; Chiba, N.; and Nakagawa, Y. Import into mitochondria of phospholipid hydroperoxide glutathione peroxidase requires a leader sequence. *Biochem. Biophys. Res. Commun.* 227: 433-439, 1996.

Baker, A.; Kanofsky, J.R. Direct observation of singlet oxygen phosphorescence at 1270 nm from L1210 leukemia cells exposed to polyporphyrin and light. *Arch. Biochem. Biophys.* 286: 70-75, 1991.

Beauchamp, C.; and Fridovich, I. Superoxide dismutase: improved assays and assay applicable to polyarylamide gels. *Anal. Biochem.* 44: 276-287, 1971.

Benchekroun, M.N.; and Robert, J. Measurement of doxorubicin-induced lipid peroxidation under the conditions that determine cytotoxicity in cultured cells. *Anal. Biochem.* 201: 326-330, 1992.

Bindoli, A. Lipid peroxidation in mitochondria. *Free Radic. Biol. Med*. 5: 247-261, 1988.

Borges, H.L.; and Linden, R. Gamma irradiation leads to two waves of apoptosis in distinct cell populations of the retina of newborn rats. *J. Cell Sci.* 112: 4315-4324, 1999.

Brigelius-Flohe, R.; Aumann, K.D.; Blocker, H.; Gross, G.; Kiess, M. Kloppel, K.D.; Maiorino, M.; Roveri, A.; Schuckelt, R.; Ursini, F.; Wingender, E.; and Flohe, L. Phospholipid-hydroperoxide glutathione peroxidase: genomic DNA, cDNA, and deduced amino acid sequence. *J. Biol. Chem*. 269: 7342-7348, 1994.

Brigelius-Flohe, R.; Friedrichs, B.; Maurer, S. Schultz, M.; and Streicher, R. Interleukin-1-induced human nuclear factor kappa B activation is inhibited by overexpression of phospholipid hydroperoxide glutathione peroxidase in a human endothelial cell line. *Biochem. J.* 328: 199-203, 1997.

Buettner, G.R. The pecking order of free radicals and antioxidants: lipid peroxidation, alpha-tocopherol, and ascorbate. *Arch. Biochem. Biophys.* 300: 535-543, 1993.

Buettner, G.R.; Kelley, E.E.; and Burns, C.P. Membrane lipid free radicals produced from L1210 murine leukemia cells by Photofrin photosensitization: an electron paramagnetic resonance spin trapping study. *Cancer Res*. 53: 3670-3673, 1993.

Buettner, G.R.; and Oberley, L.W. Considerations in the spin trapping of superoxide and hydroxyl radical in aqueous systems using 5,5-dimethyl-1-1pyrroline-1-oxide. *Biochem. Biophys. Res. Commun*. 83: 69-74, 1978.

Chan, H.W.S. Autoxidation of unsaturated lipids. *Food Science and Technology*. Academic Press, London, 1984.

Chong, K.Y.; Lai, C.C.; Lille, S.; Chang, C.; and Su, C.Y. Stable overexpression of the constitutive form of heat shock protein 70 confers oxidative protection. *J. Mol. Cell. Cardiol.* 30: 599-608, 1998.

Chu, F.F.; Doroshow, J.H.; and Esworthy, R.S. Expression, characterization, and tissue distribution of a new cellular selenium-dependent glutathione peroxidase, GSH-Px-GI. *J. Biol. Chem.* 268: 2571-2576, 1993.

Compton, C.N.; Franko, A.P.; Murrray, M.T.; Diebel, L.N.; and Dulchavsky, S.A. Signaling of apoptotic lung injury by lipid hydroperoxides. *J. Trauma-Injury Infection Critical Care* 44: 783-788, 1997.

Dougherty, T.J. Photosensitization of malignant tumors. *Semn. Surg. Oncol*. 2: 24-27, 1986.

Dypbukt, J.M.; Ankarcrona, M.; Burkitt, M.; Sioholm, A.; Strom, K.; Orrenius, S.; Nicotera, P. Different prooxidant levels stimulate growth, trigger apoptosis, or produce necrosis of insulin-secreting RINm5F cells. The role of intracellular polyamines. *J. Biol. Chem.* 269: 30553-30560

Eddy, H.A. Alterations in tumor microvasculature during hyperthermia. *Radiology* 137: 515-521, 1980.

Edgren, M.R.; and Revesz, L. Compartmentalized depletion of glutathione in cells treated with buthionine sulfoximine. *Br. J. Radiol*. 60: 723-724, 1987.

Esworthy, R.S.; Doan, K.; Doroshow, J.H.; Chu, F.F. Cloning and sequencing of the cDNA encoding a human testis phospholipid hydroperoxide glutathione peroxidase. *Gene* 144: 317-318, 1994.

Esworthy, R.S.; Ho, Y.S.; and Chu, F.F. The GPx1 gene encodes mitochondrial glutathione peroxidase in the mouse liver. *Arch. Biochem. Biophys.* 340: 59-63, 1997.

Evensen, J.F. The use of porphyrins and non-ionizing radiation for the treatment of cancer. *Acta Oncologica.* 34: 1103-1110, 1995.

Fisher, A.B.; Dodia, C.; Manevich, Y.; Chen, J.W.; and Feinstein S. Phospholipid hydroperoxides are substrates for non-selenium glutathione peroxidase. *J. Biol. Chem.* 274: 21326-21334, 1999.

Fisher, A.M.R.; Ferrario, A.; Rucker, N.; Zhang S.; and Gomer, C.J. Photodynamic therapy sensitivity is not altered in human tumor cells after abrogation of p53 function. *Cancer Res.* 59: 331-335, 1999.

Flanagan, S.W.; Moseley, P.L.; and Buettner, G.R. Increased flux of free radicals in cells subjected to hyperthermia: detection by electron paramagnetic resonance spin trapping. *FEBS Lett.* 431: 285-286, 1998.

Flohe, L. Glutathione peroxidase: enzymology and biological aspects. *Klin. Wschr.,* 49: 669-683, 1971.

Flohe, L. Glutathione peroxidases brought into focus. In: *Free Radicals in Biology.* (Pryor, A. ed.). Vol. V.W.A. pp. 223-253, Academic Press, New York, 1982.

Flohe, L.; Wingender, E.; and Brigelius-Flohe, R. The regulation of glutathione peroxidases. In: *Oxidative Stress and Signal Transduction* (Forman, H.J.; and Cadenas, E.; eds.), p415-435, New York: Chapman & Hall, 1997.

Frank, J.; Kelleher, D.K.; Pompella, A.; Thews, O.; Biesalski, H.K.; and Vaupel, P. Enhancement of oxidative cell injury and antitumor effects of localized 44 degree C hyperthermia upon combination with respiratory hyperoxia and xanthine oxidase. *Cancer Res.* 58: 2693-2681, 1998.

Freeman, M.L.; Malcolm, A.W.; and Meredith, M.J. Role of glutathione in cell survival after hyperthermic treatment of Chinese hamster ovary cells. *Cancer Res.* 45: 6308-6313, 1985.

Freeman, M.L.; and Meredith, M.J. Subcellular localization of glutathione and thermal sensitivity. *Rad. Res.* 115: 461-471, 1988.

Fridovich, I. The biology of oxygen radicals. *Science* 201: 875-880, 1978.

Geiger, P.G.; Korytowski, W.; and Girotti, A.W. Photodynamically generated 3β-hydroxy-5α-cholest-6-ene-5-hydroperoxide: toxic reactivity in membranes and susceptibility to enzymatic detoxification. *Photochem. Photobiol*. 62: 580-587, 1995.

Gewirtz, D.A. A critical evaluation of the mechanisms of action proposed for the antitumor effects of the anthracycline antibiotics adriamycin and daunorubicin. *Biochem. Pharmacol.* 57: 727-741, 1999.

Girotti, A.W. Mechanism of lipid peroxidation. *J. Free Radic. Biol. Med.* 1: 87-95; 1985.

Godeas, C.; Sandri, G.; and Panfile, E. Distribution of phospholipid hydroperoxide glutathione peroxidase (PhGPx) in rat testis mitochondria. *Biochim. Biophys. Acta* 1191: 147-150, 1994.

Godeas, C.; Tramer, F.; Micali, F.; Roveri, A.; Maiorino, M.; Nisii, C.; Sandri, G.; and Panfile, E. Phospholipid hydroperoxide glutathione peroxidase (PhGPx) in rat testis nuclei is bound to chromatin. *Biochem. Mol. Med.* 59: 118-124, 1996.

Godeas, C.; Tramer, F.; Micali, F.; Soranzo, M.; Sandri, G.; and Panfili, E. Distribution and possible novel role of phospholipid hydroperoxide glutathione peroxidase in rat epididymal spermatozoa. *Biol. Reproduction* 57: 1502-1508, 1997.

Gomer, C.J.; Rucker, N.; Ferrario, A.; and Wong S. Properties and applications of photodynamic therapy. *Rad. Res.* 120: 1-18, 1989.

Gorman, A.M.; Heavey, B.; Creagh, E.; Cotter, T.G.; and Samali, A. Antioxidant-mediated inhibition of the heat shock response leads to apoptosis. *FEBS Lett.* 445: 98-102, 1999.

Grether-Beck, S.; Olaizola-Horn, S.; Schmitt, H.; Grewe, M.; Jahnke, A.; Johnson, J.P.; Briviba, K.; Sies, H.; and Krutmann, J. Activation of transcription factor AP-2 mediates UVA radiation- and singlet oxygen-induced expression of the human intercellular adhesion molecule 1 gene. *Proc. Natl. Acad. Sci*. 93: 14586-14591, 1996.

Griffith, O.W. Biologic and pharmacologic regulation of mammalian glutathione synthesis. *Free Radic. Biol. Med.* 27: 922-935, 1999.

Griffith, O.W.; and Meister, A. Potent and specific inhibition of glutathione synthesis by buthionine sulfoximine (s-n-butyl homocysteine sulfoximine). *J. Biol. Chem.* 254: 7558-7560, 1979.

Griffith, O.W.; and Meister, A. Origin and turn over of mitochondrial glutathione. *Proc. Natl. Acad. Sci*. 82: 4668-4672, 1985.

Grossman, A.; and Wendel, A. Non-reactivity of the selenoenzyme glutathione peroxidase with enzymatically hydroperoxidized phospholipids. *Eur. J. Biochem.* 135: 549-552, 1983.

Guarnieri, C.; Muscari, C.; and Caldarera C.M. In: *Free Radicals and Aging* (Emerit I, and Chance B. eds.), pp. 73-77, Birkhauser Verlag, Basel, 1992.

Gupta, S.; Ahmad, N.; and Mukhtar, H. Involvement of nitric oxide during phthalocyanine (Pc4) photodynamic therapy-mediated apoptosis. *Cancer Res*. 58: 1785-1788, 1998.

Gutteridge, J.M. Free radicals in disease processes: a compilation of cause and consequence. *Free Radic. Res. Commun.* 19: 141-158, 1993.

Hall D.M.; Oberley, T.D.; Moseley, P.M.; Buettner, G.R.; Oberley, L.W.; Weindruch, R. and Kregel, K.C. Caloric restriction improves thermotolerance and reduces hyperthermia-induced cellular damage in old rats. *FASEB J*. 14: 78-86, 2000.

Halliwell, B.; and Gutteridge, J.M.C. Role of free radicals and catalytic metal iron in human disease: an overview. *Methods Enzymol.* 186: 1-85, 1990.

Halliwell, B.; and Gutteridge, J.M.C. In: *Free Radicals in Biology and Medicine* (Halliwell, B.; and Gutteridge, J.M.C.; eds.), Oxford University Press, 1999.

Hanning, J.; Yu, J.; Beckett, M.; Weichselbaum, R.; Lee, R.C. Poloxamine 1107 sealing of radiopermeabilized erythrocyte membranes. *Internat. J. Radic. Biol.* 75: 379-385, 1999.

Henderson, B.W.; and Dougherty, T.J. How does photodynamic therapy work? *Photochem. Photobiol.* 55: 145-157, 1992.

Huang, H.S.; Chen, C.J.; Chang, and W.C. The CCAAT-box binding factor NF-Y is required for the expression of phospholipid hydroperoxide glutathione peroxidase in human epidermoid carcinoma A431 cells. *FEBS Lett*. 455:111-116, 1999.

Huang, H.S.; Chen, C.J.; Suzuki, H.; Yamamoto, S.; Chang, W.C. Inhibitory effect of phospholipid hydroperoxide glutathione peroxidase on the activity of lipoxygenases and cyclooxygenases. *Prosglandins Other Lipid Mediators* 58: 65-75, 1999.

Hurst, R.; Bao, Y.; Jemth, P.; Mannervik, B.; and Williamson, G. Phospholipid hydroperoxide glutathione peroxidase activity of human glutathione transferases. *Biochem. J*. 332: 97-100, 1998.

Hwang, C.; Sinsk, A.; and Lodish, H.F. Oxidized redox state of glutathione in the endoplasmic reticulum. *Science* 257: 1496-1502, 1992.

Imai, H.; Hanamato, A.; Arai, M.; Sugiyama, A.; Chiba, N.; Kuchino, Y.; and Nakagawa, Y. Molecular cloning and functional expression of a cDNA for rat phospholipid Hydroperoxide glutathione peroxidase: 3'-untranslated region of the gene is necessary for function expression. *J. Biochem.* 118: 1061-1067, 1995.

Imai, H.; Narashima, K.; Arai, M.; Sakamoto, H.; Chiba, N.; and Nakagawa, Y. Suppression of leukotriene formation in RBL-2H3 cells that overexpressed phospholipid hydroperoxide glutathione peroxidase. *J. Biol. Chem.* 273: 1990-1997, 1998.

Imai, H.; Sumi, D.; Sakamoto, H.; Hanamoto, A.; Arai, M.; Chiba, N.; and Nakagawa, Y. Overexpression of phospholipid hydroperoxide glutathione peroxidase suppressed cell death due to oxidative damage in rat basophile leukemia cells (RBL-2H3). *Biochem. Biophys. Res. Commun.* 222: 432-438, 1996.

Issels, R.D.; Fink, R.M.; and Lengfelder, E. Effects of hyperthermic conditions on the reactivity of oxygen radicals. *Free Radic. Res. Commun.* 2: 7-18, 1986.

Johnson, L.V.; Walsh, M.L.; and Chen, L.B. Localiztion of mitochondria in living cells with rhodamine 123. *Proc. Natl. Acad. Sci.* 77: 990-993, 1980.

Jori, G. The molecular biology of photodynamic action. In: *Lasers in Photomedicine and Photobiology (Pratesi, R. and Sacchi, C.A. eds.)*, pp. 58-66, Springer-Verlag, Berlin, 1980.

Kapoor, M.; and Lewis, J. Heat shock induces peroxidase activity in Neurospora crassa and confers tolerance toward oxidative stress. *Biochem. Biophys. Res. Comm.* 147: 904-910, 1987.

Kappus, H. Lipid peroxidation: mechanisms, enzymology, and biological relevance. In *Oxidative Stress* (Sies, H. ed.), pp. 273-310, American Press, New York, 1985.

Karlseder, J., Wissing, D., Holzer, G., Orel, L., Sliutz, G., Auer, H.; Jaattela, M., and Simon, M.M. Hsp70 overexpression mediates the escape of a doxorubicin-induced G2 cell cycle arrest. *Biochem. Biophys. Res. Commun.* 220: 153-159, 1996.

Kato, Y.; Makino, Y.; and Osawa, T. Characterization of a specific polyclonal antibody against 13-hydroperoxyoctadecadienoic acid-modified protein: formation of lipid hydroperoxide-modified apoB-100 in oxidized LDL. *J. Lipid Res.* 38: 1334-1346, 1997.

Kelley, E.E.; Buettner, G.R.; and Burns, C.P. Production of lipid-derived free radicals in L1210 murine leukemia cells is an early oxidative event in the photodynamic action of Photofrin. *Photochem. Photobiol*. 63: 576-580,1997.

Kelner, M.J.; and Montoya, M.A. Structural organization of the human selenium-dependent phospholipid hydroperoxide glutathione peroxidase gene (GPx4): chromosomal localization to 19p13.3. *Biochem. Biophys. Res. Commun*. 249: 53-55, 1998.

Khadir, A.; Verreault, J.; and Averill, D.A. Inhibition of antioxidants and hyperthermia enhance bleomycin-induced cytotoxicity and lipid peroxidation in Chinese hamster ovary cells. *Arch. Biochem. Biophys.* 370: 163-175,1999.

Khan, S.A.; Dougherty, T.J.; and Mang, T.S. An evaluation of photodynamic therapy in the management of cutaneous metastases of breast cancer. *European J. Cancer* 29A; 1686-1690, 1993.

Knopp, E.A.; Arndt, T.L.; Eng, K.L.; Caldwell, M.; LeBoeuf, R.C.; Deeb, S.S.; and O'Brien, K.D. Murine phospholipid hydroperoxide glutathione peroxidase: cDNA sequence, tissue expression, and mapping. *Mammalian Genome* 10: 601-605, 1999.

Kosower, N.S.; and Kosower, E.M. The glutathione status of cells. *Int. Rev. Cytol.* 54: 109-160, 1978.

Kotake, Y.; Reinke, L.A.; Tanigawa, T.; and Koshida, H. Determination of the rate of superoxide generation from biology systems by spin trapping: use of rapid oxygen depletion to measure the decay rate of spin adducts. *Free Radic. Biol. Med*. 17: 215-223, 1994.

Kovacs, I.B.; Jahangiri, M.; Rees, G.M.; and Gorog, P. Elevated plasma lipid hydroperoxides in patients with coronary artery diseases. *American Heart J*. 134: 572-576, 1997.

Kretz-Remy, C.; Mehlen, P.; Mirault, M.E.; and Arrigo, A.P. Inhibition of IκB-a phosphorylation and degradation and subsequent NF-κB activation by glutathione peroxidase overexpression. *J. Cell Biol.* 133: 1083-1093, 1996.

Kriska, T.; Mal'tseva, E.; and Gal, D. In vivo experimental studies on the role of free radicals in photodynamic therapy: photodynamic effect on free radical concentration in mice tumors measured by ESR spectroscopy. *Biochem. Biophys. Res. Commun*. 223: 136-140, 1996.

Kuhn, H.; and Brash, A.R. Occurrence of lipoxygenase products in membranes of rabbit reticulocytes. Evidence for a role of the reticulocyte lipoxygenase in the maturation of red cells. *J. Biol. Chem.* 265: 1454-1458, 1990.

Kurokawa, T.; Kobayashi, H.; Nonami, T.; Harada, A.; Nakao, A.; and Takagi, H. Mitochondrial glutathione redox and energy producing function during liver ischemia and reperfusion. *J. Surg. Res.* 66: 1-5, 1996.

Lander. H.M.; Ogiste, J.S.; Teng, K.K.; and Novogrodsky, A. p21ras as a common signaling target of reactive free radicals and cellular redox stress. *J. Biol. Chem.* 270: 21195-21198, 1995.

Lemaitre, D.; Vericel, E.; Polette, A.; and Legarde, M. Effects of fatty acids on human platelet glutathione peroxidase: possible role of oxidative stress. *Biochem. Pharmacol*. 53: 479-486, 1997.

Lepock, J.R.; and Kruuv, J. In: *Hyperthermia Oncology* (Gerner, E.W.; and Cetas, T.C. eds.) Vol. 2, pp. 9-16, Arizona Board of Regents, 1992.

Leyland-Jones, B.R.; Townsend, A.J.; Tu, C.P.D.; Cowan, k.H.; and Goldsmith, M.E. Antineoplastic drug sensitivity of human MCF-7 breast cancer cells stably transfected with a human α class glutathione S-transferase gene. *Cancer Res.* 51: 587-594, 1991.

Li, J.J.; and Oberley, L.W. Overexpression of manganese-containing superoxide dismutase confers resistance to the cytotoxicity of tumor necrosis factor α and/or hyperthermia. *Cancer Res.* 57: 1991-1998, 1997.

Li, S.; Yan, T.; Yang, J.Q.; Oberley, T.D.; and Oberley, L.W. The role of cellular glutathione peroxidase redox regulation in the suppression of tumor cell growth by manganese superoxide dismutase. *Cancer Res.* 60: 3927-3939, 2000.

Lin, F.; Geiger, P.G.; and Girotti, A.W. Selenoperoxidase-mediated cytoprotection against merocyanine 540-sensitized photoperoxidation and photokilling of leukemia cells. *Cancer Res*. 52: 5282-5299, 1992.

Lopez-Barea, J.; Barcena, J.A.; Bocanegra, J.A.; Florindo, J.; Garcia-Alfonso, C.; Lopez-Ruiz, A.; Martinez-Galisteo, M.; and Peinado, J. Structure, mechanism, functions, and regulatory properties of glutathione reductase. In: *Metabolism and Physiological Function.* (Vina, J. ed.), pp. 105-112, CRC Press, Boca Raton, 1990.

Lord-Fontaine, S.; and Averill, D.A. Enhancement of cytotoxicity of hydrogen peroxide by hyperthermia in Chinese hamster ovary cells: role of antioxidant defenses. *Arch. Biochem. Biophys.* 363: 283-295, 1999.

Loven, D.P.; Leeper, D.B.; and Oberley, L.W. Superoxide dismutase levels in Chinese hamster ovary cells and ovarian carcinoma cells after hyperthermia or exposure to cycloheximide. *Cancer Res.* 45: 3029-3033, 1985.

Lu, S.C. Regulation of hepatic glutathione synthesis: current concepts and controversies. *FASEB J*. 13: 1169-1183, 1999.

Maiorino, M.; Chu, F.F.; Ursini, F.; Davies, K.J.; Doroshow, J.H.; and Esworthy, R.S. Phospholipid hydroperoxide glutathione peroxidase is the 18-kDa selenoprotein expressed in human tumor cell lines. *J. Biol. Chem.* 266: 7728-7732, 1991.

Maiorino, M.; Gregolin, C.; and Ursini, F. Phospholipid hydroperoxide glutathione peroxidase. *Method Enzymol*. 186: 448-457, 1990.

Maiorino, M.; Wissing, J.B.; Brigelius-Flohe, R.; Calabrese, F.; Roveri, A.; Steinert, P.; Ursini, F.; and Flohe, L. Testosterone mediates expression of the selenoprotein PhGPx by induction of spermatogenesis and not by direct transcriptional gene activation. *FASEB J.* 12: 1359–1370, 1998.

Marchal, C.; Weber, B.; de Lafontan, B.; Resbeut, M.; Mignotte, H.; du Chatelard, P.P.; Cutuli, B.; Reme-Saumon, M.; Broussier-Leroux, A.; Chsplain, G.; Lesaunier, F.; Dilhuydy, J.M.; and Lagrange, J.L. Nine breast angiosarcomas after conservative treatment for breast carcinoma: a survey from French comprehensive cancer centers. [review]. *Inter. J. Rad. Oncol. Biol. Phys.* 44: 113-119, 1999.

Masini, A.; Ceccarelli, D.; Gallesi, D.; Giovannini, F.; and Trenti, T. Lipid hydroperoxide induced mitochondrial dysfunction following acute ethanol intoxication in rats. The critical role of mitochondrial reduced glutathione. *Biochem. Pharmacol.* 47: 217-224, 1994.

Meister, A. Glutathione, ascorbate, and cellular protection. *Cancer Res.* 54: 1969s-1975s, 1994.

Meister, A. Glutathione. In: *The Liver: Biology and Pathobiology, Second Edition* (Aria, I.M., Jakoby, W.B., Popper H., Schachter, D., and Shafritz, D.A., eds.), pp. 401-417, Raven Press, New York, 1988.

Meister, A.; and Anderson, M.E. Glutahione. *Annual Review Biochem.* 52: 711-760, 1983.

Meister, A. Glutathione deficiency produced by inhibition of its synthesis, and its reversal; applications in research and therapy. *Pharmacol. Ther.* 51: 155-194, 1991.

Meredith, M.J.; and Reed, D.J. Status of the mitochondrial pool of glutathione in the isolated hepatocyte. *J. Biol. Chem*. 257: 3747-3753, 1982.

Mills, G.C. Hemoglobin catabolism I. Glutathione peroxidase, and erythrocyte enzyme which protects hemoglobin from oxidative breakdown. *J. Biol. Chem.* 229: 189-197, 1957.

Mitchell, J.B.; and Russo, A. Thiols, thiol depletion, and thermosensitivity. *Radiat. Res.* 95: 471-485, 1983.

Mulcahy, R.T.; Bailey, H.H.; and Gipp, J.J. Upregulation of γ-glutamylcysteine synthetase activity in melphalan-resistant human multiple myeloma cells expressing increased glutathione levels. *Cancer Chemother. Pharmacol.* 34: 67-71, 1994.

Newton, C.J.; Drummond, N.; Burgoyne, C.H.; Speirs, V.; Stalla, G.K.; and Atkin, S.L. Functional inactivation of the oestrogen receptor by the antioestrogen, ZM 182780, sensitises tumor cells to reactive oxygen species. *J. Endocinol.* 161: 199-210, 1999.

Nomura, K.; Imai, H.; Koumura, T.; Arai, M.; and Nakagawa, Y. Mitochondrial phospholipid hydroperoxide glutathione peroxidase suppresses apoptosis mediated by a mitochondrial death pathway. *J. Biol. Chem.* 274: 29294-29302, 1999.

Oberley, L.W.; McCommick, M.L.; Sierra, E.; and St.Clair, D.K. Manganese superoxide dismutase in normal and transformed human embryonic lung fibroblasts. *Free Radic. Biol. Med.* 6: 379-384, 1989.

Ochsner, M. Photophysical and photobiological processes in the photodynamic therapy of tumors. *J. Photochem. Photobiol. B: Biol*. 39: 1-18, 1997.

Ottesen, G.; Andersen, J.A.; Blichert-Toft, M.; and Axelsson, C. Frequency and types of chest wall recurrences among node negative breast cancer patients. *Acta Oncol.* 27: 601-604, 1988.

Palace, V.; Kumar, D.; Hill, M.F.; Khaper, N.; Singal, P.K. Regional differences in non-enzymatic antioxidants in the heart under control and oxidative stress conditions. *J. Mol. Cellul. Cardiol.* 31: 193-202, 1999.

Parker, S.L.; Tong, T.; Bolden, S.; and Wingo, P.A. Cancer statistics. *CA Cancer J. Clin.* 47: 5-27, 1997.

Pass, H.I.; and Pogrebniak, H.W. Photodynamic therapy for thoracic malignancies. *Semin Surg. Oncol.* 8: 217-225, 1992.

Phillips, D. Photodynamic therapy. *Sci. Progress* 77: 295-316, 1994.

Phillips, D.M.; and Balducci, L. Current management of breast cancer. *Am. Fam. Physician* 53: 657-665, 1996.

Phillips, M.I.; and Gyurko, R. Antisense oligonucleotides: new tools for physiology. *News Physiol. Sci.* 12: 99-105, 1997.

Piette, J.; Piret, B.; Bonizzi, G.; Schoonbroodt, S.; Merville, M.P.; Legrand-Poels, S.; and Bours, V. Multiple redox regulation in NF-kappaB transcription factor activation. *Biol. Chem.* 378: 1237-1245, 1997.

Porter, N.A.; Caldwell, S.E.; and Mills, K.A. Mechanisms of free radical oxidation of unsaturated lipids. *Lipids* 30: 277-290, 1995.

Pradhan, D.; Weiser, M.; Lumley-Sapanski, K.; Franzier, D.; Kemper, S.; Willianson, P.; and Schlegel, R.A. Peroxidation-induced perturbations of erythrocyte lipid organization. *Biochim. Biophys. Acta* 1023: 398-404, 1990.

Privalle, C.T.; and Fridovich, I. Induction of superoxide dismutase in Escherichia coli by heat shock. *Proc. Natl. Acad. Sci*. 84: 2723-2726, 1987.

Pushpa-Rekha, T.R.; Burdsall, A.L.; Oleksa, L.M.; Chisolm, G.M.; and Driscoll, D.M. Rat, phospholipid-hydroperoxide glutathione peroxidase. cDNA cloning and identification of multiple transcription and translation start sites. *J. Biol. Chem.* 270: 26993-26999, 1995.

Qian, S.Y.; Wang, H.P.; Schafer, F.Q.; and Buettner, G.R. EPR detection of lipid-derived radicals from PUFA, LDL, and cell oxidations. *Free Radic. Biol. Med.* 29: 568-579, 2000.

Reed, J.C. Cytochrome c: can't live with it – can't live without it [comment]. *Cell* 91: 559-562, 1997.

Robinson, D.S.; Parel, J.M.; Denham, D.B.; Gonzalea-Cirre, X.; Manns, F.; Milne, P.J.; Schachner, R.D.; Herron, A.J.; Comsnder, J.; and Hauptmann, G. Interstitial laser hyperthermia model development for minimally invasive therapy of breast carcinoma. *J. American College Surgeons* 186: 284-292, 1998.

Romero, F.J.; and Sie, H. Subcellular glutathione contents in isolated hepatocytes treated with L-buthionine sulfoximine. *Biochem. Biophys. Res. Commun*. 123: 1116-1121, 1984.

Roti Roti, J.L.; Laszlo, A. In: *Hyperthermia and Oncology* (Urano, M.; and Douple, E.; eds.), 2: 99-16, Arizona Board of Reagents, 1988.

Roveri, A.; Casasco, A.; Maiorino, M.; Dalano, D.; Calligaro, A.; and Ursini, F. Phospholipid hydroperoxide glutathione peroxidase of rat testis: gonadotropin dependence and immunocytochemical identification. *J. Biol. Chem.* 267: 6142-6146, 1992.

Roveri, A.; Maiorino, M.; and Ursini, F. Enzymatic and immunological measurements of soluble and membrane-bound phospholipid-hydroperoxide glutathione peroxidase. *Methol. Enzymol*. 233: 202-212, 1994.

Sandstrom, P.A.; Tebbey, P.W.; Cleave, S.V.; and Buttke, T.M. Lipid hydroperoxides induce apoptosis in T cells displaying a HIV-associated glutathione peroxidase deficiency. *J. Biol. Chem.* 269: 798-801, 1994.

Scaduto. R,C.; and Grotyhann, L.W. Measurement of mitochondrial membrane potential using fluorescent rhodamine derivatives. *Biophys. J.* 76: 469-475, 1999.

Schafer, F.Q.; and Buettner, G.R. Singlet oxygen toxicity is cell line-dependent: a study of lipid peroxidation in nine leukemia cell lines. *Photochem. Photobiol*. 70: 858-867, 1999.

Schnurr, K.; Belkner, J.; Ursini, F.; Schewe, T.; and Kuhn, H. The selenoenzyme phospholipid hydroperoxide glutathione peroxidase controls the activity of the 15-lipoxygenase with complex substrates and preserves the specificity of the oxygenation products. *J. Biol. Chem.* 271: 4653-4658, 1996.

Schuckelt, R.; Brigelius-Flohe, R.; Maiorino, M.; Roveri, A.; Reumkens, J.; Straβburger, W.; Ursini, F.; Wolf, B.; and Flohe, L. Phospholipid hydroperoxide glutathione peroxidase is a selenoenzyme distinct from the classical glutathione peroxidase as evidence from cDNA and amino acid sequencing. *Free Radic. Res. Commun.* 14: 343-361, 1991.

Sharkey, S.M.; Wilson, B.C.; Moorehead, R.; and Singh, G. Mitochondrial alterations in photodynamic therapy-resistant cells. *Cancer Res.* 53: 4994-4999, 1993.

Sherar, M.; Liu, F.F.; Pintilie, M.; Levin, W.; Hunt, J.; Hill, R.; Hand, J.; Vernon, C.; van Rhoon, G.; van der Zee, J.; Gonzalez, D.G.; van Dijk, J.; Whaley, J.; and Machin, D. Relationship between thermal dose and outcome in thermoradiotherapy treatments for superficial recurrences of breast cancer: data from a phase III trial. *Inter. J. Rad. Oncol. Biol. Phys.* 39: 371-380, 1997.

Shigenaga, M.K.; Hagen, T.M.; and Ames, B.N. Oxidative damage and mitochondrial decay in aging. *Proc. Natl. Acad. Sci*. 91: 10771-10778, 1994.

Shull, S.; Heintz, N.H.; Periasamy, M.; Manchar, M.; Janssen, Y.M.W.; Marsh, J.P.; and Mossman, B.T. Differential regulation of antioxidant enzymes in response to oxidants. *J. Biol. Chem.* 266: 24398-24403, 1991.

Skibba, J.L.; Quebbeman, E.J.; and Kalbfleisch, J.H. Nitrogen metabolism and lipid peroxidation during hyperthermic perfusion of human livers with cancer. *Cancer Res.* 46: 6000-6003, 1986.

Skibba, J.L.; Stadnicka, A.; Kalbfleisch, J.H.; and Powers R.H. Effects of hyperthermia on xanthine oxidase activity and glutathione levels in the perfused rat liver. *J. Biochem. Tox.* 4: 119-125, 1989.

Slyshenkov, V.S.; Omelyanchik, S.W.; Moiseenok, A.G.; Petushok, N.E.; and Wojtczak, L. Protection by pantothenol and beta-carotene against liver damage produced by low-dose gamma radiation. *Acta Biochim. Polonica* 46: 239-248, 1999.

Smith, C.V.; Jones, C.P.; Guenthner, T.M.; Lash, L.H.; and Lauterburg, B.H. Contemporary issues in toxicology. Compartmentation of glutathione: implications for the study of toxicity and disease. *Toxicol. Appl. Pharmacol.* 140: 1-12, 1996.

Soule, H.; Maloney, T.M.; Wolman, S.R.; Peterson, W.D.; Brenz, R.; McGrath, C.M.; Russo, J.; Pauley, R.J.; Jones, R.F.; and Brooks, S.C. Isolation and characterization of a spontaneously immortalized human breast epithelial cell line, MCF-10. *Cancer Res.* 50: 6075-6086, 1990.

Spitz, D.R.; and Li, G.C. Heat-induced cytotoxicity in H_2O_2-resistant Chinese hamster fibroblasts. *J. Cell. Physiol.* 142: 255-260, 1990.

Stauss, H.M; Morgan, D.A.; Anderson, K.E.; Massett, M.P.; and kregel, K.C. Modulation of baroreflex sensitivity and spectral power of blood pressure by heat stress and aging. *Am. J. Physiol*. 272: H776-784, 1997.

Steinbeck, M.J.; Kim, J.K.; Trudeau, M.J.; Hauschka, P.V.; and Karnovsky, M.J. Involvement of hydrogen peroxide in the differentiation of clonal HD-11EM cells into osteoclast-like cells. *J. Cell. Physiol.* 176: 574-587, 1998.

Su, C.Y.; Chong, K.Y.; Owen, O.E.; Dillmann, W.H.; Chang, C.; and Lai, C.C. Constitutive and inducible Hsp70 are involved in oxidative resistance evoked by heat shock or ethanol. *J. Mol. Cell Cardiol*. 30: 587-598, 1998.

Suzuki, Y.; Kondo, Y.; Himeno, S.; Nemoto, K.; Akimoto, M.; and Imura, N. Role of antioxidant systems in human androgen-independent prostate cancer cells. *Prostate* 43: 144-149, 2000.

Suzuki, Y.J.; Forman, H.F.; and Sevanian, A. Oxidant as stimulators of signal transduction. *Free Radic. Biol. Med.* 22: 269-285, 1997.

Taber, S.W.; Fingar, V.H.; and Wieman, T.J. Photodynamic therapy for palliation of chest wall recurrence in patients with breast cancer. *J. Surg. Oncol*. 68: 209-214, 1998.

Takahashi, K.; Avissar, N.; Whitin, J.; Cohen, H. Purification and characterization of human plasma glutathione peroxidase: a selenoglycoprotein distinct from the known cellular enzyme. *Arch. Biochem. Biophys.* 256: 677-686, 1987.

Tao, J.; Sanghera, J.S.; Pelech, S.L.; Wong, G.; and Levy JG. Stimulation of stress-activated protein kinase and p38 HOG1 kinase in murine keratinocytes following photodynamic therapy with benzoporphyrin derivative. *J. Biol. Chem.* 271: 27107-27115, 1996.

Thomas, J.P.; Maiorino, M.; Ursini, F.; and Girotti, A.W. Protective action of phospholipid hydroperoxide glutathione peroxidase against membrane-damaging lipid peroxidation in situ reduction of phospholipid and cholesterol hydroperoxides. *J. Biol. Chem.* 265: 454-461, 1990.

Ursini, F.; Maiorino, M.; Valente, M.; Ferri, L.; Gregolin, C. Purification from pig liver of a protein which protects liposomes and biomembranes from peroxidative degradation and exhibits glutathione peroxidase activity on phosphatidylcholine hydroperoxides. *Biochim. Biophys. Acta* 710: 197-211, 1982.

Ursini, F.; Heim, S.; Kiess, M.; Maiorino, M.; Roveri, A.; Wissing, J.; and Flohe, L. Dual function of the selenoprotein PhGPx during sperm maturation. *Science* 285: 1393-1396, 1999.

Ursini, F.; Maiorino, M.; Brigelius-Flohe, R.; Aumann, K.D.; Roveri, A.; Schomburg, D.; and Flohe, L. The diversity of glutathione peroxidases. *Methods Enzymol.* 252: 38-53, 1995.

Ursini, F.; Maiorino, M.; and Gregolin, C. The selenoenzyme phospholipid hydroperoxide glutathione peroxidase. *Biochim. Biophys. Acta* 839: 62-70, 1985.

van der Zee, J.; van der Holt, B.; Rietveld, P.J.M.; Helle, P.A.; Wijnmaalen, A.J.; van Putten, W.L.J.; and van Rhoon, G.C. Reirradiation combined with hyperthermia in recurrent breast cancer results in a worthwhile local palliation. *British J. Cancer* 79: 483-490, 1999.

van Kuijk, F.J.G.M.; Sevanian, A.; Handelman, G.J.; and Dratz, E.A. A new role for phospholipase A2: protection of membranes from lipid peroxidation damage. *Trends Biochem. Sci.* 12: 31-34, 1987.

Vile, G.F.; and Tyrrell, R.M. Oxidative stress resulting from ultraviolet A irradiation of human skin fibroblasts leads to a heme oxygenase-dependent increase in ferritin. *J. Biol. Chem*. 268: 14678-14681, 1993.

Wang, H.P.; Qian, S.Y.; Schafer, F.Q.; Domann, F.E.; Oberley, L.W.; and Buettner, G.R. Phospholipid hydroperoxide glutathione peroxidase protects against the singlet oxygen-induced damage of photodynamic therapy. Submitted, 2000.

Weishaupt, K.R.; Gormer, C.J.; and Dougherty, T.J. Identification of singlet oxygen as the cytotoxic agent in photo-inactivation of a murine tumor. *Cancer Res*. 36: 2326-2329, 1976.

Weiss, J.F.; and Landauer M.R. Radioprotection by antioxidants. *Ann. New York Acad. Sci.* 899: 44-60, 2000.

Weitzel, F.; and Wendel, A. Selenoenzymes regulate the activity of leukocyte 5-lipoxygenase via the peroxide tone. *J. Biol. Chem.* 268: 6288-6292, 1993.

Weitzel, F.; Ursini, F.; and Wendel, A. Phospholipid hydroperoxide glutathione peroxidase in various mouse organs during selenium deficiency and repletion. *Biochim. Biophys. Acta* 1036: 88-94, 1990.

Welch, W.J. Mammalian stress response: cell physiology, structure / function of stress proteins, and implications for medicine and disease. *Physiol. Reviews* 72: 1063-1081, 1992.

Wilkinson, F.; and Brummer, J.G. Rate constants for the decay and reactions of the lowest electronically excited singlet state of molecular oxygen in solution. *J. Phys. Chem. Ref. Data* 10: 809-999, 1981.

Williams, R.S., Thomas, J.A., Fina, M., German, Z., and Benjamin, I.J. Human heat shock protein (Hsp70) protects murine cells from injury during metabolism stress. *J. Clin. Invest.* 92: 503-508, 1993.

Wong, G.H.; McHugh, W.T.; Weber, R.; and Goeddel, D.V. Tumor necrosis factor alpha selectively sensitizes human immunodeficiency virus-infected cells to heat and radiation. *Proc. Natl. Acad. Sci*. 88: 4372-4376, 1991.

Yagi, K.; Komura, S.; Kojima, H.; Sun, Q.; Nagata, N.; Ohishi, N.; and Nishikimi, M. Expression of human phospholipid hydroperoxide glutathione peroxidase gene for protection of host cells from hydroperoxide-mediated injury. *Biochem. Biophys. Res. Commun.* 219: 486-491, 1996.

Yamaoka, S.; Urade, R.; and Kito, M. Cardiolipin molecular species in rat heart mitochondria are sensitive to essential fatty acid-deficient dietary lipids. *J. Nutr.* 120: 415-421, 1990.

Yan, T.; Jiang, X.; Zhang, H.J.; Li, S.; and Oberley, L.W. Use of commercial antibodies detection of the primary antioxidant enzymes. *Free Radic. Biol. Med.* 25: 688-693, 1998.

Yoshikawa, T.; Yoshida, N.; Miyagawa, H.; Takemura, T.; Tanigawa, T.; Sugino, S.; and Kondo, M. Role of lipid peroxidation in gastric mucosal lesions induced by burn shock in rats. *J. Clin. Biochem. Nutr.* 2: 163-170, 1987.

Zhang, J. Comparison of effects of two polymorphic variants of manganese-containing superoxide dismutase on human breast MCF-7 cancer cell phenotype. *Ph.D. Thesis,* The University of Iowa, 1998.